ABSTRACT

Bone morphogenetic protein (Bmp) signaling is critical for vascular development and homeostasis. Defects in this pathway lead to multiple vascular diseases, including Heritable Pulmonary Arterial Hypertension (HPAH), which is genetically linked to mutations in *Bone Morphogenetic Protein Receptor Type 2 (BMPR2)*. All forms of PAH display structural remodeling of resistance-level pulmonary arteries, suggesting that defective Bmp signaling might underlie other forms of PAH, even in the absence of *BMPR2* mutations. Therefore, we utilized a genetics-based approach in mice to examine the functional role of Bmp signaling in hypoxia-induced pulmonary hypertension (PH).

Chapters 2 and 3 describe work that is now published. These studies illustrate that both *Bmpr2* and *Bmp2* (*Bmp2*$^{+/-}$) mutant mice have defective regulation of pulmonary endothelial nitric oxide synthase (eNOS), indicating that Bmp signaling directly regulates pulmonary vascular tone. In contrast to *Bmp2*$^{+/-}$ mice, *Bmp4* deficient (*Bmp4*$^{LacZ/+}$) mice have preserved regulation of eNOS. Moreover, *Bmp2*$^{+/-}$ mice develop increased hypoxia-induced vascular remodeling and PH, while previous work showed that *Bmp4*$^{LacZ/+}$ mice are partially protected from these effects. These studies indicate that Bmp2 and Bmp4 oppositely affect the development of hypoxic PH, and that regulation of eNOS is likely a key protective effect mediated by Bmp2 and Bmpr2 in the pulmonary vasculature.

The work shown in Chapter 4, which has been submitted for publication, explores the role of Id1 as a downstream mediator of Bmp4-dependent responses in the pulmonary vasculature. A previous study showed that *Bmp4*$^{LacZ/+}$ mice display impaired hypoxia-induced vascular smooth muscle cell (VSMC) proliferation with decreased Id1 expression, suggesting that Id1 might promote VSMC proliferation in hypoxia. However, using *Id1 null*

mice, we show that Id1 expression is not required for hypoxic-induced VSMC proliferation or PH. This finding might be due to functional compensation, since expression of the closely-related Id3 is selectively up-regulated in *Id1 null* peripheral vessel VSMC.

Collectively, these studies provide functional insight into Bmp signaling in pulmonary vascular homeostasis. They add to an understanding of human PAH by illustrating distinct downstream events associated with Bmp2- vs. Bmp4-signaling *in vivo*. Additionally, they provide potential targets for future therapies.

BMP SIGNALING IN PULMONARY VASCULAR HOMEOSTASIS AND DISEASE

By

Jonathan Wayne Lowery

Dissertation

Submitted to the Faculty of the

Graduate School of Vanderbilt University

in partial fulfillment of the requirements

for the degree of

DOCTOR OF PHILOSOPHY

In

Cell and Developmental Biology

August, 2010

Nashville, Tennessee

Approved:

Professor Christopher V. Wright, Chair

Associate Professor Mark P. deCaestecker

Professor H. Scott Baldwin

Professor Chin Chiang

To my extraordinary wife, Brooklyn,

my parents, Dennis and Wanda,

and, humbly, to my mentor, Dr. Mark deCaestecker

ACKNOWLEDGMENTS

The studies described in this dissertation were performed in the Department of Cell & Developmental Biology between 2006 and 2010. I would like to thank the Department, in particular Elaine Caine, Dr. Kathy Gould, and Dr. Susan Wente, for their unwavering support of students.

This work would not have been possible without the support of many individuals, centers, and funding sources. I thank Dr. David Frank for generating much of the preliminary data on which my work was built; Dr. Lynda Anderson for being a wonderful lab mate and collaborator; Mark Jones for his essential management of the lab; Stan Poole and Dr. Jeff Reese for their crucial assistance in developing the tools to perform arteriography; Dr. Ambra Pozzi for her willingness to teach us how to isolate pulmonary microvascular endothelial cells; the Baldwin lab for access to microscopes; and Andrea Frump and Dr. Tatiana Novitskaya for their continual advice and support. I must also thank the members of the Mouse Metabolic Phenotyping Core, in which all of the physiology analyses were performed, and the Pulmonary Hypertension Interest Group (especially Drs. James West, Candice Fike, and Judy Aschner) for their bi-weekly insight.

Funding from Philip Morris Company and the National Institutes of Health has made my time in the lab possible. Additionally, a special appreciation is extended to Dr. Richard Hoover for his oversight of the Mechanisms of Vascular Disease training grant, from which I was funded for two years.

I sincerely thank Drs. Jim Patton, Roger Chalkley, and Michele Grundy of the Interdisciplinary Graduate Program in Biomedical Science. Their leadership has created a vibrant atmosphere in which graduate students can mature into scientists. Also, I am

especially thankful for the opportunity to develop teaching skills through involvement in the IGP FOCUS program.

I am infinitely appreciative to the friends and loved ones who have supported me through the ups and downs of graduate school. In particular, Chris Wolfe is the kind of best friend everyone should be lucky enough to have. I am grateful to my family, who has always given me the chance to find my own way, often through their own self-sacrifice. To my wife, Brooklyn, you are a blessing that I do not deserve. Our conversations during mutual graduate careers have ranged from signaling cascades and protein interactions to Puritan literature and Louisa May Alcott. Now, as we both graduate, I am so proud of you and all you have accomplished. Thank you for your love, support, and willingness to build a life with me.

The members of my dissertation committee have pushed me to grow and mature as a scientist. I sincerely appreciate their support, advice, guidance, and willingness to give me room to discover my calling. Thank you very much, Drs. Chris Wright, Scott Baldwin, Chin Chiang, and the late Greg Mundy.

Finally, I cannot thank my advisor, Dr. Mark deCaestecker, enough. Mark took a chance on a transfer student and allowed me to join his lab without a rotation. From the very beginning, he pushed me to work hard, even meeting with me three times a week at 8:00 a.m. when I needed direction. His door has always been open to me, and his clarity has pushed my work to completion. He has given me liberty to pursue my goals, even to the extent of taking a sabbatical to teach. He is truly my mentor, not just my advisor.

TABLE OF CONTENTS

Page

LIST OF TABLES

Table Page

LIST OF FIGURES

LIST OF ABBREVIATIONS

α-SMA	Alpha-smooth muscle actin
µL	Microliter
µM	Micromolar
µm	Micrometer
ACh	Acetylcholine
ANOVA	Analysis of variance
bHLH	Basic helix-loop-helix
Bmp	Bone morphogenetic protein
Bmpr2	Bone morphogenetic protein receptor type 2
bp	Base pair
BSA	Bovine serum albumin
cAMP	Cyclic adenosine monophosphate
cDNA	complementary DNA
cGMP	Cyclic guanosine monophosphate
CPM	Counts per minute
DAPI	4',6-diamidino-2-phenylindole
DNA	Deoxyribonucleic acid
EC	Endothelial cell
eNOS	Endothelial nitric oxide synthase
Gdf	Growth and differentiation factor
HPAH	Heritable Pulmonary Arterial Hypertension
HRP	Horseradish peroxidase
Id	Inhibitor of differentiation
IgG	Immunoglobulin G
IPA	Intrapulmonary artery
iPS	Induced pluripotent stem (cell)

KCl	Potassium chloride
kDa	Kilodalton
L-NAME	NG-nitro-L-arginine methyl ester
LV	Left ventricle
LVDP	LV diastolic pressure
mL	Milliliter
mM	Millimolar
NE	Norepinephrine
NO	Nitric oxide
NOS	nitric oxide synthase
PAH	Pulmonary arterial hypertension
PBS	Phosphate buffered saline
PCNA	Proliferating cell nuclear antigen
PCR	Polymerase chain reaction
PEC	Pulmonary microvascular EC
PH	Pulmonary hypertension
PKA	cAMP-dependent protein kinase
PKG	cGMP-dependent protein kinase
RNA	Ribonucleic acid
ROS	Reactive oxygen species
RT-PCR	Reverse transcriptase PCR
RV	Right ventricle
RVSP	RV systolic pressure
RVDP	RV diastolic pressure
SEM	Standard error of the mean
SNP	Sodium nitroprusside
VASP	Vasodilator-stimulated phosphoprotein
VE-cadherin	Vascular endothelial cadherin

Vegfr2	Vascular endothelial growth factor receptor 2
VSMC	Vascular smooth muscle cell
vWF	vonWillebrand Factor

CHAPTER I

INTRODUCTION

Part I. The Bmp signaling pathway

Bone morphogenetic proteins

The Bone morphogenetic protein (Bmp) family of proteins has ancient origins in the evolution of animals, arising 1.2-1.4 billion years ago (144). The first observation of their signaling abilities was in 1965, when Marshall Urist found that demineralized bone matrix could induce ectopic bone formation after intramuscular injection (212). The term "Bmp" was coined in 1971 to signify the mysterious molecule(s) that caused autoinduction of bone (213). Since these original findings, it has been revealed that this multi-member signaling cascade plays essential roles in the development of nearly all vertebrate organs (reviewed in (97, 240)).

Bmps, some of which are also called growth and differentiation factors (Gdfs), are now considered to be the largest subfamily of the TGF-β superfamily of ligands. This superfamily can be organized into clades based on sequence similarity and conservation among primitive animals (Figure 1). This organization helps to clarify the difference in receptor binding and cellular responses between Bmps and other TGF-β superfamily ligands. On this basis, there are 15 *bona fide* mammalian Bmp ligands that activate typical Bmp-dependent responses, some of which are context dependent. For example, the

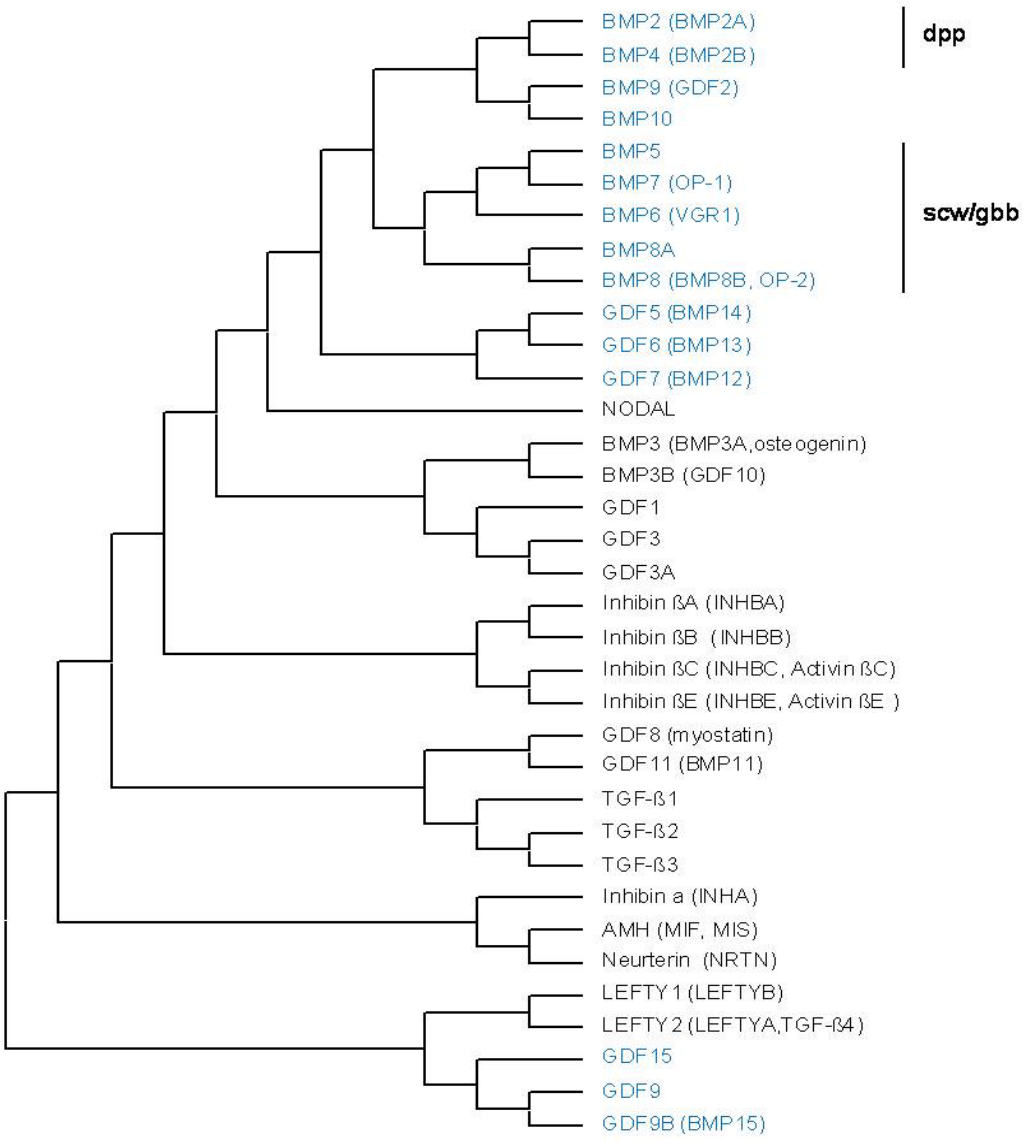

Figure 1. Phylogenic comparison of TGF-β superfamily ligands based upon full length human protein sequences. Sequence similarity to Drosophila Bmp orthologues is indicated. Alternative names are listed in parentheses. Ligands in blue are bona fide BMP/GDF proteins that have been shown to activate Bmp Smads. Phylogenetic analyses were conducted in MEGA4 using the Neighbor-Joining method.

distantly related Gdf15 group of ligands (Gdf15, Gdf9, and Gdf9b) can activate Bmp-dependent responses but can also act as inhibitors of Bmp signaling (46, 137). Other ligands, such as Gdf8, Gdf11, Gdf1, and Gdf3, are misnamed since they activate pathways more typical of the TGF-β/Activin ligands (4-5). Still others, such as Bmp3, should be classified as Bmp antagonists since they act by sequestering inactive Bmp receptor signaling complexes (62).

Bmp signal transduction

Bmp signal transduction occurs by formation of heterotetrameric complexes of type I (Activin-like kinase (Alk) 1, 2, 3, and 6) and type II receptors (Bmp receptor 2 (Bmpr2), Activin receptor (Actr) 2A, and Actr2B) (reviewed in (134, 141)). Both receptor types have extracellular ligand binding, transmembrane, and cytoplasmic serine/threonine kinase domains. These receptors have distinct ligand binding properties (Table 1, Table 2), but show considerable promiscuity in binding to different members of the TGF-β superfamily (reviewed in (146)). Alk3 and Alk6 are activated by Bmp2 and Bmp4 equally well, while Bmp5-8 group ligands principally activate Alk2. The order of receptor oligomerization can also differ between Bmp ligands: Bmp2 and Bmp4 recruit type II receptors after first binding with high affinity to a type I receptor, while Bmp5-8 group ligands bind first with high affinity a type II receptor and then recruit type I receptor. Upon ligand-induced oligomerization, the type II receptor phosphorylates the GS box of the type I receptor, altering the type I receptor conformation and activating its kinase domain (reviewed in (184)).

Table 1. Demonstrated type I receptor interactions for *bona fide* Bmp ligands. Alternative names are listed in parentheses.

Receptor	Ligand	References
Alk1 (Acvrl1)	Bmp9 (Gdf2)	(23, 39, 133, 177, 183)
	Bmp10	(39, 133)
Alk2 (Acvr1)	Bmp6 (Vgr1)	(47)
	Bmp7 (OP-1)	(125, 206, 229)
	Bmp9 (Gdf2)	(177)
Alk3 (Bmpr1A)	Bmp2 (Bmp2A)	(2, 92, 95-96, 98, 145, 226, 229)
	Bmp4 (Bmp2B)	(73, 206, 226)
	Bmp5	(15)
	Bmp6 (Vgr1)	(47)
	Bmp7 (OP-1)	(206)
	Bmp10	(127)
	Gdf5 (Bmp14)	(50)
	Gdf6 (Bmp13)	(50)
	Gdf9	(217)
Alk6 (Bmpr1B)	Bmp2 (Bmp2A)	(227)
	Bmp4 (Bmp2B)	(206)
	Bmp6 (Vgr1)	(47)
	Bmp7 (OP-1)	(206, 229)
	Bmp10	(127)
	Gdf5 (Bmp14)	(50, 147)
	Gdf6 (Bmp13)	(50)
	Gdf9	(217)
	Gdf9B (Bmp15)	(136)

Table 2. Demonstrated type II receptor interactions for *bona fide* Bmp ligands. Alternative names are listed in parentheses.

Receptor	Ligand	References
Bmpr2	Bmp2 (Bmp2A)	(94, 114)
	Bmp4 (Bmp2B)	(169)
	Bmp6 (Vgr1)	(47)
	Bmp7 (OP-1)	(114, 169)
	Bmp9 (Gdf2)	(177, 183)
	Bmp10	(127)
	Gdf5 (Bmp14)	(50, 147)
	Gdf6 (Bmp13)	(50)
	Gdf9	(217)
	Gdf9B (Bmp15)	(136)
Actr2A (Acvr2A)	Bmp2 (Bmp2A)	(2, 225)
	Bmp4 (Bmp2B)	(225)
	Bmp6 (Vgr1)	(47)
	Bmp7 (OP-1)	(67, 125)
	Bmp9 (Gdf2)	(177)
	Gdf9	(217)
Actr2B (Acvr2B)	Bmp2 (Bmp2A)	(94)
	Bmp4 (Bmp2B)	(125)
	Bmp6 (Vgr1)	(47)
	Bmp9 (Gdf2)	(177)

Type I Bmp receptor activation leads to C-terminal phosphorylation of the Bmp-restricted Smad signaling intermediates (Smad1, Smad5, and Smad8). This helps to distinguish the effects of Bmp versus TGF-β/Activin activated type I receptors (Alk4, 5 and 7) which generally activate Smad2 and Smad3. However, it should be noted that, in certain instances, TGF-β can induce phosphorylation of Smad1/5/8 (36, 66) and Gdf9 can induce phosphorylation of Smad2/3 (128). A number of Smad-independent signaling responses have also been described. Among these, the MAP kinase family, PI3 kinase/AKT, PKC, and Rho-GTPases can be activated by Bmps in certain contexts (reviewed in (239)).

Beyond type I and II receptors, several Bmp co-receptors have been identified. These molecules modulate Bmp signaling by modifying Bmp ligand-receptor interactions (Table 3). For example, endoglin interacts with a variety of TGF-β family ligands, including Bmp2, Bmp7, and Bmp9, and is required for TGF-β to activate Smad1/5 (13, 19, 104, 177). Endoglin also enhances Bmp7 and Bmp9-dependent Smad responses (40, 178), although the mechanism by which this occurs is unknown.

Bmp-mediated regulation of gene expression

C-terminal phosphorylation of the receptor-activated (RA) Smad by the type I Bmp receptor leads to increased affinity of the RA-Smad for the co-activator Smad4 (reviewed in (184)). The RA-Smad/Smad4 complex translocates to the nucleus and controls target gene transcription by directly binding to Smad binding elements (SBE) or by interacting with other transcription factors (reviewed in (170)). Smad binding to DNA is relatively weak and often depends on additional DNA binding transcription factors. This allows for considerable crosstalk with a variety of signaling pathways. For example, Smad1 synergizes with the Wnt pathway member Lef1 (44) and the Notch intracellular domain (84).

Table 3. Co-receptors of Bmp signaling. Alternative names are listed in parentheses.

Co-receptor	Partner	References
Endoglin (CD105)	Bmp2 (Bmp2A)	(14)
	Bmp7 (OP-1)	(14)
	Bmp9 (Gdf2)	(39)
TGFβR3 (betaglycan)	Bmp2 (Bmp2A)	(93)
	Bmp4 (Bmp2B)	(93)
	Bmp7 (OP-1)	(93)
	Gdf5 (Bmp14)	(93)
RGMa	Bmp2 (Bmp2A)	(11, 69)
	Bmp4 (Bmp2B)	(11)
	Gdf7 (Bmp12)	(69)
RGMb (DRAGON)	Bmp2 (Bmp2A)	(69, 173)
	Bmp4 (Bmp2B)	(173)
	Gdf7 (Bmp12)	(69)
RGMc (Hemojuvelin)	Bmp2 (Bmp2A)	(10, 69, 99, 224, 232)
	Bmp4 (Bmp2B)	(224)
	Bmp6 (Vgr1)	(6, 224)
	Gdf7 (Bmp12)	(69)
Bambi (Nma)	Alk1 (Acvrl1)	(152)
	Alk3 (Bmpr1A)	(152)
	Alk6 (Bmpr1B)	(152)
	Actr2A (Acvr2A)	(152)
TrkC	Bmpr2	(89)
Ror2	Alk6 (Bmpr1B)	(174-175)

One of the best characterized Bmp target genes is *Inhibitor of differentiation 1 (Id1)* (135, 205). Id1 acts as a dominant negative regulator of transcription by heterodimerization with bHLH proteins (83). Thus, Bmp-induced expression of Id1 leads to an secondary network of Bmp-mediated gene regulation. Id1 has been shown to participate in several Bmp-induced cellular effects, including promoting proliferation, inhibiting differentiation, and, in some cases, inducing apoptosis (171, 186, 220).

In addition to direct transcriptional control, Smads have recently been shown to modulate gene expression through transcription and maturation of microRNAs (26, 41). Given that a single microRNA can regulate expression of hundreds of proteins (reviewed in (12, 182)), this allows Bmp signaling an even larger network of control than previously thought.

Regulation of Bmp signaling

Transduction of Bmp signaling is regulated at multiple levels. The expression of Bmp ligands may be controlled at long-range by *cis*-acting elements (162) or locally by altered mRNA stability (57). Most Bmp ligands are secreted as dimers in their active, cleaved form, the production of which can also be regulated in a tissue-specific manner (64). Once secreted, Bmp ligands are subject to interaction with a host of extracellular modulators (reviewed in (210)). Many of these act as inhibitors by sequestering ligands from interacting with receptors, reducing diffusion in the extracellular space, and/or promoting their uptake and degradation. Still others are capable of both promoting and inhibiting Bmp signals. Thus, the *in vivo* modulation of Bmp ligand activity is entirely dependent on context. Further, each individual modulator has varying affinity for Bmp ligands; for example, Noggin efficiently binds Bmp2, 4, 5, and 7 but does not inhibit Bmp9 or

10 at all (180). Additionally, the duration of Bmp signals can be regulated: activated receptor complexes and RA-Smads are targeted for proteosomal degradation by inhibitory Smads (I-Smads) and Smad ubiquitin ligases respectively (reviewed in (117)), thus establishing negative feedback.

Bmp signaling in vascular maintenance and disease

In addition to critical roles in vascular development, Bmp pathway components have been reported to be altered in human vascular disease. For example, several Bmp ligands have been shown to affect angiogenic response *in vitro* and some, such as Bmp2 and Bmp4, are up-regulated in endothelial cells (ECs) at sites of atherosclerosis and vascular injury (20, 32, 194). Bmp2 is also up-regulated in two experimental models of systemic hypertension (35). Moreover, exogenous administration of Bmp4 causes systemic hypertension and endothelial dysfunction in mice (132). These studies suggest that Bmp signaling might play a role in regulating vascular stability and/or function. Further evidence for this comes from the analysis of vascular phenotypes that are associated with genetic mutations in Bmp signaling components in mice and man (Table 4).

Of particular interest to us is the finding that a number of pathway components are functionally implicated in protection against Pulmonary Hypertension (PH) (Table 4). PH is a broad classification of diseases of varying etiology that is diagnostically defined as elevated pulmonary artery pressure. However, regardless of underlying cause, all forms of PH display the same structural remodeling of small, resistance-level arterioles of the lung periphery (187). This argues that defects in similar regulatory mechanisms might underlie the development of all forms of PH. Significant insight into these mechanisms has come from rare genetic forms of Pulmonary Arterial Hypertension (PAH) that are associated with

Table 4. Vascular phenotypes of Bmp mutations in humans and mice. All mutations are global unless noted otherwise. Human mutations are denoted by all capital letters. Embryonic lethality is indicated in parenthesis as day post coitum. PH: pulmonary hypertension, VSMC: vascular smooth muscle cell, EC: endothelial cell, HPAH: Heritable Pulmonary Arterial Hypertension, HHT: Hereditary Hemorrhagic Telangiectasia, SMC: smooth muscle cell, JP: Juvenile Polyposis

Genetic Modification	Het/Homozygous	Vascular Phenotype	Survival	References
Bmp2 null	Heterozygous	Susceptible to hypoxic PH	Viable	(3)
Bmp4 null-LacZ	Heterozygous	Less severe hypoxic PH, impaired vascular remodeling	Viable	(54)
Bmpr2 null	Heterozygous	Susceptible to PH, defective vascular remodeling, abnormal vascular tone	Viable	(17, 116, 193)
Bmpr2 hypomorph (ΔEx2)	Heterozygous	Susceptible to hypoxic PH; endothelial dysfunction and abnormal vascular tone	Viable	(55)
Bmpr2 knockdown	90% knockdown by RNAi	Hemorrhage; vascular dysplasia; impaired VSMC recruitment	Viable	(113)
Bmpr2 conditional	Pulmonary EC	Spontaneous PH, vascular inflammation	Viable	(79)
BMPR2 (mis-sense, non-sense)	Heterozygous	HPAH, HPAH with HHT	Viable	(121-122, 168)
Alk1 null	Homozygous	Angiogenesis defects, impaired VSMC recruitment	Lethal (E10.5)	(151, 214)
	Heterozygous	Models HHT	Viable	(195)
Alk1 conditional	EC-specific	Vascular dysplasia	Viable	(159)
ALK1(mis-sense, non-sense)	Heterozygous	HHT2, HPAH with and without HHT2	Viable	(58, 90, 122)

Table 4, continued.

Alk3 conditional	Mesoderm deletion	Hemorrhage, cardiac defects, impaired VSMC recruitment	Lethal (E10.5)	(157)
	SMC (embryo)	Cardiac defects, hemorrhage, impaired vascular remodeling	Lethal (E11.5)	(48)
	SMC (adult)	Impaired vascular remodeling	Viable	(49)
Endoglin null	Homozygous	Angiogenesis defects	Lethal (E10.5)	(7)
	Heterozygous	Models HHT, spontaneous PH, abnormal vascular tone	Viable	(21, 208)
ENDOGLIN (mis-sense, non-sense)	Heterozygous	HHT1, HPAH with HHT1	Viable	(71, 122, 129)
Smad1 null	Homozygous	Defects in fusion of the chorioallantoic membrane and (minor) yolk sac angiogenesis	Lethal (E9.5)	(105)
SMAD1 (mis-sense)	Heterozygous	HHT	Viable	(108)
Smad4 conditional	EC	Cardiac and angiogenesis defects , VSMC recruitment	Lethal (E10.5)	(102)
SMAD4 (mis-sense, non-sense)	Heterozygous	HHT (with and without JP)	Viable	(59-60)
Smad5 null	Homozygous	Cardiac and angiogenesis defects	Lethal (E9.5)	(28-29, 234)
Smad6 null	Homozygous	Cardiac defects, vascular calcification, systemic hypertension	Some viable	(61)
Smad8 null-LacZ	Homozygous	Spontaneous pulmonary vascular remodeling	Viable	(82)
SMAD8 (non-sense)	Heterozygous	HPAH	Viable	(185)
Tak1 null	Homozygous	Angiogenesis/cardiac defects	Lethal (E10.5)	(85)

mutations in multiple Bmp pathway genes. More than 70% of patients with Heritable PAH (HPAH) and approximately 20% of Idiopathic PAH patients inherit heterozygous germline mutations in *BMPR2* (124). Additionally, there is one case report of HPAH due to mutation in *SMAD8* (185) and some patients with Hereditary Hemorrhagic Telangiectasia (HHT), which is linked to mutations in *ALK1* and *ENG*, develop PAH (58, 71, 90, 122, 129). Collectively, these findings indicate that Bmp signaling exerts critical protective effects on the pulmonary vasculature. However, *in vitro* studies have been insufficient in determining the molecular mechanisms by which Bmps maintain pulmonary vascular homeostasis. For example, Bmp4 inhibits proliferation and promotes apoptosis in cultured proximal pulmonary artery VSMCs (100, 202), but promotes proliferation and inhibits apoptosis in VSMCs derived from more peripheral vessels (235). Moreover, Bmp4 promotes proliferation in early passage mouse proximal pulmonary VSMCs but has the opposite effect on the same cells at late passage (54). Thus, the context-specific effects of Bmps must be evaluated *in vivo*, which is a substantial hurdle due to a lack of reliable reagents.

That being said, considerable functional evidence for these Bmp pathway components in pulmonary vascular homeostasis has come from genetic studies in mice. Even with the functional strength of these studies, however, it is still not immediately discernable how Bmps exert their protective effects. For instance, while both *Eng* and *Smad8* mutant mice develop spontaneous pulmonary vascular remodeling (82, 208), heterozygous *Bmpr2 null* (*Bmpr2*$^{+/-}$) mice do not, and, if anything, display impaired vascular remodeling in response to hypoxia (17). Further, *Bmpr2*$^{+/-}$ mice do not develop PH without exposure to additional stimuli such as serotonin or inflammatory stress (17, 116, 193). The role of inflammation in the development of PH may be of significance as two other mouse models of impaired Bmpr2-dependent signaling, both of which lead to spontaneous PH, exhibit local pulmonary vascular inflammation (79, 219). This is consistent with the

observation that the pulmonary vascular lesions of patients with PAH often contain infiltrating mononuclear cells and lymphocytes (reviewed in (72)).

In addition to anti-inflammatory roles, Bmp signaling has been shown to promote vascular stability. Using RNAi in the germline to reduce Bmpr2 expression by 90% leads to massive intestinal hemorrhage, vascular dysplasia, and impaired VSMC recruitment to pulmonary vessels (113). This phenotype is similar to the defects observed in *Alk1* and *Eng* mutant mice (7, 151, 214), suggesting that Bmpr2, Alk1, and Endoglin coordinately regulate vascular stability *in vivo*. Each of these is dominantly expressed in the endothelium (8, 55, 166, 181, 199, 208), and EC-specific deletion of *Bmpr2* is sufficient to cause spontaneous PH in some mice (79). This indicates that the endothelial compartment might be the primary site of Bmp signaling in pulmonary vascular homeostasis.

Several Bmp ligands (BMP4, BMP6, and BMP9) are found at biologically active concentrations in human serum (38, 77), which allows for direct access to affect EC function. The endothelium plays a major role in regulating angiogenesis, and Bmp signaling has been shown to modulate this process. For example, Bmp4 and Bmp6 have pro-angiogenic effects on cultured ECs (75, 167). On the other hand, Bmp9 exerts potent anti-angiogenic effects (38, 177). This finding might be of significance, as recent evidence shows that Bmp9 is a ligand for Bmpr2, Alk1, and endoglin (23, 39, 133, 177, 183) and therefore may provide a link between PAH and HHT. However, the mechanism that determines the net pro- vs. anti-angiogenic effects of circulating Bmp ligands is unknown.

In addition to angiogenesis, ECs also play a major role in regulating vascular tone through the release of vasodilators (78). Bmp2 and Bmp4 have been shown to impair nitric oxide (NO)-dependent vasodilation of aortas and carotid arteries (33-34, 132) by causing increased production of reactive oxygen species (ROS). However, this action might be

vascular bed-specific since Bmp4 does not have this effect on pulmonary arteries (34). Additionally, endoglin promotes production of NO through endothelial NO synthase (eNOS) (87, 176, 207), and *Eng* mutant mice display defects in vascular tone that are mediated by impaired eNOS function due to increased ROS (16, 208).

In conclusion, the functional roles of Bmp signaling in pulmonary vascular homeostasis remain unclear. However, genetic studies in mice indicate that different components of the Bmp signaling pathway promote vascular stability, regulate vascular reactivity, EC function, and inflammation *in vivo*. Future studies are required to determine how these diverse effects coordinate vascular homeostasis, and when perturbed, lead to disease.

Part II. Experimental models of pulmonary hypertension

The characteristic pathology of human PAH involves structural remodeling of peripheral pulmonary arterioles, including media hypertrophy, neointimal lesions, adventitial thickening, and obliterative plexiform lesions (reviewed in (187)). These events serve to increase pulmonary vascular resistance, thereby placing strain on the right side of the heart, which leads to right ventricular hypertrophy and eventual right-sided heart failure. This section will discuss similarities and differences between human PAH and the experimental models used to study it.

Some genetic studies in mice have demonstrated the development of spontaneous PH. Most studies, however, have required additional stimuli to cause disease. The stimulus by which this occurs, however, can be vastly different. As shown in Table 5, several

experimental models, ranging from chemical, mechanical, and environmental, exist to study PH. Each model has its own strengths and weaknesses. For example, all models develop increased muscularization of peripheral pulmonary vessels, but most do not allow for direct genetic manipulation in the intact organism.

Table 5. Established experimental models of pulmonary hypertension.

Species	**Model**
Mice	Chronic hypoxia Serotonin infusion Inflammatory stress Pneumonectomy Schistosomiasis Genetic modification
Rats	Chronic hypoxia Monocrotaline Pneumonectomy Fawn-Hooded genetic background
Sheep	Air embolism Chronic hypoxia/high altitude Ligation of ductus arteriosus
Cows	Chronic hypoxia/high altitude
Pigs	Hypoxia/high altitude

For the studies in this dissertation, we have chosen the well-established mouse model of chronic hypoxia to induce PH. In response to hypoxia, mice develop increased

pulmonary artery pressure, right ventricular hypertrophy, and increased peripheral muscularization (reviewed in (196)). The true strength of this model comes when chronic hypoxia is combined with genetic manipulation in mice, thus allowing for evaluation of function *in vivo*. However, this model is criticized because hypoxic mice do not develop the severe obliterative lesions seen in human PAH (218). While we agree this is an obvious limitation, findings using the chronic hypoxia model provide insight into how the Bmp signaling pathway can modify pulmonary vascular function. Therefore, even though these mice do not develop severe vascular remodeling, they show defects in pulmonary vascular function that may also occur in the early course of human disease. Further, studies using the chronic hypoxia model are also relevant to the analysis of alveolar hypoxia, which plays a critical role in promoting PH associated with chronic lung disease (reviewed in (163)). Since chronic lung disease is the most common cause of PH worldwide, findings using the chronic hypoxia model have important clinical implications for our understanding of an important human disease. That being said, future studies, proposed in Chapter 5, will attempt to develop additional models of PH that are able to utilize mouse genetics while more closely mimicking human PAH.

Part III. Functional evaluation of Bmp signaling in hypoxic pulmonary hypertension

Even though loss-of-function mutations in *BMPR2* are linked to HPAH in humans (188), genetic studies in mice exposed to chronic hypoxia have revealed unexpected roles for Bmp signaling in the pulmonary vasculature. In fact, the evidence suggests multiple Bmp pathways exist in the lung, with some signaling events protecting against hypoxic PH

while others promote hypoxic PH development. This section will discuss these findings in order to provide a basis for the studies presented in this dissertation.

Previous studies have demonstrated that *Bmpr2*$^{+/-}$ mice are not susceptible to hypoxic PH and, if anything, display impaired hypoxia-induced vascular remodeling (17, 116). However, when *Bmpr2*$^{+/-}$ mice are subjected to chronic hypoxia combined with infusion of serotonin, they develop worse PH than wild type controls (116). Further, main pulmonary artery sections from *Bmpr2*$^{+/-}$ mice exhibit increased contractile responses to serotonin *ex vivo* (116). These findings suggest that abnormal vascular tone may exacerbate the defects associated with *Bmpr2* haploinsufficiency to cause PH in these mice.

In contrast, David Frank, a graduate from our lab, found that another *Bmpr2* mutant mouse line (*Bmpr2*$^{\Delta Ex2/+}$) develops PH in response to hypoxia alone (55). *Bmpr2*$^{\Delta Ex2/+}$ mice are different from *Bmpr2*$^{+/-}$ mice in that instead of a null allele they carry a hypomorphic allele of *Bmpr2 (45)* . Like *Bmpr2*$^{+/-}$ mice, though, *Bmpr2*$^{\Delta Ex2/+}$ mice do not exhibit increased hypoxic pulmonary vascular remodeling over wild type controls. Interestingly, *Bmpr2*$^{\Delta Ex2/+}$ mice display impaired hypoxic induction of eNOS expression, which has been shown to play a critical role in the maintenance of low pulmonary vascular resistance (51, 197-198). This suggests that impaired eNOS expression might participate in the development of hypoxic PH in these mice. However, taken together with increased vasoconstriction in *Bmpr2*$^{+/-}$ mice (116), this also raises the possibility that defective regulation of vascular tone may be a direct result of impaired Bmp signaling. The studies described in Chapter 2 were designed to address this question directly.

In Chapter 2, we provide the first evidence for Bmpr2-dependent signaling in the direct regulation of vascular tone. Arteriographic analysis of isolated intrapulmonary arteries shows that *Bmpr2*$^{\Delta Ex2/+}$ mice suffer defects in vascular reactivity, including severely

impaired NO-dependent vasodilation. Further, Bmpr2-dependent signaling directly regulates the expression and activity of eNOS. These findings, which are now published, suggest that the primary defect in *Bmpr2*$^{\Delta Ex2/+}$ mice might be reduced Bmp-mediated regulation of eNOS. They also raise the question as to which ligand is responsible for this signaling *in vivo*.

Pulmonary *Bmp2* and *Bmp4* expression are selectively up-regulated in mice exposed to chronic hypoxia (54), indicating that these ligands might signal through Bmpr2 in the protective response to hypoxia. Surprisingly, though, a previous study from our lab indicated that Bmp4 promotes the development of hypoxic PH (54). In contrast, the studies described in Chapter 3, which are now published, illustrate that Bmp2 exerts protective effects in the pulmonary vascular response to hypoxia. Here, we show that, similar to *Bmpr2*$^{\Delta Ex2/+}$ mice, *Bmp2* deficient (*Bmp2*$^{+/-}$) mice are susceptible to hypoxic PH. Further, *Bmp2*$^{+/-}$ mice display dysregulation of eNOS expression and activity while *Bmp4* deficient mice do not. Collectively, these findings indicate that Bmp2 and Bmp4 exert opposing effects in the development of hypoxic PH, and that Bmp2 is the predominant ligand for Bmpr2 *in vivo*. However, it also raises the question of the how Bmp4 promotes hypoxic PH.

Bmp4 deficient mice display impaired hypoxic pulmonary vascular remodeling and are partially protected from the development of hypoxic PH (54). Given the contrast between this phenotype and that of *Bmp2* and *Bmpr2*$^{\Delta Ex2/+}$ mutant mice, pulmonary Bmp4 likely signals through Actr2a and Actr2b *in vivo*; however, there are no published data regarding their expression in the intact pulmonary vasculature. Alk3 is likely the major type I receptor for Bmp4 in pulmonary VSMCs, given that, like *Bmp4* deficiency (54), patchy deletion of *Alk3* in VSMCs impairs hypoxia-induced pulmonary vascular remodeling (49). *Bmp4* deficient mice have impaired hypoxia-induced VSMC proliferation (54) *in vivo*,

suggesting that Bmp4 likely promotes hypoxic pulmonary vascular remodeling through proliferation of VSMCs. However, the downstream signaling events by which Bmp4 exerts this effect are largely unknown. One possible mediator is Id1, the expression of which is selectively reduced in pulmonary VSMCs of *Bmp4* deficient mice (54). The studies described in Chapter 4, which have been submitted for publication, were designed to examine this directly.

Because *Id1* is a well-characterized Bmp target gene, its expression has been used as a downstream readout of active Bmp signaling in multiple systems, including the study of PH (54, 68, 140, 203, 233). Yet, little is known about the functional role Id1 plays in the events leading to the development of PH. In Chapter 4, we use a genetics-based approach to show that Id1 expression is not essential for hypoxia-induced pulmonary vascular remodeling or PH; however, loss of Id1 expression leads to a selective increase in expression of Id3 in pulmonary VSMCs. Given the known functional redundancy between Id1 and Id3 *in vivo* (53, 119), we suggest that Id3 compensates for loss of Id1 expression in the pulmonary vasculature of *Id1 null* mice.

Collectively, these studies provide functional insight into Bmp signaling in pulmonary vascular homeostasis. They demonstrate a novel role branch of the Bmp pathway that directly regulates pulmonary vascular tone and add to an understanding of human PAH by illustrating distinct downstream events associated with Bmp2 versus Bmp4 signaling *in vivo*. Additionally, our studies provide potential targets in the treatment of human PAH. Future studies will build upon these findings to further examine the spatial regulation of Bmp2 versus Bmp4 signaling, attempt to rescue Bmp signaling defects by eNOS overexpression *in vivo*, and evaluate the potential role of dominant negative *BMPR2* mutations in HPAH pathogenesis.

CHAPTER II

BMPR2$^{\Delta Ex2/+}$ MUTANT MICE DISPLAY DEFECTS IN VASCULAR REACTIVITY

Introduction

Genetic studies have shown that most patients with HPAH have inherited heterozygous mutations at the *BMPR2* locus (123). Most of these mutations encode premature termination codons or are predicted to disrupt critical functional domains of the mature protein (123). This implies that defective BMPR2-dependent signaling predisposes individuals to the development of PH. Yet the protective role that BMPR2 normally plays in the pulmonary vasculature has yet to be firmly established.

One approach to answer these questions has been to study the pulmonary vasculature of mice that carry mutations at the *Bmpr2* locus. Heterozygous *Bmpr2* knock-out (*Bmpr2*$^{+/-}$) mice display a mild increase in pulmonary vascular resistance (17) and increased susceptibility to PH in response to inflammatory stress or a combination of hypoxia and serotonin infusion (116, 193). In support of this, our lab has shown that another *Bmpr2* mutant mouse (*Bmpr2*$^{\Delta Ex2/+}$), which carries a partially-inactivating version of *Bmpr2* (45), develops increased hypoxic PH. However, neither of these *Bmpr2* mutant mice develops increased pulmonary vascular remodeling (17, 55). This indicates that impaired Bmpr2-dependent signaling might promote events other than increased pulmonary vascular remodeling that lead to hypoxic PH. Intriguingly, *Bmpr2*$^{\Delta Ex2/+}$ mutant mice display impaired hypoxia-induced expression of pulmonary eNOS (55), an enzyme that is critically important in maintaining low pulmonary vascular resistance (51, 197-198).

These findings suggest that defective regulation of pulmonary vascular reactivity might underlie the development of hypoxic PH in *Bmpr2*$^{\Delta Ex2/+}$ mutant mice. However, the ability of Bmp signaling to directly regulate eNOS expression, and the functional role that Bmpr2 plays in this regulation, are unknown.

To address these questions, we evaluated the Bmp-mediated regulation of eNOS in the pulmonary vasculature. We show that Bmp activation regulates eNOS expression and activity in a Bmpr2-dependent manner. Furthermore, the *Bmpr2*$^{\Delta Ex2/+}$ mutation is associated with increased vasoconstriction and severe defects in nitric oxide (NO)-mediated vasodilation. These findings indicate that defective Bmp-mediated regulation of pulmonary vascular tone could play a role in the pathogenesis of human PH. I performed the studies outlined in this chapter, which were, in part, published in a larger study on *Bmpr2*$^{\Delta Ex2/+}$ mutant mice (55).

Methods

Mouse lines

Mutant mice carrying a partially inactivating mutation at the *Bmpr2* locus (*Bmpr2*$^{\Delta Ex2/+}$) were a gift from Karen Lyons (45). *Bmpr2*$^{\Delta Ex2/+}$ mutant mice were maintained on a Balb/cJ x 129SvJ background. H-2Kb-tsA58 transgenic mice (Immortomouse) (86), on a C57Bl/10 background, and wild type ICR mice were purchased from Charles River. *eNOS null* mutant mice were purchased from Jackson Laboratories. Because some pure background *eNOS null* mutant mice have severe cardiovascular defects (70, 106, 111, 131), *Bmpr2*$^{\Delta Ex2/+}$;*eNOS null* double mutant mice were generated on a mixed Balb/cJ x 129SvJ x C57Bl/6 genetic

background. *Bmpr2*$^{\Delta Ex2/+}$*eNOS null* double mutant mice are born at near-expected Mendelian ratios and do not differ in body weight from wild type mice (data not shown). Genotyping was performed on ear clip DNA using the primers and conditions described in Table 6.

Intrapulmonary artery tree isolation

Intrapulmonary artery (IPA) trees were carefully trimmed free from surrounding tissue of the left lung by tracing the main pulmonary artery from the hilum of whole lungs under a dissecting microscope (SZ61, Olympus). Isolation was performed in cold PBS (Gibco) and completed within 30 minutes post-mortem in order to preserve tissue integrity. Isolated IPA trees contain continuous first, second, and third generation (approximate diameter of 75 μm) vessels beginning at the hilum. These preparations, which contain ECs, VSMCs, and adventitia, yield ~100 μg total protein and provide a means for specific analysis of protein content in the arterial vasculature of the lung. For Bmp-response studies, freshly isolated IPAs were cultured in DMEM with 10% FBS and treated ± 50 ng/ml recombinant Bmp2 or Bmp4 (R&D systems) for 18 hours prior to lysis.

Isolation and treatment of pulmonary endothelial cells

The isolation of conditionally immortalized pulmonary microvascular ECs (PECs) has been described previously (54). In order to obtain wild type and *Bmpr2*$^{\Delta Ex2/+}$ PECs, *Bmpr2*$^{\Delta Ex2/+}$ mutant mice were crossed with the Immortomouse (86). The Immortomouse is a transgenic mouse strain that carries a temperature sensitive mutant of the SV40 large T antigen. When cultured at 33°C, the SV40 large T antigen protein is in an active

Table 6. Genotyping PCR primers for mouse lines utilized. Primer sequence, annealing temperature, and amplicon size are listed. All PCR reactions were performed in a MJ Mini Gradient thermalcycler (Bio-Rad).

Gene	Forward Primer	Reverse Primer	Annealing Temp (Celsius)	Product Size
Bmp2 (wild type allele)	AGCATGAACCCTCATGT CTTGG	GTGACATTAGGCTGC TGTAGCA	62	322 bp
Bmp2 (mutant allele)	AGCATGAACCCTCATGT CTTGG	GAGACTAGTGAGACG TGCTACT	62	367 bp
5' Bmp2 BAC LacZ (transgene)	GTTGCAGTGCACGGCGA TACACTTGCTG	GCCACTGGTGTGGGC CATAATTCATTCGC	58	350 bp
Bmp4^{LacZ} (knock-in)	GTTGCAGTGCACGGCGA TACACTTGCTG	GCCACTGGTGTGGGC CATAATTCATTCGC	58	350 bp
Bmpr2 (wild type allele)	CCATGCTCTTTTGAAGATG G	GGCCGCTTTTCTGGATT CATC	60	1000 bp
Bmpr2 (mutant allele)	CCATGCTCTTTTGAAGATG G	GGCCGCTTTTCTGGATT CATC	60	700 bp
eNOS (wild type allele)	ATTTCCTGTCCCCTGCCTTC	GGCCAGTCTCAGAGCCA TAC	65	442 bp
eNOS (mutant allele)	ATTTCCTGTCCCCTGCCTTC	TGGCTACCCGTGATATT GCT	65	500 bp
H-2Kb-tsA58 (transgene)	AGCGCTTGTGTCGCCAT TGTATTC	GTCACACCACAGAAG TAAGGTTCC	58	1000 bp
Id1 (wild type allele)	CCTCAGCGACACAAGATGC GATCG	GGTTGCTTTTGAACGTT CTGAACC	66	850 bp
Id1 (mutant allele)	CCTCAGCGACACAAGATGC GATCG	GCACGAGACTAGTGAGA CGTG	66	650 bp

conformation, binding to p53 and allowing for cellular transformation. However, under non-permissive conditions (culture at 37°C), conformation of the gene product changes and it no longer binds to p53 or immortalizes the cell. Importantly, we have characterized PECs extensively: These cells behave like differentiated ECs – cobblestone appearance, capillary structures in 3D culture, expression of eNOS and CD31 – when grown under non-permissive conditions (3, 54-55). For normal culturing, PECs were maintained in EGM-2 MV (Lonza) supplemented with 40 units/ml IFN-Ɣ (Peprotech) at 33°C. For use in experiments, PECs were shifted to 37°C for at least 72 hours in EGM-2 MV without IFN-Ɣ.

For Bmp-response studies, PECs were treated with 10 ng/ml recombinant Bmp2 (R&D Systems) under serum-free conditions for up to 4 hours before lysis to evaluate protein expression by western blot. For analysis of NOS activity, PECs were cultured in basal EBM-2 (Clonetics) supplemented with 2.5 mM ascorbic acid (Sigma) and [H^3]-arginine to citrulline conversion evaluated using a NOS Activity Assay Kit (Cayman). For this, PECs were exposed to 160 nM [H^3]-arginine (NOS substrate) for the indicated times. Cells were lysed and mixed with equilibrated resin, then [H^3]-citrulline (NOS by-product) eluate was collected and quantified by liquid scintillography. Pre-treatment with 1 mM L-NAME for 45 minutes served as a control for NOS-specific accumulation of [H^3]-citrulline. Assays were performed in triplicate and results expressed as CPM/μg protein.

Western blot

Cell and tissue lysis was carried out in Triton-X100 lysis buffer (25 mM HEPES pH 7.4, 150 mM NaCl, 5 mM EDTA, 1% Triton X-100, 10% glycerol, 5 mM AEBSF, 2 mM NaOV, 50 mM NaF) on ice for 15 minutes at room temperature followed by clarification at 14k rpm in 4°C. Concentration of the clarified supernatant was then determined by the DC Protein

Assay (Bio-Rad). Equal quantities of total protein were denatured for 10 minutes at 100°C in sample reducing buffer (50 mM Tris pH 6.8, 10% glycerol, 2 mM EDTA, 2% SDS, 144 mM β-mercaptoethanol, 0.008% bromophenol blue) and resolved using SDS-PAGE (Bio-Rad) in running buffer (2.5 mM Tris, 200 mM Glycine, 3.5 mM SDS) followed by transfer to PVDF membrane (Bio-Rad) in transfer buffer (2.5 mM Tris, 200 mM Glycine, 3.5 mM SDS). After blocking for 1 hour in 10% milk in TBST (25 mM Tris pH 8.0, 100 mM NaCl, 0.1% Tween-20) with gentle rocking**,** primary antibodies were applied in either 5% milk in TBST or 5% BSA in TBST (when detecting phospho-specific isoforms) overnight at 4°C. The next day, after washing three times for 10 minutes each in TBST, HRP-conjugated secondary antibodies raised against the host species of the primary antibody were applied in 5% milk in TBST at room temperature for 30 minutes with gentle rocking. This was followed by three washes in TBST for 10 minutes each. Western blots were visualized by ECL (Perkin Elmer), exposed to X-ray film (HPI), and processed by a film developer (Merry X-Ray Corporation). Blots that were re-probed were stripped in Restore Western Blot Stripping Buffer (Pierce) for 10 minutes at room temperature with gentle rocking, followed by 3 TBST washes. Stripped membranes were then subjected to the western blot protocol detailed above. Primary and secondary antibodies utilized are detailed in Table 7.

IPA pressure arteriography

Intact IPA segments were carefully trimmed free from surrounding tissue of the left lung by tracing the main pulmonary artery from the hilum of whole lungs under a dissecting microscope (SMZ 1500, Nikon). Vessel isolation was performed under ice-cold modified Krebs buffer: 118 mM NaCl, 25 mM $NaHCO_3$, 4.7 mM KCl, 0.9 mM $MgSO_4$-7(H_20), 2.5 mM $CaCl_2$-2(H_20), 1 mM KH_2PO_4, and 11.1 mM glucose equilibrated with 5% CO_2 balanced to

Table 7. Antibodies utilized for western blot analyses.

Antigen	Manufacturer	Species	Dilution
β-actin	Sigma (A5316)	Mouse	1:5000
Bmpr2	Clone 18 BD (612292)	Mouse	1:250
Bmpr2	ASQ (In-house)	Rabbit	1:250
eNOS	BD (610296)	Mouse	1:1000
eNOS (pSer1177)	Cell Signaling (9571)	Rabbit	1:500
Flk-1 (Vegfr2)	Santa Cruz (sc-504)	Rabbit	1:250
Id1	BioCheck (BCH-1/195-14)	Rabbit	1:250
Id2	Santa Cruz (sc-489)	Rabbit	1:250
Id3	BioCheck (BCH-1/17-3)	Rabbit	1:250
IgG (Goat)	Santa Cruz (sc-2020)	Donkey	1:2000
IgG (Rabbit)	Cell Signaling (7074)	Goat	1:2000
IgG (Mouse)	KPL (04-18-06)	Goat	1:2000
Smad1	Santa Cruz (sc-7965)	Mouse	1:250
pSmad1/5/8	Cell Signaling (9511)	Rabbit	1:1000
VASP (pSer239)	Cell Signaling (3114)	Rabbit	1:500
VE-cadherin	Santa Cruz (sc-6458)	Goat	1:250

room air to maintain a constant pH of 7.35. Isolated vascular segments were transferred to a custom arteriography chamber (University of Vermont, Instrument and Model Facility, Burlington, VT) with two micrometer-controlled positioning arms holding glass micropipettes in a 5 mL perfusion bath. All studies were performed using invariant, second branch, second and third generation IPAs with resting external diameters of 75-100 μm. These were mounted on glass micropipettes at proximal and distal ends and secured using single filaments of 10-0 braided nylon suture. Side branches from the mounted vessel were individually tied off. The arteriography chamber was transferred to the stage of an inverted microscope (Motic AE-21, Richmond, BC, Canada) equipped with a video camera and computer-based monitoring system. The vessel image was captured and processed for continuous measurement of the lumen diameter using video dimension analysis software (IonOptix, Milton, MA). The perfusion chamber was initially connected to a 1 L non-recirculating reservoir for superfusion of cannulated, pressurized IPAs. A second, 100 mL recirculating reservoir was used for all drug studies. All studies were performed in Krebs buffer pre-warmed to 37°C.

Experimental PH

Mice were exposed to normoxia or 10% normobaric oxygen for defined time periods as described previously (55). At completion, 12-week-old mice were anesthetized with 375 mg/kg Avertin (Sigma), ventilated by tracheotomy, and opened at the chest. Right ventricular systolic pressure (RVSP) and diastolic pressures (RVDP), and left ventricular diastolic pressure (LVDP) were measured by direct cardiac puncture using a pressure gauge needle as described previously (55). Pressure wave forms were visualized and measured in mmHg using a Digi-Med Blood Pressure Analyzer with Gould printer. Mean RVSP was

calculated from ≥15 seconds of stable measurement with heart rate above 300 beats/minute. Right and left ventricular + septal (RV/LV+S) dry weights were determined to evaluate right ventricular hypertrophy as described previously (55). Hematocrit was measured using a Drummond Scientific Company micro-hematocrit centrifuge according to manufacturer's instructions. All experimental methods were approved by Vanderbilt University's Institutional Animal Care and Use Committee.

Histological evaluation of pulmonary vascular remodeling

After hemodynamic analysis, lungs were inflated and fixed overnight in 10% formalin in PBS before mounting in paraffin. With the observer blinded to genotype and treatment condition, the percentage of muscularized peripheral vessels in the pulmonary vasculature was assessed by two color immunofluorescence staining for α-smooth muscle actin (α-SMA) and von Willebrand factor (vWF) as described previously (54-55). Vessels were identified by vWF staining and considered non-muscularized or muscularized when surrounding α-SMA-positive VSMCs were absent/present, respectively.

Immunoprecipitation

Immunoprecipitation (IP) for Bmpr2 was carried out on ~100 μg total protein obtained from wild type and *Bmpr2*$^{\Delta Ex2/+}$ IPA and PEC preparations. Lysates were pre-cleared with Protein A/G conjugated sepharose (Santa Cruz SC-2003), then specific IP was achieved with 2 μg anti-Bmpr2 mouse monoclonal antibody (BD #612292) overnight at 4°C. The next day, 40 μl Protein A/G conjugated sepharose was added for 1 hour at 4°C with rotation, then samples were pelleted at 14k rpm at 4°C, aspirated, and washed in Triton X-

100 lysis buffer. This washing procedure was repeated for a total of five washes. Samples were then subjected to further analysis by glycosidase treatment or western blot.

Endoglycosidase treatment

Cleavage of specific asparagine-linked carbohydrate modifications by endoglycosidases allows for evaluation of precise progress in the trafficking of proteins (56). While PNGase F cleaves all asparagine-linked carbohydrate residues, Endoglycosidase H (EndoH) cleaves only high mannose and hybrid structures which are modified by enzymes resident in the *medial*-Golgi complex. Therefore, a glycoprotein that is EndoH-sensitive has not been trafficked beyond the *cis*-Golgi. In order to analyze the trafficking of Bmpr2, IP was performed as described above, samples were resuspended in 9 µl water, and subjected to treatment with endoglycosidase H (NEB #P0702) or PNGase F (NEB #P0704). Digestion was performed in 20 µl total volume using 2000 units EndoH or 1000 units PNGase F for 2 hours at 37°C as per manufacturer's protocol. Samples were then denatured in reducing buffer at 100°C for 10 minutes and analyzed by western blot.

Statistical analyses

Statistical analyses were performed using GraphPad Prism 5 with two-tailed t-test for pair-wise comparisons and one-way ANOVA for multiple, between group comparisons using Bonferroni correction for post-hoc, pair-wise comparisons. The minimal level of significance was set at $p<0.05$.

Results

Bmp signaling regulates eNOS expression and activity via Bmpr2

To explore the regulation of eNOS by Bmp signaling in the pulmonary vasculature, we developed a novel assay in which isolated intrapulmonary artery (IPA) trees were treated *ex vivo* with recombinant Bmp2. IPA preparations were carefully isolated from lung parenchyma and airways under a dissecting microscope (Figure 2A). IPAs cultured up to 18 hours remain viable and express the EC markers eNOS, VE-cadherin, and Vegfr2 (Figure 2B). Upon treatment with Bmp2, there is a dose-dependent increase of eNOS and phosphorylated-Smad1/5/8 (pSmad1/5/8) expression in wild type IPAs (Figure 2C), indicating that Bmp pathway activation leads to increased expression of pulmonary eNOS. To explore Bmp2-dependent regulation of eNOS further, we evaluated Bmp2-dependent responses in cultured pulmonary microvascular ECs (PECs) from the Immortomouse. Similar to IPAs, PECs show a rapid induction of eNOS and pSmad1/5/8 in response to Bmp2 (Figure 2D). To evaluate the role of Bmpr2 in mediating these effects, we isolated PECs from *Bmpr2*$^{\Delta Ex2/+}$ Immortomice. *Bmpr2*$^{\Delta Ex2/+}$ PECs display impaired induction of pSmad1/5/8 in response to Bmp2 (Figure 2E, F). Furthermore, NOS activity in wild type PECs is significantly increased following 4-hour treatment with Bmp2, but this effect is absent in *Bmpr2*$^{\Delta Ex2/+}$ PECs (Figure 2G). The increase in NOS activity following Bmp2 treatment is blocked by the NOS inhibitor L-NAME (Figure 2G), indicating that this response reflects Bmp2-induced changes in NOS activity. Therefore, Bmp signaling increases eNOS expression and NOS activity in pulmonary ECs via Bmpr2-dependent effects.

Figure 2. Bmp-mediated regulation of eNOS expression and function. A: Isolated IPA tree from the left lobe of a freshly harvested wild type lung. Preparations contain 1st to 7th branches of the main intrapulmonary artery through the subsequent 2nd and 3rd generation branchpoint. **B:** Expression of EC markers Vegfr2, eNOS, and VE-cadherin compared to β-actin as assessed by western blot in wild type IPAs after culture for 18 hours. Lanes 1 and 2 are from two separate IPA preparations. **C:** eNOS and phosphorylated-Smad1/5/8 (pSmad1/5/8) in wild type IPAs treated with Bmp2 for 18 hours. **D:** Western blot for eNOS and pSmad1/5/8 in PECs treated with 10 ng/ml Bmp2 over 4 hours compared to β-actin loading control. **E, F:** Bmp2-mediated phosphorylation of Smad1/5/8 (pSmad1/5/8) in wild type and *Bmpr2*$^{\Delta Ex2/+}$ PECs determined by western blot (E) and quantified by densitometry relative to β-actin loading control (F). **G:** Bmp2-mediated effect on NOS activity in intact wild type and *Bmpr2*$^{\Delta Ex2/+}$ PECs assessed using a radio-labeled arginine conversion assay +/- treatment with 10 ng/ml Bmp2 for 4 hours and +/- NOS inhibition with 1 mM L-NAME. Assay was performed in triplicate and repeated with similar results. Results from one experiment are shown. Data are expressed as mean +/- SEM. One-way ANOVA with Bonferroni correction, $p<0.05$: **a**, vs. untreated control; **b**, vs. wild type 4 hour Bmp2.

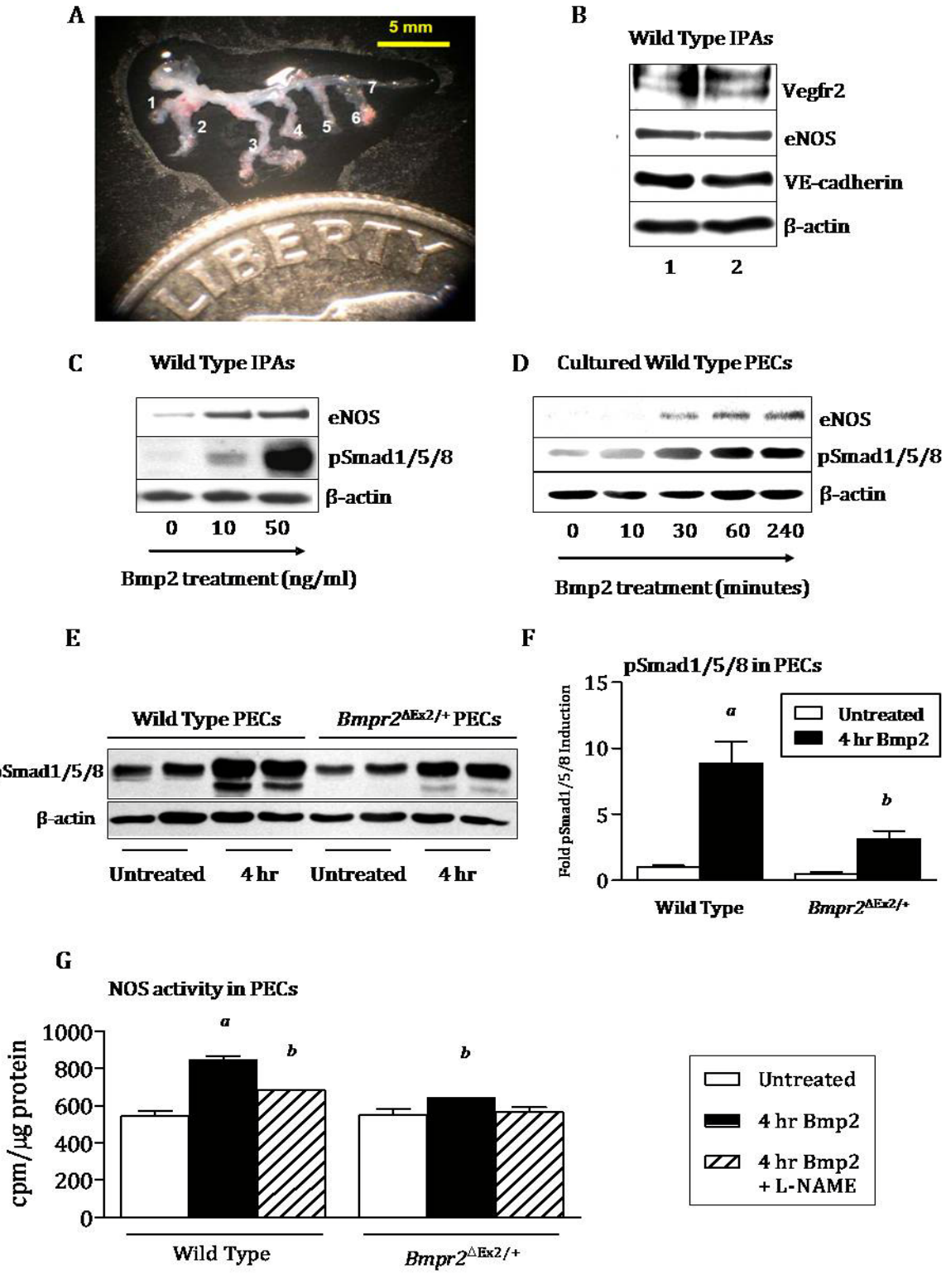
A
5 mm
1
2
3
4
5
6
7
LIBERTY
B
Wild Type IPAs
Vegfr2
eNOS
VE-cadherin
β-actin
1
2
C
Wild Type IPAs
eNOS
pSmad1/5/8
β-actin
0
10
50
Bmp2 treatment (ng/ml)
D
Cultured Wild Type PECs
eNOS
pSmad1/5/8
β-actin
0
10
30
60
240
Bmp2 treatment (minutes)
E
Wild Type PECs
Bmpr2ΔEx2/+ PECs
pSmad1/5/8
β-actin
Untreated
4 hr
Untreated
4 hr
F
pSmad1/5/8 in PECs
Fold pSmad1/5/8 Induction
15
10
5
0
a
b
Untreated
4 hr Bmp2
Wild Type
Bmpr2ΔEx2/+
G
NOS activity in PECs
cpm/μg protein
1000
800
600
400
200
0
a
b
b
Wild Type
Bmpr2ΔEx2/+
Untreated
4 hr Bmp2
4 hr Bmp2
+ L-NAME

Abnormal pulmonary arterial tone in *Bmpr2*$^{\Delta Ex2/+}$ mutant mice

Having established that Bmpr2-dependent signaling regulates eNOS expression and activity, we sought to directly determine whether impaired Bmpr2-dependent signaling leads to functional changes in the pulmonary vasculature. To do so, we established a pressure arteriography system to evaluate vasoconstrictor and vasodilator responses in isolated blood vessels. In order to evaluate physiologically relevant vasculature, we focused our analyses upon IPAs. To minimize variability, we strictly limited our evaluation to IPA segments from invariant, third branch, second and third generation IPAs with resting external diameters of 75-100 μm (Figure 3A, yellow rings). These were mounted on glass micropipettes at proximal and distal ends and side branches from the mounted vessel were individually tied off (Figure 3B). The arteriography chamber was transferred to the stage of an inverted microscope equipped with a video camera and computer-based monitoring system (Figure 3C). IPAs were visualized by real-time video capture software and processed for continuous measurement of the lumen diameter (Figure 3D). Our analysis, the first to utilize murine IPAs in the study of PH, allows for quantification of vessel reactivity in response to specific vasoactive agents (Figure 3E). Importantly, we are able to evaluate both endothelial-dependent and endothelial-independent vasodilation through the nitric oxide (NO) pathway. By combining this technique with the power of mouse genetics, we are the first group with the ability to directly evaluate the physiological consequence of a desired mutation in the context of experimental PH.

Vessel reactivity in IPAs from wild type and *Bmpr2*$^{\Delta Ex2/+}$ mutant mice was evaluated in a variety of ways: vasoconstriction in response to membrane depolarization (KCl) and adrenergic stimulation (norepinephrine; NE); endothelial-dependent vasodilation with a muscarinic receptor agonist (acetylcholine; ACh) and calcium ionophore (A23187); and

Figure 3. Pressure arteriography using isolated intrapulmonary arteries. A: Arteriogram of a left lung lobe from a wild type mouse. Yellow rings indicate segments of the invariant, third branch, second and third generation intrapulmonary arteries (IPAs) excised for arteriographic analysis. **B:** IPA after excision and mounting on glass canulae. **C:** Custom pressure arteriography chamber used for vessel reactivity studies. **D:** Photo showing a mounted IPA during vessel reactivity study. Yellow arrows indicate vessel wall (dark lines). External vessel diameter is determined using real-time video image analysis software. **E:** Representative arteriography tracing from a wild type IPA showing changes in external vessel diameter in response to vasoactive stimulation as indicated. Arteriogram modified from TCV Surgery Research Lab, University of Virginia.

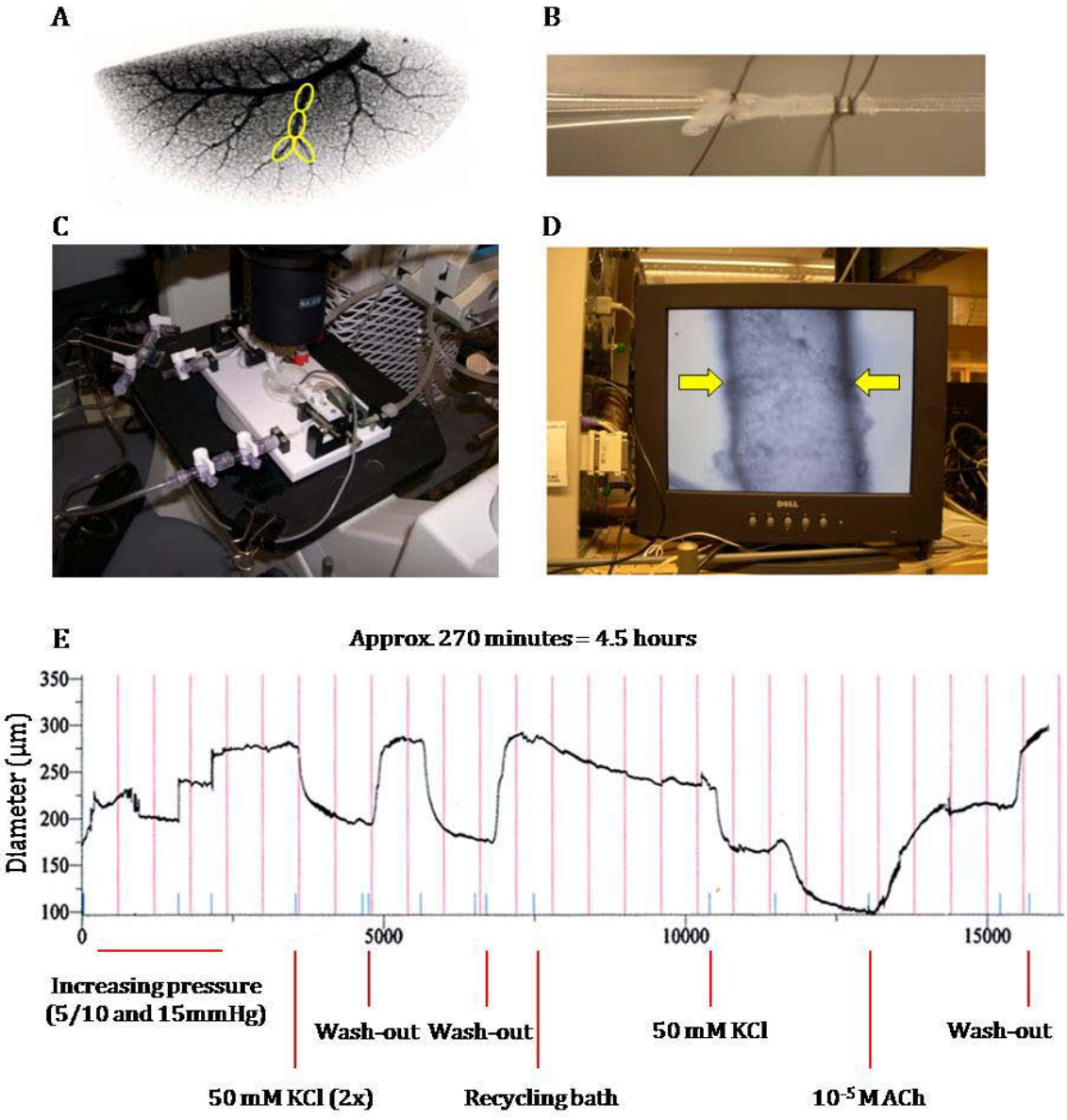
A
B
C
D
E
Approx. 270 minutes = 4.5 hours
Diameter (µm)
350
300
250
200
150
100
0
5000
10000
15000
Increasing pressure
(5/10 and 15mmHg)
Wash-out
Wash-out
50 mM KCl
Wash-out
50 mM KCl (2x)
Recycling bath
10-5 M ACh

endothelial-independent vasodilation with NO donor (sodium nitroprusside; SNP) (Figure 4A, B). While membrane depolarization with KCl causes similar vasoconstriction in both wild type and *Bmpr2*$^{\Delta Ex2/+}$ IPAs (Figure 4C), *Bmpr2*$^{\Delta Ex2/+}$ mutant IPAs show a significant increase in NE-induced vasoconstriction compared with wild type littermates (Figure 4D). In addition, endothelial-dependent vasodilation of submaximally constricted vessels with both ACh and A23187, which induce vasodilation through eNOS, was absent in *Bmpr2*$^{\Delta Ex2/+}$ mutant IPAs (Figure 4E). This was also associated with a partial impairment in endothelial-independent vasodilation in response to SNP (Figure 4E). These findings indicate that *Bmpr2*$^{\Delta Ex2/+}$ IPAs have multiple defects in NO-dependent vasodilation; namely, in addition to impaired Bmp-mediated regulation of eNOS, *Bmpr2*$^{\Delta Ex2/+}$ IPAs are hyper-constrictive and NO-resistant. The exact functional role that the *Bmpr2*$^{\Delta Ex2}$ allele plays in these defects is unknown. Furthermore, it is unclear if defective eNOS-expression is the primary cause of exacerbated hypoxic PH in *Bmpr2*$^{\Delta Ex2/+}$ mutant mice. Preliminary data to evaluate both of these questions are described below.

Genetic analysis of the *Bmpr2*$^{\Delta Ex2}$ mutation in the context of eNOS deficiency

We hypothesized that, if the primary downstream defect in *Bmpr2*$^{\Delta Ex2/+}$ mice is diminished eNOS expression, then adding the *Bmpr2*$^{\Delta Ex2}$ mutation to an *eNOS null* background would not cause hypoxic PH that is exacerbated over that seen in *eNOS null* mutants alone. However, if hypoxic PH is exacerbated in double mutants over *eNOS null* mutants, it would suggest that diminished eNOS expression alone is not sufficient to cause the degree of hypoxic PH seen in *Bmpr2*$^{\Delta Ex2/+}$ mice. Therefore, we crossed *Bmpr2*$^{\Delta Ex2/+}$ mutant mice with *eNOS null* mutant mice and then exposed wild type, *Bmpr2*$^{\Delta Ex2/+}$, *eNOS null*, and *Bmpr2*$^{\Delta Ex2/+}$*eNOS null* double mutant mice to hypoxia for 5 weeks. Upon evaluating

Figure 4. Abnormal pulmonary vasoconstriction and NO-mediated vasodilation in *Bmpr2*$^{\Delta Ex2/+}$ mutant mouse IPAs. A, B: Representative arteriography tracing of wild type (A) and *Bmpr2*$^{\Delta Ex2/+}$ (B) mutant IPAs showing response to defined vasoactive agents. **C, D**: Vasocontriction responses to KCl (C) and norepinephrine (NE; D) at the indicated concentrations. **E:** Cumulative NO-mediated vasodilation in IPAs pre-constricted with 10^{-6} M NE followed by treatment with the EC-dependent vasodilators ACh and A23187 (both 10^{-6} M) and the EC-independent vasodilator SNP (10^{-5} M). Data are expressed mean +/- SEM. n=3 vessels/group. Kruskal Wallis ANOVA, $p<0.05$: ***a***, vs. wild type at same treatment condition.

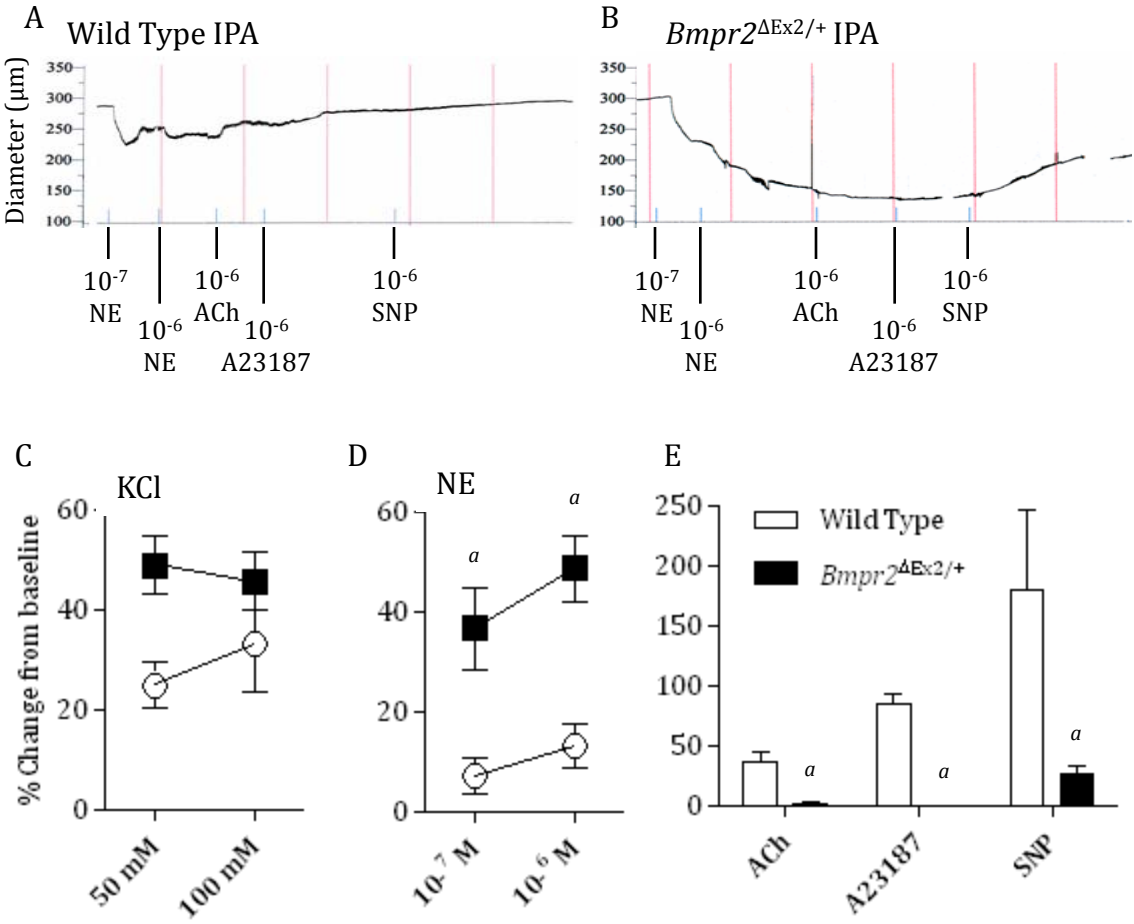
A
Wild Type IPA
Diameter (µm)
350
300
250
200
150
100
10-7 NE
10-6 NE
10-6 ACh
10-6 A23187
10-6 SNP
B
Bmpr2ΔEx2/+ IPA
350
300
250
200
150
100
10-7 NE
10-6 NE
10-6 ACh
10-6 A23187
10-6 SNP
C
KCl
% Change from baseline
60
40
20
0
50 mM
100 mM
D
NE
a
a
60
40
20
0
10-7 M
10-6 M
E
Wild Type
Bmpr2ΔEx2/+
250
200
150
100
50
0
a
a
a
a
ACh
A23187
SNP

hypoxic PH development, we found that there is a significant increase in RVSP in response to hypoxia in each genotype; however, in contrast to our expectation, there is no difference in RVSP between wild type and mutant mice under any of the treatment conditions (Table 8). Male mice tend to develop more severe PH after 5 weeks of hypoxia than female mice, but this effect is not modulated within either gender by *Bmpr2*$^{\Delta Ex2/+}$, *eNOS null*, or *Bmpr2*$^{\Delta Ex2/+}$*eNOS null* double mutation (Table 8). No elevation of RVDP or LVDP was observed in any genotype, confirming that the increase in RVSP is not due to left-sided heart failure (data not shown). These hemodynamic data are supported by measurements of RV hypertrophy, which also show an increase after 5 weeks of hypoxia, but reveal no differences between genotypes (Table 8). There is also no difference in sedated heart rate or hypoxia-induced increase in hematocrit between genotypes (Table 8).

To determine whether *Bmpr2*$^{\Delta Ex2/+}$*eNOS null* double mutation is associated with alterations in hypoxia-induced pulmonary vascular remodeling, we evaluated the degree of hypoxia-induced peripheral vessel muscularization in wild type, *Bmpr2*$^{\Delta Ex2/+}$, *eNOS null*, and *Bmpr2*$^{\Delta Ex2/+}$*eNOS null* double mutant mice. Supporting our hemodynamic data, the characteristic increase in peripheral muscularization is not different between genotypes (Table 8).

One explanation for our findings is that genetic strain background may be complicating direct analysis of mutation-specific effects. To address this possibility, we evaluated the distribution of RVSP within each genotype. This revealed subpopulations of mutant mice that developed greater hypoxic PH than wild type controls (Figure 5A, above red dashed line: *Bmpr2*$^{\Delta Ex2/+}$ - 3/18 (16.7%), *eNOS null* - 2/16 (12.5%), *Bmpr2*$^{\Delta Ex2/+}$*eNOS null* double mutants - 2/12 (16.7%)). Interestingly, these subpopulations are only observed among male mice (females, Figure 5B; males, Figure 5C, above red dashed line: *Bmpr2*$^{\Delta Ex2/+}$ -

Table 8. Assessment of hypoxic PH in wild type, *Bmpr2* $^{\Delta Ex2/+}$, *eNOS null*, and *Bmpr2*$^{\Delta Ex2/+}$*eNOS null* double mutant mice. Data are expressed as mean +/- SEM and numbers per group are as indicated (n). One-way ANOVA with Bonferroni correction, p<0.05: ***b***, vs. corresponding genotype normoxic control.

	Normoxia				3 Weeks Hypoxia			
	Wild Type Mean±SEM (n)	***Bmpr2*$^{\Delta Ex2/+}$** Mean±SEM (n)	***eNOS Null*** Mean±SEM (n)	**Double Mut.** Mean±SEM (n)	**Wild Type** Mean±SEM (n)	***Bmpr2*$^{\Delta Ex2/+}$** Mean±SEM (n)	***eNOS Null*** Mean±SEM (n)	**Double Mut.** Mean±SEM (n)
RVSP, mmHg	22.10±1.18 (17)	21.99±1.06 (20)	26.97±2.80 (7)	20.32±0.21 (2)	32.78±1.17 *b* (14)	34.53±1.72 *b* (18)	34.00±1.97 (14)	35.5±2.07 *b* (12)
Female RVSP, mmHg	19.66±1.82 (7)	19.38±1.08 (11)	26.0±0.66 (3)	ND	31.14±1.65 *b* (7)	28.88±1.48 *b* (7)	29.3±3.16 *b* (4)	32.63±3.14 (6)
Male RVSP, mmHg	23.80±1.37 (10)	25.18±1.36 (9)	27.66±1.82 (4)	20.32±0.21 (2)	34.42±1.52 *b* (7)	38.12±2.02 *b* (11)	35.89±2.2 (10)	38.37±2.39 *b* (6)
RV/LV+S, mg/mg	0.256±0.01 (17)	0.260±0.01 (21)	0.247±0.02 (8)	0.239±0.01 (2)	0.375±0.01 *b* (15)	0.395±0.01 *b* (22)	0.347±0.01 *b* (20)	0.355±0.02 (17)
Hematocrit, %	36.77±1.45 (15)	39.03±0.70 (16)	36.38±2.51 (8)	40.5±0.50 (2)	59.17±1.25 *b* (6)	58.25±1.79 *b* (14)	50.57±1.97 *b* (14)	52.38±1.78 (16)
Heart Rate, bpm	492.5±14.9 (17)	472.5±11.8 (20)	506.3±17.7 (7)	438.5±1.93 (2)	437.0±8.3 (7)	439.3±10.5 (18)	425.8±11.6 (13)	431.4±11.4 (13)
Muscularized Vessels, %	ND	ND	ND	ND	29.29±5.81 (7)	31.20±7.95 (5)	26.00±4.00 (2)	31.33±5.89 (3)

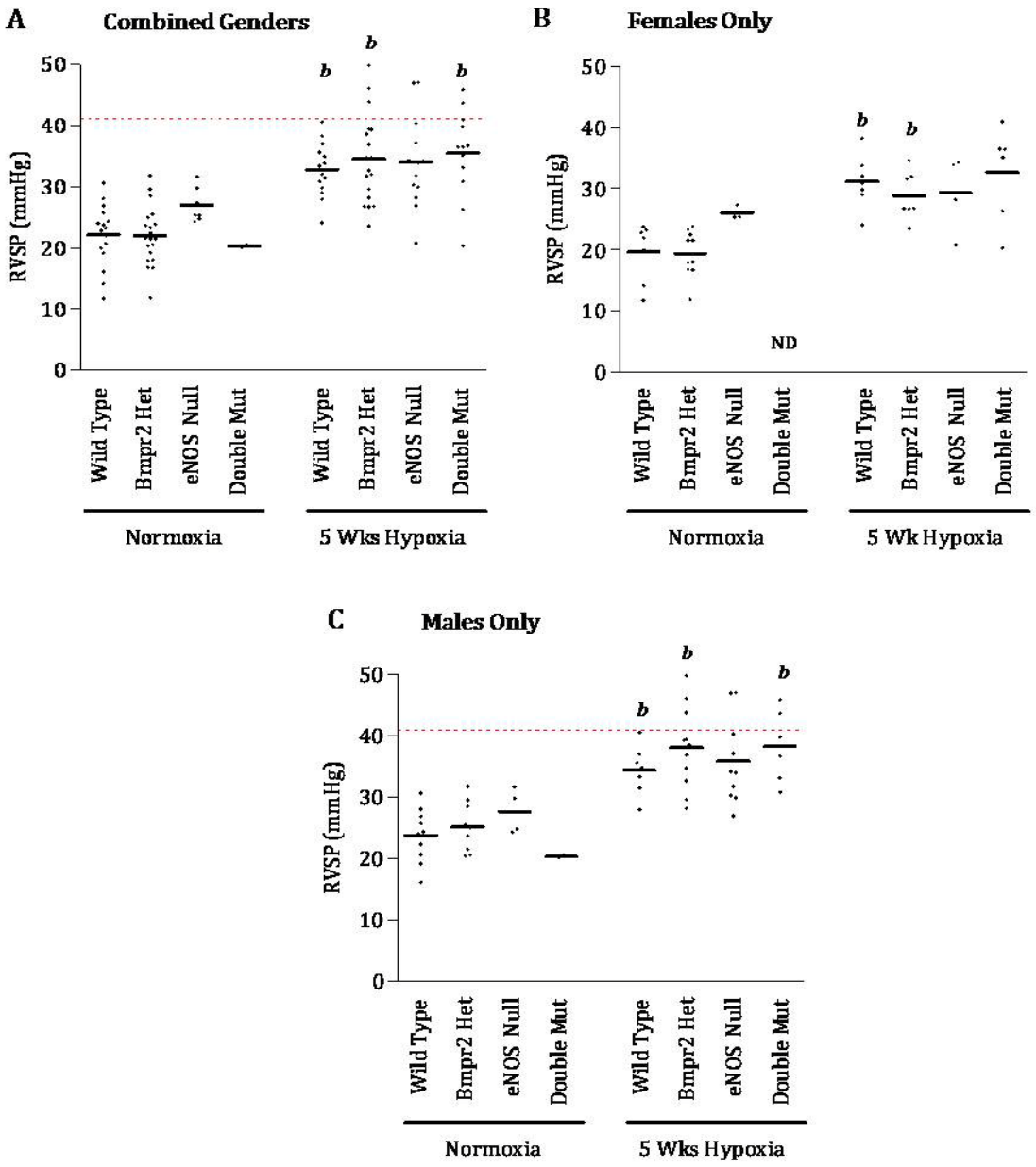

Figure 5. RVSP in wild type, *Bmpr2*$^{\Delta Ex2/+}$, *eNOS null*, and *Bmpr2*$^{\Delta Ex2/+}$*eNOS null* double mutant mice exposed to normoxia or 5 weeks hypoxia. A: RVSP for each genotype with genders combined. **B, C:** RVSP for female (B) and male (C) mice of each genotype. (Double Mut) mice are *Bmpr2*$^{\Delta Ex2/+}$*eNOS null*. Each dot represents the mean RVSP from a single mouse. Bars indicate mean RVSP for each group. Dashed line is set at highest wild type 5 week hypoxic RVSP. One-way ANOVA with Bonferroni correction, $p<0.05$: **b**, vs. corresponding genotype normoxic control.

3/11 (27.2%), *eNOS null* - 2/10 (20%), *Bmpr2*$^{\Delta Ex2/+}$*eNOS null* double mutants - 2/6 (33.3%)). However, these findings are insufficient to confirm or refute our hypothesis, since both genetic strain background and gender greatly affect the development of hypoxic PH in these studies.

Bmpr2-ΔEx2 is retained in the endoplasmic reticulum

To explore the underlying mechanism of defective vascular reactivity in *Bmpr2*$^{\Delta Ex2/+}$ mutant IPAs, we focused our attention on the expressed Bmpr2-ΔEx2 protein. While homozygous *Bmpr2*$^{-/-}$ mutant mice suffer embryonic lethality at gastrulation (18), homozygous *Bmpr2*$^{\Delta Ex2/\Delta Ex2}$ mutant mice die at embryonic day 13.5 due to cardiovascular defects (45). This indicates that the *Bmpr2*$^{\Delta Ex2}$ allele gives rise to a partially functioning protein, i.e. a hypomorphic Bmpr2 (Bmpr2-ΔEx2). This raises the possibility that defects in *Bmpr2*$^{\Delta Ex2/+}$ mutant mice may be directly due the expression of Bmpr2-ΔEx2 instead of impaired Bmpr2-dependent signaling alone. To begin to address this, we first characterized Bmpr2 expression by western blot using a commercially available mouse monoclonal antibody (Clone 18, BD) raised against the C-terminus of Bmpr2. In wild type whole lung lysates, Clone 18 resolves Bmpr2 predominantly as a 150 kDa band, whose expression is decreased in *Bmpr2*$^{\Delta Ex2/+}$ whole lung lysates (Figure 6A, left). Clone 18 also resolves a band of approximately 130 kDa that is only present in *Bmpr2*$^{\Delta Ex2/+}$ whole lung lysates, suggesting that this protein is Bmpr2-ΔEx2. This possibility is supported using an in-house rabbit polyclonal antibody (ASQ) that is raised against a peptide encoded by exon 2, which is deleted in the *Bmpr2*$^{\Delta Ex2}$ allele. ASQ recognizes the 150 kDa band in wild type and *Bmpr2*$^{\Delta Ex2/+}$ whole lung lysates, but not the 130 kDa band (Figure 6A, right). The expression of the 130 kDa protein is consistently observed in *Bmpr2*$^{\Delta Ex2/+}$ IPAs and is enriched in

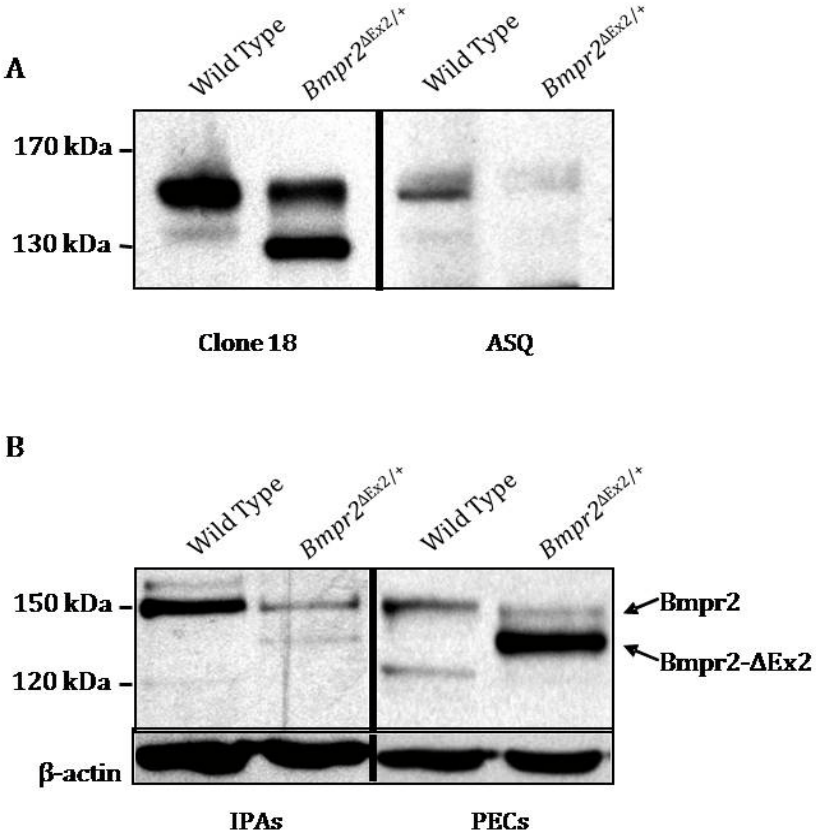

Figure 6. Western blot analysis of Bmpr2 expression in wild type and *Bmpr2*$^{\Delta Ex2/+}$ mutant mice. A: The in-house rabbit polyclonal antibody (ASQ) raised against a peptide encoded by exon 2 of Bmpr2 only resolves the wild type 150 kDa band (right), while Clone 18 (BD), raised against the C-terminus of Bmpr2, resolves both wild type and the 130 kDa Bmpr2-ΔEx2 bands (left) in whole lung lysates. **B:** Bmpr2-ΔEx2 is expressed in *Bmpr2*$^{\Delta Ex2/+}$ IPAs (left) and PECs (right).

Bmpr2$^{\Delta Ex2/+}$ PECs (Figure 6B). Therefore, the 150 kDa band represents expression of wild type Bmpr2, while the 130 kDa band represents expression of Bmpr2-ΔEx2.

To evaluate whether Bmpr2-ΔEx2 undergoes proper sub-cellular trafficking, we took advantage of the step-wise and sub-cellular compartment-specific modification of asparagine-linked glycosyl residues (74). Asparagine-linked glycosylation events define specific points of protein maturation, i.e. trafficking through the ER, *cis*-, *medial*-, and *trans*-Golgi network. While the endoglycosidase PNGase F cleaves all asparagine-linked oligosaccharides regardless of complexity, endoglycosidaseH (EndoH) cleaves only immature asparagine-linked oligosaccharides that exist in the ER or *cis*-Golgi network. As such, a glycoprotein that is EndoH-sensitive has not been trafficked beyond the *cis*-Golgi. Upon subjecting wild type Bmpr2 and Bmpr2-ΔEx2 to endoglycosidase treatment, we found that wild type Bmpr2 from IPAs and PECs (Figure 7A: bands 1 and 2; Figure 7B: band 4) is not EndoH-sensitive but is cleaved by PNGase F (Figure 7A: bands 1' and 2'; Figure 7B: band 4'), indicating that it has been trafficked beyond the *cis*-Golgi. Similar results are also observed for wild type Bmpr2 expressed in *Bmpr2*$^{\Delta Ex2/+}$ IPAs and PECs. On the other hand, the truncated Bmpr2-ΔEx2 protein (Figure 7A: band 3; Figure 7B: band 5) is fully EndoH sensitive and is not further cleaved by PNGaseF (Figure 7A: band 3'; Figure 7B: band 5'), representing immature processing of this mutant protein. These results indicate that Bmpr2-ΔEx2 is improperly trafficked in the pulmonary endothelium, which may play a significant role in the vascular defects observed in *Bmpr2*$^{\Delta Ex2/+}$ mutant mice. Future studies to further evaluate this possibility are proposed in Chapter 5.

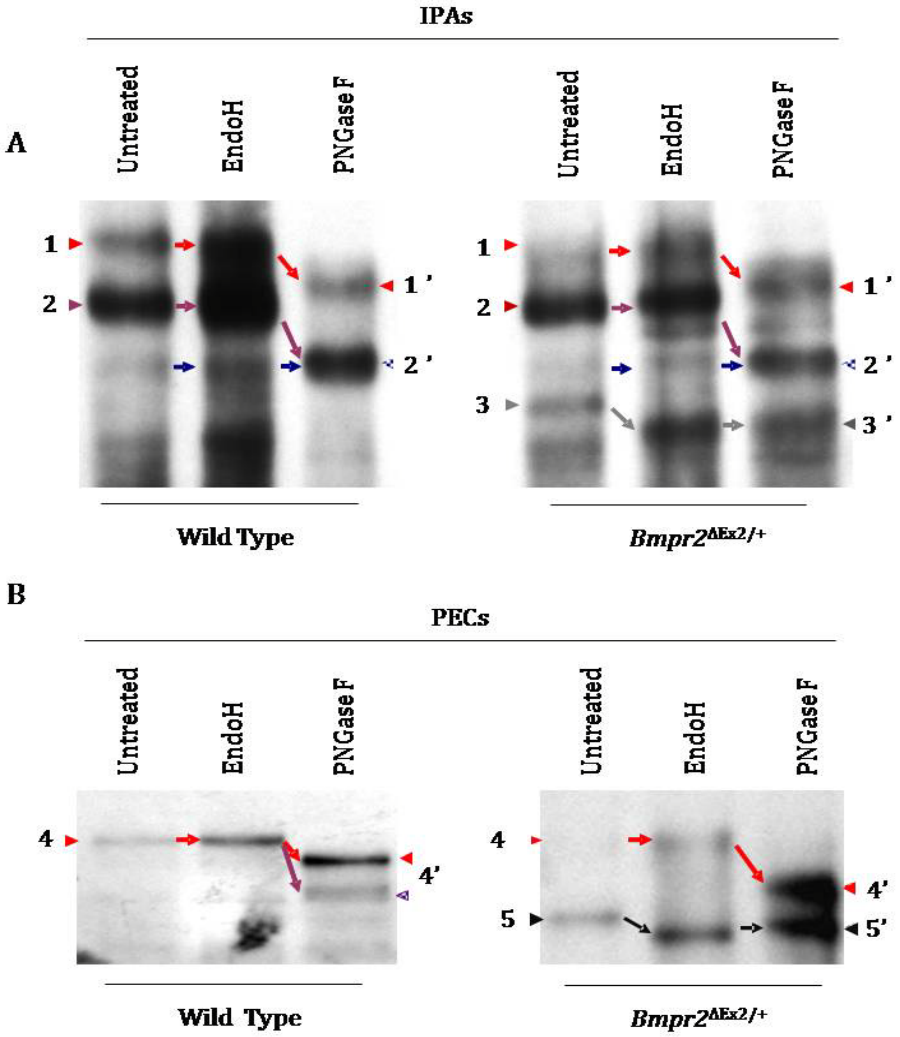

Figure 7. Trafficking defect of Bmpr2-ΔEx2 in *Bmpr2*$^{\Delta Ex2/+}$ IPAs and PECs. A, B: Bmpr2 was immunoprecipitated from total protein of wild type and *Bmpr2*$^{\Delta Ex2/+}$ IPAs (A) or PECs (B) and then treated +/- endoglycosidase for assessment of sub-cellular compartment-specific glycosylation. Wild type Bmpr2 (A: bands 1 and 2; B: band 4) is not EndoH-sensitive but is cleaved by PNGaseF (A: bands 1' and 2'; B: band 4'), indicating trafficking beyond the cis-Golgi. Hypomorphic Bmpr2-ΔEx2 (A: band 3; B: band 5) is fully EndoH sensitive (A: band 3'; B: band 5'), indicating incomplete trafficking. Blue arrow in A highlights assay sensitivity in the ability to resolve trafficking intermediates of Bmpr2. Each lane represents immunoprecipitate from a single IPA or PEC culture dish.

Discussion

The majority of HPAH patients inherit heterozygous mutations at the *BMPR2* locus (123). Given that pulmonary BMPR2 is dominantly expressed in ECs (8, 55, 166, 199), the pulmonary endothelium is likely a major target of defective BMPR2-dependent signaling. Previous data from our lab has shown that *Bmpr2*$^{\Delta Ex2/+}$ mutant mice develop exacerbated hypoxic PH that is associated with impaired hypoxic regulation of pulmonary eNOS expression (55). In the present study, we show that Bmp signaling regulates eNOS expression and function in the pulmonary vasculature via Bmpr2. Furthermore, *Bmpr2*$^{\Delta Ex2/+}$ mutant IPAs have severe endothelial dysfunction, exhibiting defects in NO-mediated vasodilation coupled with increased vasoconstriction. These findings indicate that Bmpr2 plays a previously unknown role in regulating vascular tone in the normoxic and hypoxic pulmonary vasculature through the direct regulation of eNOS.

The role of eNOS in maintaining low pulmonary vascular resistance has been demonstrated in a number of studies. Mice that are either heterozygous or homozygous deficient for *eNOS* have increased hypoxic PH and pulmonary vascular tone (51, 197-198). Additionally, there is evidence that there may be a reduction in eNOS expression in the pulmonary endothelium of patients with PAH (63, 126). Therefore, our observation that eNOS expression is reduced in the pulmonary vasculature of *Bmpr2*$^{\Delta Ex2/+}$ mutant mice suggests that Bmp-mediated regulation of eNOS could be of importance in human disease.

Our analyses indicate that *Bmpr2*$^{\Delta Ex2/+}$ mutant mice have abnormalities in endothelial function. In support of this, we have demonstrated that there is a marked defect in NO-mediated vasodilation of preconstricted IPAs from *Bmpr2*$^{\Delta Ex2/+}$ mutant mice. These findings are consistent with loss of eNOS expression in *Bmpr2*$^{\Delta Ex2/+}$ mutant IPAs, given that

previous studies have shown complete loss of endothelium-dependent vasodilation in *eNOS null* pulmonary arteries (197). However, our studies were performed on IPA preparations from normoxic lungs, which do not display a difference in eNOS expression between wild type and *Bmpr2*$^{\Delta Ex2/+}$ mutants. As eNOS activity can be regulated independently of expression levels (52), this raises the question as to whether there might also be a defect in eNOS activity in *Bmpr2*$^{\Delta Ex2/+}$ mutant IPAs. In support of this possibility, PECs isolated from *Bmpr2*$^{\Delta Ex2/+}$ mutant mice display decreased NOS activity in response to Bmp activation in *Bmpr2*$^{\Delta Ex2/+}$ PECs under normoxic conditions. Furthermore, there is a reduction in the expression of activated phospho-eNOS (S1177) and the NO-target sGC in normoxic *Bmpr2*$^{\Delta Ex2/+}$ mutant lungs (55). Collectively, these data indicate that basal Bmp signaling regulates eNOS expression and function in the pulmonary endothelium. Additionally, since sGC is a marker of NOS activity and is required to mediate NO-dependent vasodilation, reduced sGC expression may account for the defect in NO-donor-mediated vasodilation in *Bmpr2*$^{\Delta Ex2/+}$ IPAs.

Earlier studies have demonstrated enhanced pulmonary vasoconstrictor responses to exogenous serotonin in isolated pulmonary artery preparations from *Bmpr2*$^{+/-}$ mutant mice (116). This finding has been used to support the hypothesis that increased pulmonary vascular smooth muscle contractility accounts for increased susceptibility to PH in *Bmpr2*$^{+/-}$ mutant mice. To explore this further, we developed a novel approach to study pulmonary vascular responses in IPA preparations. Functional analysis of these smaller vessels is likely to more closely reflect functional changes in pulmonary resistance vessels than the analysis of extrapulmonary conduit vessels. Our studies confirmed that *Bmpr2*$^{\Delta Ex2/+}$ mutant IPAs have increased vasoconstrictor responses to NE, but contrast with earlier studies that did not detect differences between wild type and *Bmpr2*$^{+/-}$ mutant mice to phenylephrine (PE) (116). Like NE, PE induces vasoconstriction through activation of the α-adrenergic

receptors in VSMCs. This discrepancy is likely to reflect differences in vascular responses to conduit artery preparations used in the earlier studies (external diameters of 350-450 μm), and the smaller IPA preparations used in our studies (resting external diameters of 75-100 μm, increasing to 250-350 μm after inflation). Regardless, results from both studies indicate that there is increased pulmonary VSMC contractility in mice carrying heterozygous mutations at the *Bmpr2* locus that contributes to their increased susceptibility to PH. The mechanisms by which these mutations give rise to defects in VSMC function remain to be established; however, Bmp-mediated regulation of eNOS may play a role since previous studies found that vasoconstriction responses can be augmented by eNOS deficiency (101).

In addition to impaired NO-mediated vasodilation and increased vasoconstriction, other mechanisms may contribute to the development of exacerbated hypoxic PH in *Bmpr2*$^{\Delta Ex2/+}$ mutant mice. To explore these possibilities, we chose a genetics-based approach to evaluate the role of Bmpr2-mediated regulation of eNOS *in vivo* by examining the *Bmpr2*$^{\Delta Ex2}$ mutation in an *eNOS null* background. We hypothesized that, if the primary downstream defect in *Bmpr2*$^{\Delta Ex2/+}$ mice is diminished eNOS expression, then adding the *Bmpr2*$^{\Delta Ex2/+}$ mutation to an *eNOS null* background would not cause hypoxic PH that is exacerbated over that seen in *eNOS null* mutants alone. Contrary to prior findings, neither *Bmpr2*$^{\Delta Ex2/+}$ or *eNOS null* mutant mice in this study displayed exacerbated hypoxic PH as compared to wild type mice. However, a subset of *Bmpr2*$^{\Delta Ex2/+}$, *eNOS null*, and *Bmpr2*$^{\Delta Ex2/+}$*eNOS null* double mutant mice developed more severe hypoxic PH than wild type controls. These findings are consistent with an earlier study describing that a subset of mice in which Bmpr2 is deleted in pulmonary ECs *in vivo* spontaneously develop PH (80). Of note, all of the *Bmpr2*$^{\Delta Ex2/+}$, *eNOS null*, and *Bmpr2*$^{\Delta Ex2/+}$*eNOS null* double mutant mice in our study that developed exacerbated hypoxic PH were male. This finding is likely related

to eNOS deficiency, as the *eNOS null* mutation has greater impact on the male pulmonary vasculature than female (111). Taken together, therefore, these studies neither confirm nor refute our hypothesis that the primary defect in *Bmpr2*$^{\Delta Ex2/+}$ mutant mice results from loss of eNOS expression in the pulmonary vasculature. On this basis we are presently unable to rule out that additional defects contribute to the development of exacerbated hypoxic PH in *Bmpr2*$^{\Delta Ex2/+}$ mutant mice. The wide spread in our data and the failure to confirm previous reports that *Bmpr2*$^{\Delta Ex2/+}$ or *eNOS null* mice develop more severe hypoxic PH than their wild type littermates (51, 55, 197-198) suggests that the failure of these studies is primarily a reflection of the mixed genetic background used for these studies. Unfortunately, this problem was unavoidable, since pure background *eNOS null* mutant mice suffer severe cardiovascular defects and post-natal mortality (70, 106, 111, 131). Therefore, to test our original hypothesis, another genetic approach, rescue of hypoxic PH in *Bmpr2*$^{\Delta Ex2/+}$ by overexpression of eNOS, is proposed in Chapter 5.

It is important to stress that these studies have been performed using *Bmpr2*$^{\Delta Ex2/+}$ mutant mice, which express a truncated, hypomorphic version of Bmpr2 (Bmpr2-ΔEx2) (45). This mutant mouse, in which the majority of the Bmpr2 ligand binding domain has been deleted, exactly replicates an inherited mutation in one HPAH family, while approximately 20-30% of all mutations in *BMPR2* occur in the ligand binding domain. *Bmpr2*$^{\Delta Ex2/+}$ mutant mice are different than the heterozygous null *Bmpr2* mutant mice (*Bmpr2*$^{+/-}$) used in earlier studies. Our lab has recently reported that *Bmpr2*$^{\Delta Ex2/+}$ are more susceptible to hypoxic PH than wild type littermates (55). On the other hand, *Bmpr2*$^{+/-}$ mutant mice do not develop PH with hypoxia alone (17, 116). This raises the possibility that the defects observed in *Bmpr2*$^{\Delta Ex2/+}$ mutant mice are partially related to the expression of Bmpr2-ΔEx2 instead of decreased Bmpr2-dependent signaling alone. This idea is consistent with the finding that HPAH patients who carry expressed inactivating *BMPR2*

mutations have more severe disease than those who carry non-expressed *BMPR2* mutations (9). Therefore, we investigated Bmpr2-ΔEx2 more closely and found that this mutant protein displays defective sub-cellular trafficking. Examination of Bmpr2-ΔEx2 glycosylation revealed that this protein is retained in the ER or *cis*-Golgi. While this preliminary evidence does not rule out that some Bmpr2-ΔEx2 reaches the cell surface, it raises the possibility that mis-trafficked Bmpr2-ΔEx2 may exert dominant negative interference on normal cellular processes. This hypothesis is more fully explored in Chapter 5.

Collectively, the data presented in this chapter suggest a novel role for Bmpr2 in regulation of pulmonary vascular tone. In this model, Bmp ligands signal through Bmpr2 to regulate eNOS expression, thereby positively affecting NO production and promoting vasodilation. In the presence of *Bmpr2* mutation, the Bmp-mediated regulation of eNOS is impaired, leading to endothelial dysfunction and increased pulmonary VSMC contractility. These defects are exaggerated in chronic hypoxia when NO-mediated vasodilation is imbalanced with hypoxic pulmonary vasoconstriction, thus exacerbating hypoxic PH in *Bmpr2*$^{\Delta Ex2/+}$ mutant mice. Our findings have implications for the understanding of human HPAH and potentially identify areas of therapeutic intervention in other forms of PAH.

Acknowledgments

The studies described in this chapter were a collaborative effort among several individuals. A particular debt of gratitude is owed to David Frank, Lynda Anderson, Mark Jones, Ambra Pozzi, Stan Poole, and Jeff Reese.

CHAPTER III

BMP2 EXERTS PROTECTIVE EFFECTS IN HYPOXIC PULMONARY HYPERTENSION

Introduction

The observation that most patients with the rare disease HPAH inherit heterozygous mutations in *BMPR2* (123) suggests that dysregulated BMPR2-dependent signaling contributes to the pathogenesis of this disease. All forms of PH display structural remodeling of resistance-level pulmonary arteries and increased pulmonary vascular tone and reactivity (165), suggesting that defects in similar regulatory mechanisms may underlie the development of most forms of PH. This also raises the wider question as to the role of BMPR2-dependent signaling in more common forms of PH that are not associated with inherited *BMPR2* mutations.

To explore the role of Bmps in regulating pulmonary vascular function in the absence of *Bmpr2* mutations, we evaluated pulmonary expression of Bmpr2 ligands in a mouse model of hypoxic PH. Pulmonary Bmp2 and Bmp4 expression (but not Bmp5, Bmp6, or Bmp7) are up-regulated following exposure to hypoxia (54). Surprisingly, loss of hypoxia-induced Bmp4 expression in heterozygous null *Bmp4*$^{LacZ/+}$ mutant mice is associated with reduced PH and decreased pulmonary vascular remodeling and VSMC proliferation. These findings suggest that Bmp4 promotes hypoxic PH by increasing VSMC proliferation and vascular remodeling. This is consistent with the observation that conditional loss of Alk3 (a type 1 Bmp receptor required for some Bmpr2-signaling (42)) in VSMCs protects mice against hypoxic pulmonary vascular remodeling (49). These findings

contrast with our observations in *Bmpr2*$^{\Delta Ex2/+}$ mutant mice, which show greater susceptibility to hypoxic PH (55). Furthermore, ~30% of mice with conditional deletion of *Bmpr2* in ECs spontaneously develop PH (80). This indicates that loss of Bmpr2-mediated signaling in ECs is sufficient to promote PH. Therefore, observations in *Bmp4*$^{LacZ/+}$ and *Bmpr2* mutant mice suggest that Bmp signaling exerts opposing effects on the pulmonary vasculature through its effect on VSMC and EC function. Furthermore, they raise the questions as to the dominant ligand activating Bmpr2 in the pulmonary endothelium. Since Bmp2 is also up-regulated in the hypoxic lung (54) and is a Bmpr2 ligand, we therefore hypothesized that hypoxia-induced expression of Bmp2 exerts opposing effects to Bmp4 in the hypoxic pulmonary vasculature, and that Bmp2 is the dominant ligand activating Bmpr2 in pulmonary ECs.

To test this hypothesis, we investigated the role of Bmp2 in hypoxic PH using mice deficient for *Bmp2* (*Bmp2*$^{+/-}$ mutant mice). We show that these mice develop more severe hypoxic PH than their wild type littermates. Unlike *Bmp4*$^{LacZ/+}$ mutant mice, *Bmp2*$^{+/-}$ mutant mice have decreased hypoxia-induced expression and activation of eNOS in the pulmonary vasculature. These findings suggest that Bmp2 and Bmp4 exert opposing effects on the pulmonary vasculature *in vivo*, and that the effects of Bmp2 are likely to be mediated through activation of protective, Bmpr2-dependent effects in pulmonary ECs in hypoxic PH. Our findings outlined in this chapter have recently been published as a co-first authored study (3).

Methods

Mouse lines

Bmp2$^{+/-}$ mice bred on a C57Bl/6 background were a gift from Stephen Harris (236). *Bmp4*$^{LacZ/+}$ mice bred on an ICR background were a gift from Brigid Hogan (103). 5' and 3' *Bmp2* BAC transgenic reporter mice have been described (27). Wild type ICR mice for IPA response studies were purchased from Charles River. Genotyping was performed by PCR of ear punch DNA using the primer sets outlined in Table 6.

Quantitative RT-PCR

Total RNA from snap frozen left lung was extracted in Trizol reagent (Invitrogen) and quantified by UV spectrophotemetry (NanoDrop, Thermo Scientific). Reverse transcription of 1 μg RNA by Superscript III (Invitrogen) was used to generate cDNA for analysis by quantitative PCR (Biosystems 7300 Real Time PCR, Applied Biosystems) using SYBR Green (Applied Biosystems). Primers complementary to mouse mRNA sequences were designed to cross exon boundaries to avoid detection of contaminating genomic DNA and are outlined in Table 9. Changes in mRNA expression were determined by comparison of sample Ct values against a standard curve generated using pooled sample cDNA. All data were normalized to *β-actin* mRNA and expressed as fold change of normoxic control.

Table 9. Quantitative PCR primers utilized for RT-PCR analysis of mRNA. Primer sequences and amplicon size are listed for each target mRNA. All Quantitative PCR reactions were performed in a Biosystems 7300 Real-Time PCR (Applied Biosystems) using SYBR Green (Applied Biosystems).

mRNA	Forward Primer	Reverse Primer	Amplicon Size
Bmp2	TGTGGGCCCTCATAAAGAAGCAG A	AGCAAGCTGACAGGTCAGAGAAC A	164 bp
Bmp4	CCTCAAGGGAGTGGAGATTG	GACTACGTTTGGCCCTTCTG	102 bp
eNOS	GGGAAAGCTGCAGGTATTTG	TGATGGCTGAACGAAGATTG	115 bp
β-actin	ACGGCCAGGTCATCACTATTG	AGGGGCCGGACTCATCGTA	371 bp

Western blot

Western blot analyses were performed as described in Chapter 2 using antibodies detailed in Table 7.

Experimental PH

Experimental PH was performed as described in Chapter 2.

Histological evaluation of pulmonary vascular remodeling, proliferation, and vascular density

Evaluation of pulmonary vascular remodeling was performed as described in Chapter 2. With the observer blinded to genotype and treatment condition, VSMC proliferation was determined as described using two-color immunofluorescence staining for α-SMA and PCNA with DAPI nuclear stain (54-55). In this assay, proliferating VSMCs stain positive for PCNA and are identified by expression of α-SMA. Vascular cell proliferation is expressed as number of PCNA-positive VSMC/vessel. Because significant hypoxia-induced proliferation is not observed at the 3 week time-point (130), proliferation was scored after 1 week of hypoxia only. Vessel density, expressed as vessels per 100 alveoli, was determined after H&E staining and counting of peripheral vessels and alveoli from 100X fields of view.

Analysis of β-galactosidase expression in *Bmp2* BAC LacZ transgenic mice

Lungs were inflated and fixed in 0.2% glutaraldehyde in PBS with 2 mM MgCl2 and 5 mM EGTA overnight. Tissue processing and β-galactosidase staining were performed as described (22). Results were quantified by counting the number of blue cells per alveolus or vessel in cross section, excluding vessels if their longitudinal length was >2X their width. Cell counts were obtained in peripheral vessels (20-50 μm and distal to terminal bronchioles) and larger vessels (50-200 μm and associated with muscularized airways). We evaluated >300 alveoli, >30 small, and >20 large vessels per mouse.

Isolation of IPA trees

The isolation of IPA trees was performed as described in Chapter 2. For Bmp-response studies, freshly isolated IPA s were cultured in DMEM with 10% FBS and treated ± 50 ng/ml recombinant Bmp2 or Bmp4 (R&D systems) for 18 hours prior to lysis.

Statistical analyses

Statistical analyses were performed as described in Chapter 2.

Results

Bmp2-dependent signaling is impaired in *Bmp2*$^{+/-}$ mutant mice

To determine the functional role of Bmp2 in hypoxic PH, we obtained mice in which the *Bmp2* genomic locus has been disrupted. While homozygous deficiency of *Bmp2* results in embryonic lethality, *Bmp2*$^{+/-}$ mutant mice are phenotypically normal (236). Similar to previous observations (54), wild type mice display increased pulmonary *Bmp2* mRNA and phosphorylation of Smad1/5/8 (pSmad1/5/8) in response to chronic hypoxia (Figure 8A, C, D). However, both responses are significantly blunted in *Bmp2*$^{+/-}$ mutant mice (Figure 8A, C, D). There is no compensatory change in *Bmp4* mRNA levels in hypoxic *Bmp2*$^{+/-}$ mutant mice (Figure 8B). Because *Bmp2*$^{+/-}$ mutant mice display impaired Bmp2-dependent signaling, they provide a useful model to study the functional role of Bmp2 in hypoxic PH.

Bmp2$^{+/-}$ mutant mice develop exacerbated hypoxic pulmonary hypertension

The role of Bmp2 in hypoxia was investigated by exposing wild type and *Bmp2*$^{+/-}$ mutant mice to 10% normobaric oxygen for up to 3 weeks. Compared to wild type littermates, *Bmp2*$^{+/-}$ mutant mice develop higher RVSP after 3 weeks hypoxia (Figure 9A, B; Table 10). RV hypertrophy also tended to be higher in *Bmp2*$^{+/-}$ mutant mice than wild type littermates after 3 weeks hypoxia, but this difference failed to reach statistical significance (Table 10). Increased RVSP in *Bmp2*$^{+/-}$ mutant mice is not due to left ventricular failure as no elevation in LVDP was observed (data not shown), and did not result from differences in polycythemic responses to hypoxia between genotypes (Table 10).

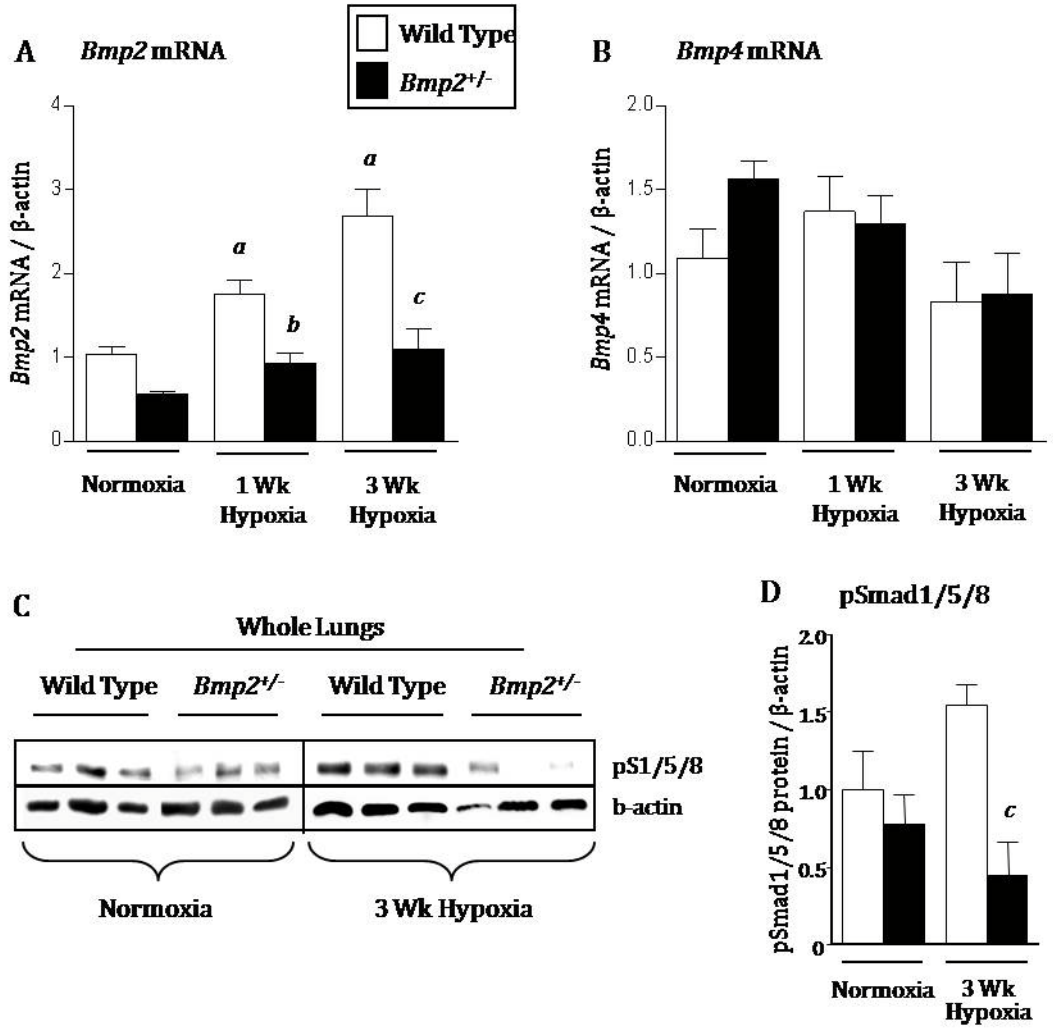

Figure 8. Bmp signaling in *Bmp2*$^{+/-}$ mutant mice. A, B: Quantitative RT-PCR for *Bmp2* (A) and *Bmp4* (B) mRNA expression in wild type and *Bmp2*$^{+/-}$ mouse lungs under normoxia (wild type n=8, *Bmp2*$^{+/-}$ n=6), 1 week hypoxia (wild type n=6, *Bmp2*$^{+/-}$ n=6), and 3 weeks hypoxia (wild type n= 5, *Bmp2*$^{+/-}$ n=5). **C, D:** Whole lung phospho-Smad1/5/8 (pSmad1/5/8) in wild type and *Bmp2*$^{+/-}$ mutant mice detected by western blot (C) and quantified by densitometry (D). Data expressed as mean +/- SEM for wild type mice (white bars), and *Bmp2*$^{+/-}$ mutant mice (black bars). One-way ANOVA with Bonferroni correction, $p<0.05$: **a**, vs. wild type normoxia; **b**, vs. wild type 1 week hypoxia, and **c**, vs. wild type 3 weeks hypoxia.

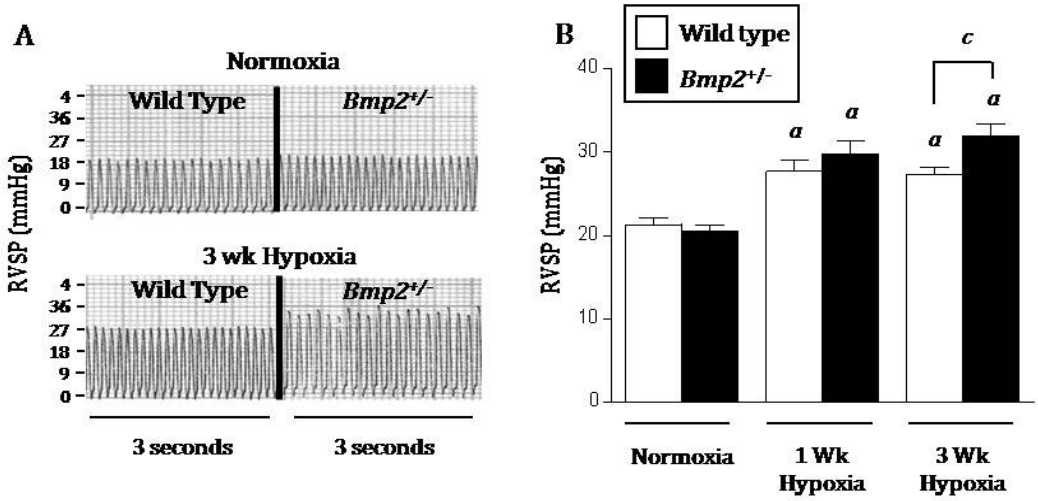

Figure 9. Hypoxic PH responses in *Bmp2*$^{+/-}$ mutant mice. A: Representative RV pressure tracings from wild type and *Bmp2*$^{+/-}$ mutant mice exposed to normoxia or 3 weeks hypoxia. **B:** Mean RVSP in wild type and *Bmp2*$^{+/-}$ mutant mice exposed to normoxia or 3 weeks hypoxia. Mouse numbers per group are indicated in Table 10 (page 60). Data are expressed as mean +/- SEM for wild type mice (white bars) and *Bmp2*$^{+/-}$ mice (black bars). One-way ANOVA with Bonferroni correction, $p<0.05$: **a**, vs. wild type normoxia; **c,** vs. wild type 3 week hypoxia.

Table 10. Hypoxic PH in *Bmp2*$^{+/-}$ mutant mice. RVSP, RV/LV+Septal ratio, and hematocrit in wild type and *Bmp2*$^{+/-}$ mutant mice exposed to normoxia, 1 week, or 3 weeks hypoxia. Data are expressed as mean +/- SEM. Mouse numbers indicated in parentheses. One-way ANOVA with Bonferroni correction, $p<0.05$: ***a***, vs. wild type normoxia; ***c***, vs. wild type 3 weeks hypoxia. RV/LV+S ratio and hematocrit measurements were determined by L. Anderson.

	Normoxia		1 Week Hypoxia		3 Weeks Hypoxia	
	Wild Type	***Bmp2*$^{+/-}$**	**Wild Type**	***Bmp2*$^{+/-}$**	**Wild Type**	***Bmp2*$^{+/-}$**
	Mean+/- SEM (n)	Mean+/- SEM (n)	Mean+/- SEM (n)	Mean+/- SEM (n)	Mean+/- SEM (n)	Mean+/- SEM (n)
RVSP, mmHg	21.26+/- 0.822 (18)	20.49+/- 0.69 (17)	27.66+/- 1.41 (6) *a*	29.8+/- 1.47 (6) *a*	27.29+/- 0.86 (16) *a*	31.95+/- 1.40 (8) *a c*
RV/LV+S, mg/mg	0.313+/- 0.020 (14)	0.309+/- 0.011 (11)	0.363+/- 0.028 (6)	0.330+/- 0.020 (7)	0.397+/- 0.032 (19) *a*	0.371+/- 0.046 (9) *a*
Hematocrit, %	42.75+/- 1.57 (8)	43.00+/- 1.81 (5)	ND	ND	56.27+/- 3.27 (11)	60.11+/- 3.58 (9)

In addition to increased RVSP, *Bmp2*$^{+/-}$ mutant mice, when compared to wild type littermates, show a marked increase in peripheral vessel muscularization after exposure to hypoxia for 3 weeks (Table 11). Increased vessel remodeling is not associated with significant differences in alveolar vascular density in wild type and *Bmp2*$^{+/-}$ mutant mice under normoxic or hypoxic conditions (Table 11), suggesting that aberrant remodeling and PH responses to hypoxia do not result from a developmental defect in small vessel patterning in the lung. Since previous studies indicate that proliferative effects of hypoxia occur early in the development of hypoxic PH (130, 164), we went on to evaluate pulmonary VSMC proliferation after 1 week of hypoxia in both small, peripheral muscularized vessels (20-50 μm diameter) and larger, airway-associated muscularized vessels (50-200 μm diameter). There are very few α-SMA-positive, small, peripheral muscularized vessels in normoxic lungs of either wild type or *Bmp2*$^{+/-}$ mutant mice. For this reason, we were unable to evaluate basal, normoxic VSMC proliferation rates in these vessels. Studies were therefore performed by comparing genotypes exposed to hypoxia only. VSMC proliferation in these small, muscularized peripheral vessels is reduced in hypoxic *Bmp2*$^{+/-}$ mouse lungs, although these differences are not significantly different from VSMC proliferation rates in wild type littermates (Table 11). Basal VSMC proliferation in larger, muscularized vessels is slightly increased in *Bmp2*$^{+/-}$ versus wild type mice, but this is not statistically significant. There is, however, a significant reduction in VSMC proliferation in larger muscularized vessels from *Bmp2*$^{+/-}$ mice compared to wild type littermates after 1 week of hypoxia (Table 11). Taken together, these findings indicate that *Bmp2*$^{+/-}$ mutant mice have increased susceptibility to hypoxic PH. This is associated with increased muscularization of the peripheral pulmonary vasculature which occurs without evidence of increased VSMC proliferation.

Table 11. Hypoxia-induced vascular remodeling and proliferation in wild type and *Bmp2*$^{+/-}$ mutant mice. Peripheral pulmonary vessel muscularization, VSMC proliferation in small, muscularized peripheral and larger proximal vessels, and peripheral vessel density ratios in wild type and *Bmp2*$^{+/-}$ mutant mice exposed to normoxia, 1 week, or 3 weeks hypoxia. Data are expressed as mean +/- SEM. Mouse numbers indicated in parentheses. One-way ANOVA with Bonferroni correction, $p<0.05$: ***a***, vs. wild type normoxia; ***b***, vs. wild type 1 week hypoxia; ***c***, vs. wild type 3 weeks hypoxia. Peripheral muscularization and density ratios were determined by L. Anderson.

	Normoxia		1 Week Hypoxia		3 Weeks Hypoxia	
	Wild Type	***Bmp2*$^{+/-}$**	**Wild Type**	***Bmp2*$^{+/-}$**	**Wild Type**	***Bmp2*$^{+/-}$**
	Mean+/- SEM (n)	Mean+/- SEM (n)	Mean+/- SEM (n)	Mean+/- SEM (n)	Mean+/- SEM (n)	Mean+/- SEM (n)
Peripheral Muscularization, %	1.33+/-0.49 (6)	8.00+/-4.03 (5)	ND	ND	23.66+/-5.57 (6) *a*	45.00+/-4.92 (5) *a c*
Proximal Vessel VSMC Proiferation, PCNA+/Vessel	0.59+/-0.07 (3)	1.47+/-0.35 (3)	2.43+/-0.34 (5) *a*	1.36+/-0.23 (4)	0.64+/-0.08 (3)	1.01+/-0.25 (3)
Peripheral Vessel VSMC Proiferation, PCNA+/Vessel	ND	ND	0.20+/-0.03 (3)	0.11+/-0.03 (4)	0.07+/-0.01 (5) *b*	0.04+/-0.01 (4)
Muscularized Peripheral Vessel Density, Vessel/100 Alveoli	3.68+/-0.61 (6)	3.73+/-0.31 (5)	ND	ND	3.59+/-0.36 (6)	3.31+/-0.29 (5)

Bmp2 expression in the lung is closely associated with the vasculature

To determine the mechanism by which Bmp2 regulates pulmonary vascular responses to chronic hypoxia, we first evaluated its cellular localization in hypoxic lungs. We were unsuccessful in detecting Bmp2 protein expression by immunohistochemical analysis using commercially available antibodies (data not shown). Therefore, to determine which pulmonary cell types express Bmp2, we evaluated LacZ expression by β-galactosidase activity in the lungs of two *Bmp2* BAC LacZ reporter mice (27). The 5' *Bmp2* BAC LacZ and 3' *Bmp2* BAC LacZ mice encompass most of the 5' and 3' *cis*-acting regulatory sequences for *Bmp2*, respectively. The 5' *Bmp2* BAC reporter expresses LacZ in the embryonic lung while the 3' *Bmp2* BAC reporter does not (27). Consistent with these findings, there are only occasional (<1% of the total cells) intra-alveolar cells that show β-galactosidase activity after 3 weeks of hypoxia in the 3' *Bmp2* BAC reporter mouse (data not shown). In contrast, there is abundant β-galactosidase activity in the adult lungs of 5' *Bmp2* BAC reporter mice (Figure 10A-F), indicating that pulmonary regulation of *Bmp2* in the adult is dependent on *cis*-acting elements in the 5' *Bmp2* BAC reporter. Using these mice, we show that *Bmp2* LacZ is expressed at low levels in alveolar and bronchial epithelium and in a small number of vessels under normoxic conditions, and that there is a step-wise increase in the number of LacZ-positive cells in the lung after exposure to hypoxia for 1 and 3 weeks (Figure 10G). While there is an increased number of LacZ-positive alveolar cells, there is a marked increase in LacZ-positive cells in small, peripheral pulmonary vessels following 1 and 3 weeks of hypoxia but no change in the number of LacZ-positive cells in larger vessels. Higher magnification images of LacZ-positive cells in small, peripheral pulmonary vessels indicate that the majority of these cells are located in the intimal wall under hypoxic conditions (Figure 10F). This suggests that ECs are the main site of Bmp2 expression in the hypoxic peripheral pulmonary vasculature. These findings contrast with

Figure 10. LacZ expression in the 5' *Bmp2* BAC reporter mice. A-F: β-galactosidase staining of lung tissue sections from 5' *Bmp2* BAC LacZ reporter mice under normoxia (A), 1 week hypoxia (B), or 3 weeks hypoxia (C, D). Higher power images of LacZ-expressing cells under normoxic conditions (E) and after 3 weeks hypoxia (F). LacZ staining is indicated in alveoli (thin black arrows), small vessels (<50 μm and distal to terminal bronchioles, thick black arrows) and larger vessels (50-200 μm and associated with muscularized airways, clear block arrows). Black scale bars 100 μm (A-D), white scale bars 50 μm (E, F). **G:** Quantification of LacZ-expressing cells. LacZ-positive cells were counted and expressed as stained cells/unit. Data are mean +/- SEM (n=5 per group). One-way ANOVA with Bonferroni correction, $p<0.05$: **a**, vs. normoxic control. Staining and counts performed by M. deCaestecker.

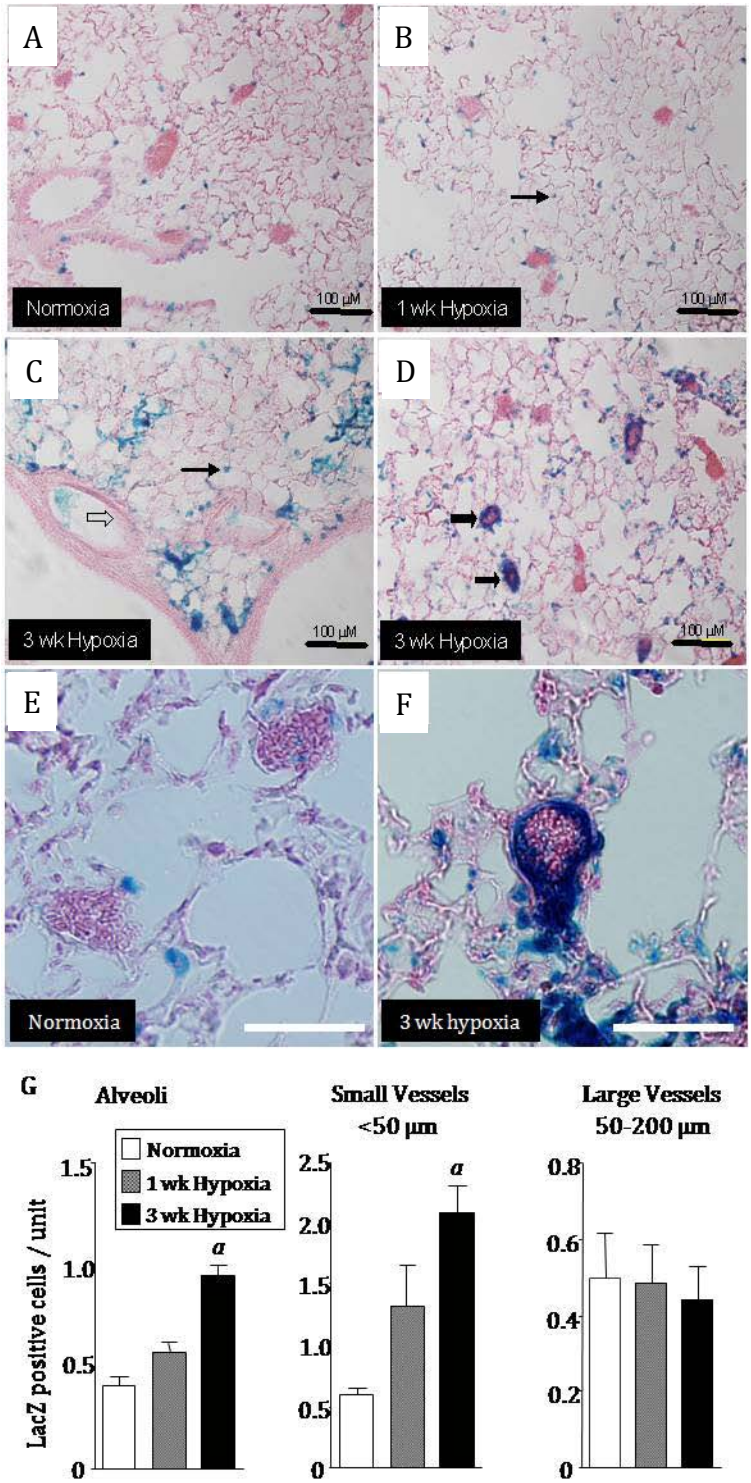
A
Normoxia
100 µM
B
1 wk Hypoxia
100 µM
C
3 wk Hypoxia
100 µM
D
3 wk Hypoxia
100 µM
E
Normoxia
F
3 wk hypoxia
G
Alveoli
Small Vessels
<50 µm
Large Vessels
50-200 µm
Normoxia
1 wk Hypoxia
3 wk Hypoxia
LacZ positive cells / unit
a
a
1.5
1.0
0.5
0
2.5
2.0
1.5
1.0
0.5
0
0.8
0.6
0.4
0.2
0

our previous observations using *Bmp4* LacZ knock-in reporter mice (54). *Bmp4* LacZ is also widely expressed in bronchial and alveolar epithelium, but unlike the 5' *Bmp2* LacZ reporter, we do not see increased *Bmp4* LacZ expression in these small, peripheral vessels.

Bmp2$^{+/-}$ mutant mice display decreased pulmonary eNOS expression and activity

Given that Bmp signaling has been shown to regulate expression and activity of eNOS (Chapter 2), and since abnormalities in the eNOS pathway play an important role in regulating pulmonary vascular responses in PH (31), we evaluated the regulation of pulmonary eNOS in hypoxic *Bmp2*$^{+/-}$ mutant mice. While chronic hypoxia increases pulmonary eNOS protein expression in wild type mice, hypoxia-induced eNOS expression is markedly reduced in *Bmp2*$^{+/-}$ mutant mouse lungs (Figure 11A, B). Pulmonary eNOS expression is also reduced in normoxic *Bmp2*$^{+/-}$ mutant mice when compared with wild type littermates but this difference did not reach statistical significance. There are no differences in pulmonary *eNOS* mRNA expression in hypoxic wild type or *Bmp2*$^{+/-}$ mutant mice, suggesting that the associated changes in eNOS protein expression are regulated at a post-transcriptional level. Decreased pulmonary eNOS in *Bmp2*$^{+/-}$ mutant mice is associated with a reduction in hypoxia-induced phosphorylation of vasodilator stimulated phosphoprotein (VASP) Serine-239 (Figure 11A, C). VASP is phosphorylated at Ser239 by cGMP-dependent protein kinases (PKGs) (24). As PKGs are downstream mediators of nitric oxide signaling, analysis of phosphorylation at VASP Ser239 (pSer239 VASP) provides a sensitive indicator of NOS activity *in vivo* (150). The pSer239 VASP antibody also recognizes a higher molecular weight band corresponding to pSer157 VASP, a target of cAMP-dependent protein kinases (PKAs) (24). There is no significant change in pSer157 VASP expression between wild type and *Bmp2*$^{+/-}$ mutant mice under normoxic or hypoxic conditions (Figure

Figure 11. eNOS expression in *Bmp2*$^{+/-}$ mutant mouse lungs. A-D: Western blot and quantification of eNOS (A, B), phospho-Ser239 VASP (A, C), and phospho-Ser157 VASP (A, D) in whole lung lysates from wild type and *Bmp2*$^{+/-}$ mutant mice exposed to normoxia or 3 weeks hypoxia. **E:** Pulmonary *eNOS* mRNA expression assessed by quantitative RT-PCR under normoxic conditions (wild type n=8; *Bmp2*$^{+/-}$ n=6) or after 3 weeks hypoxia (wild type n=5; *Bmp2*$^{+/-}$ n=5). **F, G:** Western blot and quantification for eNOS expression in intrapulmonary artery preparations (IPAs) isolated from normoxic or 3 week hypoxic wild type and *Bmp2*$^{+/-}$ mutant mice. Data are expressed as mean +/- SEM for wild type (white bars) and *Bmp2*$^{+/-}$ (black bars). One-way ANOVA with Bonferroni correction, $p<0.05$: **a**, vs. wild type normoxia; **c**, vs. wild type 3 weeks hypoxia. Western blot analysis in A performed by L. Anderson.

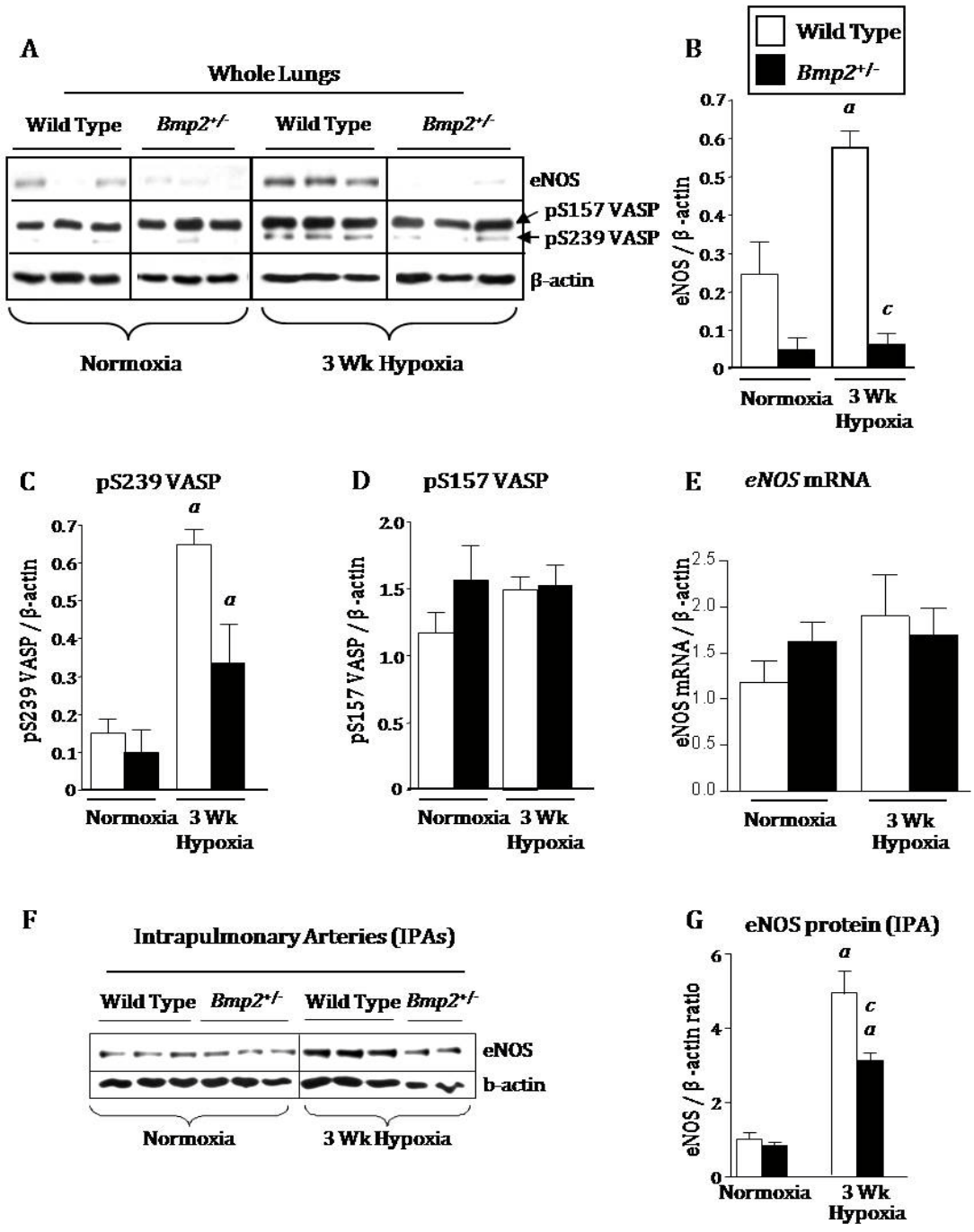
A
Whole Lungs
Wild Type
Bmp2+/-
Wild Type
Bmp2+/-
eNOS
pS157 VASP
pS239 VASP
β-actin
Normoxia
3 Wk Hypoxia
B
Wild Type
Bmp2+/-
eNOS / β-actin
a
c
Normoxia
3 Wk Hypoxia
C
pS239 VASP
pS239 VASP / β-actin
a
a
Normoxia
3 Wk Hypoxia
D
pS157 VASP
pS157 VASP / β-actin
Normoxia
3 Wk Hypoxia
E
eNOS mRNA
eNOS mRNA / β-actin
Normoxia
3 Wk Hypoxia
F
Intrapulmonary Arteries (IPAs)
Wild Type
Bmp2+/-
Wild Type
Bmp2+/-
eNOS
b-actin
Normoxia
3 Wk Hypoxia
G
eNOS protein (IPA)
eNOS / β-actin ratio
a
c
a
Normoxia
3 Wk Hypoxia

11A, D). This suggests that alterations in pSer239 VASP expression reflect differences in pulmonary PKG activity, and that reduced eNOS expression is associated with reduced pulmonary NOS activity in hypoxic *Bmp2*$^{+/-}$ mutant mice.

To examine the regulation of eNOS expression in the pulmonary vasculature of *Bmp2*$^{+/-}$ mice, we isolated whole intrapulmonary arterial (IPA) trees from wild type and *Bmp2*$^{+/-}$ mutant mice exposed to normoxia or 3 weeks hypoxia. This revealed that eNOS protein expression is significantly reduced in IPAs of hypoxic *Bmp2*$^{+/-}$ vs. wild type IPAs (Figure 11F, G). These findings are consistent with our observations in whole lungs and indicate that there is a defect in hypoxia-induced eNOS expression in the pulmonary vasculature of *Bmp2*$^{+/-}$ mice.

Bmp2, not Bmp4, is the ligand mediating Bmp-dependent regulation of eNOS *in vivo*

Our studies suggest that reduced eNOS expression in hypoxic *Bmp2*$^{+/-}$ mutant mice results from decreased expression of Bmp2 in the hypoxic lung. Since heterozygous null *Bmp4*$^{LacZ/+}$ mutant mice are protected from the development of hypoxic PH (54), we went on to evaluate the regulation of eNOS in hypoxic *Bmp4*$^{LacZ/+}$ mouse lungs. Unlike *Bmp2*$^{+/-}$, *Bmp4*$^{LacZ/+}$ mutant mice show a normal eNOS response to chronic hypoxia (Figure 12A, B), indicating that Bmp2 and Bmp4 have different effects on hypoxic regulation of eNOS *in vivo*. To evaluate this further, we compared eNOS responses to exogenous Bmp2 and Bmp4 treatment in IPAs. Bmp2 and Bmp4 induce similar increases in eNOS expression in wild type IPAs (Figure 13A, B). These findings indicate that the different effects of Bmp2 and Bmp4 in the hypoxic regulation of eNOS *in vivo* are unlikely to result from differences in direct ligand-dependent cellular responses. Based on our analyses of Bmp2 and Bmp4 expression domains in the hypoxic lung, we propose that the differential effects of these

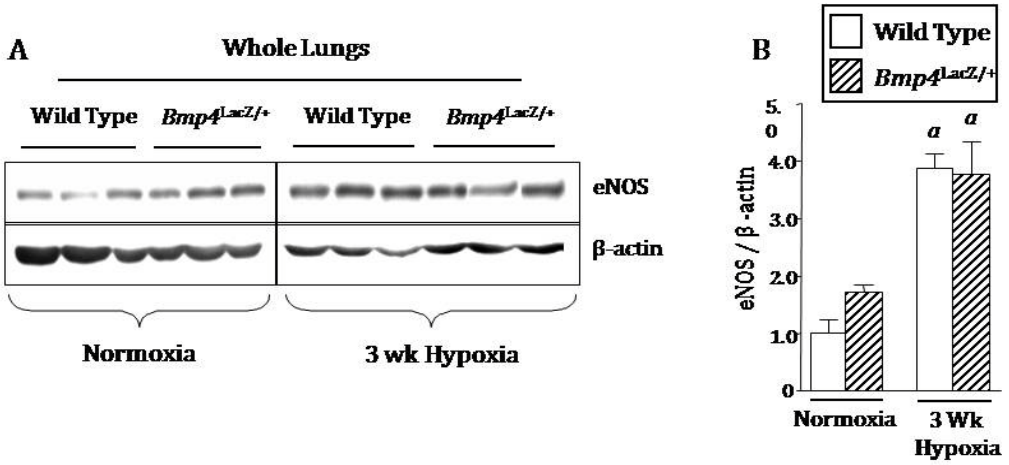

Figure 12. eNOS expression in *Bmp4*$^{LacZ/+}$ mutant mouse lungs. A-B: eNOS protein expression (A) and quantification (B) in wild type and *Bmp4*$^{LacZ/+}$ mutant lungs. Data are expressed as mean +/- SEM for wild type (white bars) and *Bmp4*$^{Lacz/+}$ mutant mice (hatched bars). One-way ANOVA with Bonferroni correction, $p<0.05$: **a**, vs. wild type normoxic.

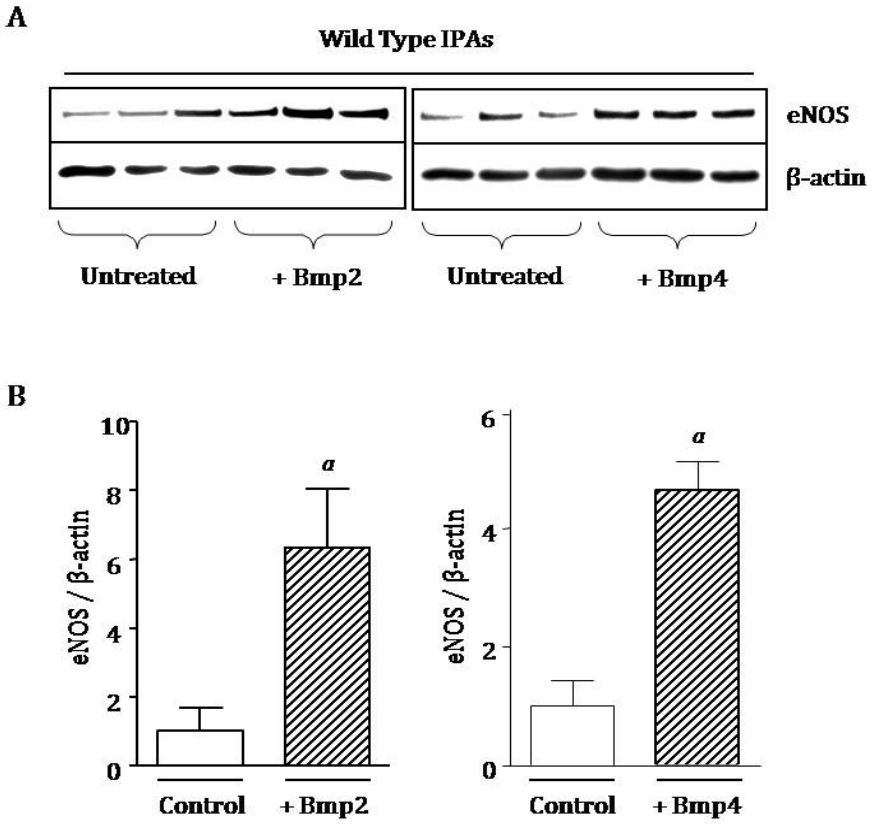

Figure 13. Regulation of eNOS by Bmp2 and Bmp4 in isolated IPA preparations. A: Western blot for eNOS expression in IPAs cultured +/- 50 ng/ml Bmp2 or Bmp4 for 18 hours before lysis. **B:** Quantification of eNOS blots by densitometry normalized to β-actin. Data are expressed as mean +/- SEM. Unpaired t-test, $p<0.05$: **a**, vs. untreated controls.

ligands on vascular function and eNOS expression *in vivo* result from their distinct cellular expression domains in the hypoxic lung.

Discussion

The majority of patients with HPAH inherit heterozygous *BMPR2* mutations (123), indicating that dysregulated BMPR2-dependent signaling contributes to the development of this disease. This suggest that defective BMPR2-dependent signaling might also play a role in more common forms of PH not associated with inherited *BMPR2* mutations. To address this, we have explored the mechanisms by which two of the Bmpr2 ligands that are expressed in the adult mouse lung, Bmp2 and Bmp4, modulate pulmonary vascular function and remodeling in hypoxic PH.

Bmp4 is expressed widely in bronchial and alveolar epithelium and, to a lesser extent, pulmonary ECs, and is up-regulated by chronic hypoxia; Bmp4 levels do not increase with hypoxia in *Bmp4*$^{LacZ/+}$ mutant mice, and these mice are protected from the development of hypoxic PH (54). As *Bmpr2*$^{\Delta Ex2/+}$ mutant mice develop more severe hypoxic PH (55), these data suggest that dominant effects of the *Bmpr2* mutation do not result from loss of Bmp4-dependent responses in the pulmonary vasculature. This led us to explore whether Bmp2, which is also up-regulated in the hypoxic lung (54), is the predominant intrapulmonary Bmp ligand responsible for activating these Bmpr2-dependent responses in the pulmonary vasculature. We now show that Bmp2 levels do not increase with hypoxia in heterozygous null *Bmp2*$^{+/-}$ mutant mice, and that these mice develop more severe hypoxic PH than wild type littermates. Furthermore, like *Bmpr2*$^{\Delta Ex2/+}$ mutant mice, there is marked

reduction in hypoxia-induced eNOS expression in the pulmonary vasculature of *Bmp2*$^{+/-}$ mutant mice. This is associated with a reduction in phosphorylation of VASP Ser239, which is a sensitive indicator of defective NO/cGMP signaling in the vasculature (150), suggesting that there is a decrease in pulmonary NOS activity in hypoxic *Bmp2*$^{+/-}$ mutant mice. This indicates that eNOS deficiency is a common feature in hypoxic *Bmp2*$^{+/-}$ and *Bmpr2*$^{\Delta Ex2/+}$ mutant mice. Furthermore, while it has been suggested that other intrapulmonary Bmp ligands (including Bmp6 and Bmp7) and/or circulating Bmp ligands (including Bmp9) may activate Bmpr2 in the pulmonary vasculature (211), our studies suggest that effects of *Bmpr2* mutations may in part result from loss of Bmp2-dependent responses in the vasculature.

Increased PH in *Bmp2*$^{+/-}$ mutant mice is associated with increased peripheral muscularization, a marker of pulmonary vascular remodeling. This is not associated with an increase in pulmonary VSMC proliferation in hypoxic *Bmp2*$^{+/-}$ mutant mice. VSMC proliferation in larger muscularized vessels is actually decreased in *Bmp2*$^{+/-}$ mutant mice after 1 week of hypoxia. These findings were unexpected as hypoxia-induced peripheral vessel muscularization is usually associated with increased VSMC proliferation (130). This expansion of peripheral muscularized vessels does not result from decreased VSMC apoptosis in hypoxic *Bmp2*$^{+/-}$ versus wild type mice, as our lab has been unable to detect pulmonary VSMC apoptosis in wild type mice exposed to 10% oxygen by TUNEL assay or cleaved caspase 3 staining (54). Therefore, while exogenous Bmp2 promotes growth inhibition and induces apoptosis in cultured VSMCs (54, 139, 202, 235, 238), our findings indicate that these responses do not play significant roles in promoting enhanced vascular remodeling in the hypoxic pulmonary vasculature of *Bmp2*$^{+/-}$ mutant mice *in vivo.* It has been proposed that peripheral vascular remodeling in hypoxia results from increased migration of differentiated pulmonary VSMCs from more proximal sites and/or increased

differentiation of non-muscularized peripheral vessel pericytes into VSMCs (130). Exogenous Bmp2 (and Bmp4) increase migration of cultured pulmonary VSMCs (54). On this basis, reduced expression of Bmp2 would be expected to reduce, not increase, the degree of hypoxia-induced peripheral vascular muscularization in *Bmp2*$^{+/-}$ mutant mice. Therefore, our studies suggest that increased hypoxic peripheral muscularization in *Bmp2*$^{+/-}$ mutant mice is most likely to result from increased vascular pericyte differentiation into VSMCs. The mechanism by which this occurs is unknown.

Bmp2 and Bmp4 have 92% amino acid sequence identity and are essentially indistinguishable in most *in vitro* functional assays. However, studies from our lab suggest that Bmp2 and Bmp4 have opposing effects in hypoxic PH *in vivo*. Furthermore, there is a marked reduction in hypoxia-induced eNOS expression in *Bmp2*$^{+/-}$ mutant mice while eNOS expression is unaffected in *Bmp4*$^{LacZ/+}$ mutant mouse lungs. As discussed in Chapter 2, eNOS deficiency could account for the differences in PH responses to chronic hypoxia in the two *Bmp* mutant mouse lines. However, our studies also show that eNOS expression is induced equally after treating cultured IPA preparations with exogenous Bmp2 and Bmp4. This suggests that the opposing effects of these ligands *in vivo* do not result from differences in direct cellular responses to Bmp2 and Bmp4. One explanation is that vascular target cells respond differently to these ligands *in vivo* because Bmp2 and Bmp4 are expressed in distinct cellular domains of the lung. Our findings using *Bmp2* BAC transgenic reporter mice to identify cellular expression domains of Bmp2 in the hypoxic lung support this hypothesis. Together with our lab's earlier observations using *Bmp4* LacZ knock-in mice to evaluate Bmp4 localization in the hypoxic lung (54), these findings indicate that Bmp2 and Bmp4 are expressed in overlapping expression domains in the alveolar epithelium, but that Bmp2 is more strongly expressed than Bmp4 in small peripheral vessels in the hypoxic lung. Therefore, reduced expression of the two Bmp ligands in *Bmp2*$^{+/-}$ versus *Bmp4*$^{LacZ/+}$ mutant

mice may have different effects on vascular function and eNOS expression as a result of differences in local Bmp concentrations in and around the hypoxic pulmonary vasculature. Future studies to further evaluate these possibilities are proposed in Chapter 5.

In summary, these studies demonstrate for the first time the opposing roles of Bmp2 and Bmp4 ligands in the development of hypoxic PH. We show that eNOS deficiency is a common feature in hypoxic *Bmp2*$^{+/-}$ and *Bmpr2*$^{\Delta Ex2/+}$ mutant mice and suggest that Bmp2 is the predominant ligand mediating Bmpr2-dependent effects in the hypoxic pulmonary vasculature. As the functional effects of Bmp2 and Bmp4 are indistinguishable *in vitro*, these findings underscore the importance of studies to evaluate the functional role of the Bmp pathway *in vivo*. These studies shed new light on the mechanisms by which aberrant BMP signaling associated with *BMPR2* mutations may contribute to the pathogenesis of HPAH as well as other, more common forms of PH not associated with inherited *BMPR2* mutations.

Acknowledgments

The studies described in this chapter were a collaborative effort among several individuals. A particular debt of gratitude is owed to Lynda Anderson, Mark Jones, Tatiana Novitskaya, David Frank, Mark deCaestecker, and Doug Mortlock, without whom these studies would not have been possible.

CHAPTER IV

ROLE AND REGULATION OF ID FAMILY MEMBERS IN HYPOXIC PH

Introduction

Advances in our understanding of the mechanisms underlying HPAH will likely come from investigation of the downstream signaling effectors of Bmp signaling. The receptor Bmpr2 is a component of the Bmp signaling cascade which is activated when members of this family of growth factors bind to specific combinations of type I and type II Bmp receptors. Activation of these receptors leads to C-terminal phosphorylation of the receptor-activated Smads (Smad1/5/8), their nuclear translocation, and transactivation of target genes (42). One such well-characterized transcriptional target of Bmp-activated Smads is the gene encoding the basic helix-loop-helix (bHLH) protein Inhibitor of Differentiation 1 (Id1) (135, 205). Id proteins, of which there are four known members in mammals (Id1-4), lack the DNA binding basic domain, thereby serving as dominant negative regulators of transcription by heterodimerization with other bHLH proteins (83). The best described targets of Id1 are members of the ubiquitously expressed family of "E" proteins, which are sequestered and prevented from binding to tissue-specific bHLH proteins (149). This negative regulatory function allows Id1 to play a role in multiple cellular processes. For example, Id1 promotes proliferation, inhibits differentiation, and in some cases induces apoptosis (171, 186, 220). Being a well-characterized Bmp target, expression of Id1 has been used as a downstream readout of active Bmp signaling in multiple systems, including

the study of PH (54, 68, 140, 203, 233). However, little is known about the role Id1 plays in the events leading to the development of PH.

The vascular remodeling that is characteristic of human PAH has been suggested to arise from increased proliferation and migration of VSMCs, reduced vascular cell apoptosis, and trans-differentiation of pericytes (130). Previous *in vitro* work suggests a complex and cell-dependent functional role for Id1 in mediating many of these functions. For example, it has been shown that ID1 promotes proliferation, tube formation, and migration of human umbilical vein and bovine aortic ECs (107, 148, 172, 215). ID1 also promotes migration of human umbilical vein VSMCs (30). On the other hand, another group of investigators has shown that ID1 exerts anti-proliferative effects in human pulmonary artery smooth muscle cells (233). In these studies, BMP-mediated regulation of ID1 was shown to be BMPR2-dependent, leading these authors to conclude that reduced expression of ID1 in pulmonary VSMCs from HPAH patients with *BMPR2* mutations might promote pulmonary vascular remodeling in this disease.

In vivo studies on Id1 expression also suggest a complex regulation of Id1 in different models of PH. For example, pulmonary Id1 expression is reduced in the monocrotaline-injury rat model (115, 140), unchanged (115) or reduced (200) in the rat model of chronic hypoxia, but increased in murine hypoxic PH (54). Furthermore, we have shown that pulmonary Id1 expression is reduced in mice that are heterozygous deficient for the ligand *Bmp4*, suggesting that *Id1* is an *in vivo* target of Bmp4 (54). Since these studies also revealed that *Bmp4* mutant mice are protected from the development of hypoxic PH, pulmonary vascular remodeling, and hypoxia-induced VSMC proliferation, these findings also suggest that Id1 could be acting as a downstream mediator of Bmp4 to promote hypoxia-induced remodeling of the pulmonary vasculature. This is consistent with

numerous studies indicating that Id1 promotes proliferation in a variety of cell types (171, 186, 220), but contrasts with *in vitro* studies suggesting that Id1 mediates anti-proliferative effects of Bmp4 in pulmonary VSMCs (233).

To address these inconsistencies in the literature, we sought to determine the definitive *in vivo* role of Id1 in a model of chronic hypoxia-induced PH using a genetic approach in mice. Despite robust induction of Id1 expression in the pulmonary vasculature of wild type mice by hypoxia, we found no differences in hypoxic PH, pulmonary vascular remodeling, or proliferation in wild type mice and mice with germ line *Id1* deficiency. However, loss of Id1 expression led to up-regulation of other Id family members in the lung – *Id1 null* mutant mice display a selective increase in expression of Id3 in pulmonary VSMCs. Taken together, these findings indicate that Id1 is not required for the development of hypoxic PH or pulmonary vascular remodeling, but suggest that Id3 compensates for loss of Id1 expression in the pulmonary vasculature of *Id1* null mice. On this basis, we propose that there could be functional redundancy between Id1 and Id3 in the hypoxic pulmonary vasculature. Results from these studies have been submitted for publication and are currently under revision (118).

Methods

Mouse lines

Germ line, *Id1 null* mutant mice (230) bred on a C57Bl/6J x 129 genetic background were a gift from Robert Benezra (Memorial Sloan-Kettering Cancer Center). Genotyping was performed by PCR of ear punch DNA using primers outlined in Table 6.

Experimental pulmonary hypertension

Experimental PH was carried out as described in Chapter 2.

Histological evaluation of pulmonary vascular remodeling and proliferation

Evaluation of pulmonary vascular remodeling was performed as described in Chapter 2. Vascular cell proliferation was determined as described in Chapter 3. Proliferating ECs and VSMCs stain positive for PCNA and are identified by their respective location in the vessel wall by α-SMA staining. Vascular cell proliferation is expressed as cell type-specific index (number of proliferating EC or VSMC/total number of EC or VSMC counted).

Intrapulmonary artery tree isolation

IPA trees were isolated as described in Chapter 2.

Western blot

Western blot analyses were performed as described in Chapter 2 using the antibodies outlined in Table 7. Western blots for Id1 were performed using three different anti-Id1 antibodies: rabbit monoclonal antibodies Clone 195-14 and Clone 37-2 (BioCheck), and rabbit polyclonal (Santa Cruz, SC-488), as indicated. Specificity for each antibody was confirmed by lack of signal in lung lysates from *Id1 null* mice (Figure 14). Additionally, rabbit polyclonal anti-Id2 (Santa Cruz, SC-489), rabbit monoclonal anti-Id3 Clone 17-3

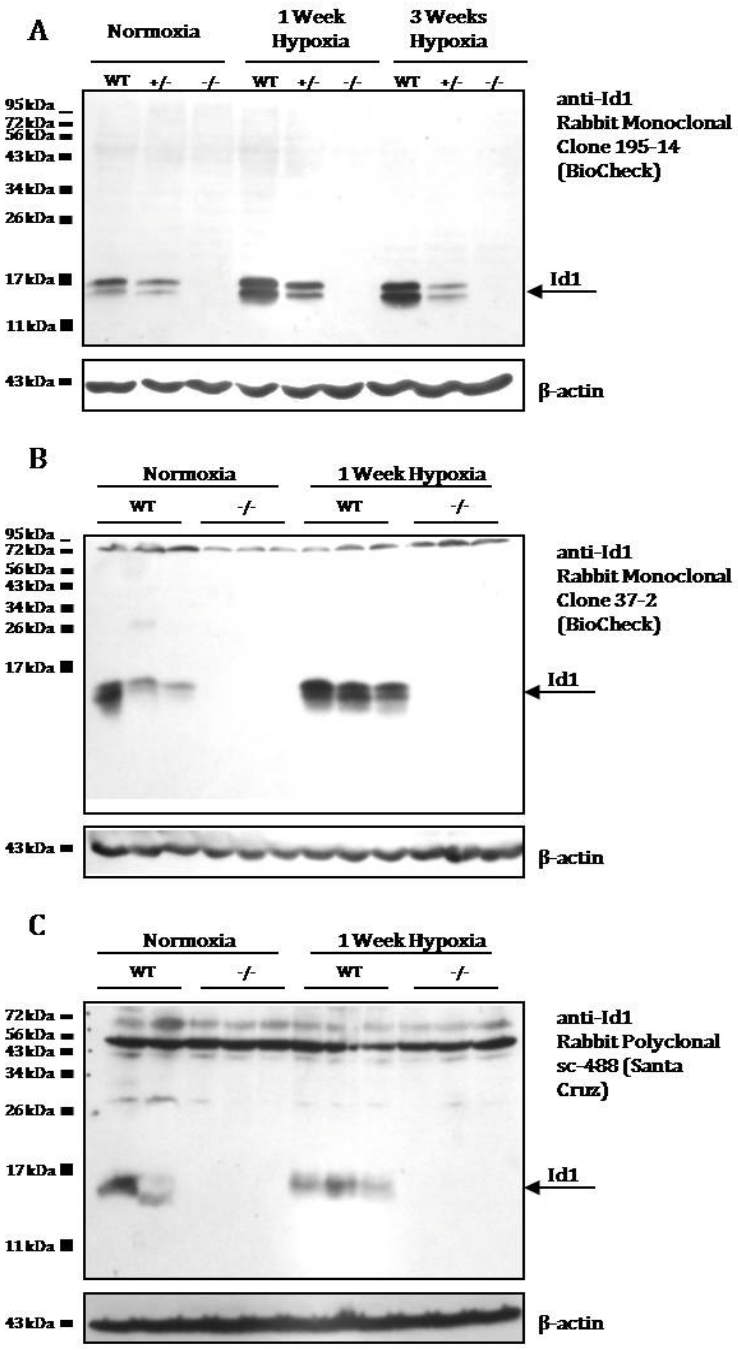

Figure 14. Western blot specificity of anti-Id1 antibodies. Western blot for Id1 and β-actin in normoxic, 1 week hypoxic, and 3 week hypoxic wild type, *Id1*$^{+/-}$, and *Id1* null whole lung lysates, as indicated. Specificity of staining was determined by the absence of signal in lung lysates from *Id1 null* mice using rabbit monoclonal anti-Id1 antibodies Clones 195-14 (**A**) and 37-2 (**B**) (Biocheck) and a rabbit polyclonal anti-Id1 antibody (Santa Cruz, SC-488) (**C**).

(BioCheck), rabbit polyclonal anti-C-terminal phospho-Smad1/5/8 (Cell Signaling, 9511), and mouse monoclonal anti-β-actin antibody Clone AC-74 (Sigma) were used. Specific bands (doublet for Id1, single bands for Id2 and Id3) were quantified by densitometry and normalized to β-actin loading controls.

Immunohistochemistry

Immunoperoxidase staining for Id1, Id2, and Id3 was performed on formalin-fixed, paraffin-embedded lung sections using diamino benzidine with ABC amplification (Vector) and counterstained with Mayer's hematoxylin (Fluka). Rabbit monoclonal anti-Id1 Clone 37-2, anti-Id2 Clone 92-8, and anti-Id3 Clone 17-3 antibodies were used (Id1-3 antibodies from Biocheck). Cells positive for Id protein expression were quantified from ten 200X fields while blinded to treatment and genotype. For these studies we evaluated airway-associated vessels separated into small (20-50 μm) and larger vessel sizes (50-100μm). Vessels were only scored if in cross-section, and counts were expressed as number of positive cells per vessel.

Immunofluorescence was performed on formalin-fixed, paraffin-embedded lung sections with the antibodies outlined above and detected with a rabbit IgG specific HRP-conjugated secondary antibody amplified using Cy3 labeled tyramide signal amplification, according to the manufacturer's instructions (Perkin Elmer). DNA was stained with DAPI (Vector). VSMCs were identified by α-smooth muscle actin (α-SMA) staining using mouse monoclonal anti-α-SMA (Sigma) and a FITC-labeled anti-mouse IgG secondary antibody (Vector). While blinded to genotype and treatment conditions, Id1-3 positive cells were quantified in ten 200X fields of view. For these studies, we focused on small (20-50 μm) peripheral muscularized vessels distal to terminal bronchioles as these are the major site of

pulmonary vascular remodeling in hypoxic PH (130). Cells were defined as VSMCs if α-SMA positive, and EC when located internal to α-SMA positive smooth muscle cells. Vessels were only scored if in cross-section. Id1-3 positive cells were expressed as compartment-specific Id1-3 positive cellular indices (Id1-3 positive VSMC or EC/total VSMC or EC DAPI stained nuclei).

Statistical analyses

Statistical analyses were performed as described in Chapter 2.

Results

Regulation of pulmonary Id1 expression by hypoxia

To evaluate the regulation of pulmonary Id1 in response to hypoxia, we first performed western blot analyses of whole lung lysates. This revealed low level expression of Id1 in normoxic lungs with a robust induction of Id1 after 1 week and 3 weeks of hypoxia (Figure 15A, B). This increase in Id1 expression was confirmed using two other commercially available antibodies (Figure 14). All of the antibodies detect a doublet for Id1 that is lost in *Id1 null* lysates, confirming that both bands represent Id1 isoforms. Increased Id1 expression is associated with correlative activation of the Bmp pathway, as indicated by increased C-terminal phosphorylation of the receptor activated Smads 1, 5 and 8 (pS1/5/8) in response to hypoxia (Figure 15A). Since Id1 may be expressed in different cell types in the lung, we went onto evaluate Id1 expression in the pulmonary arterial vasculature by

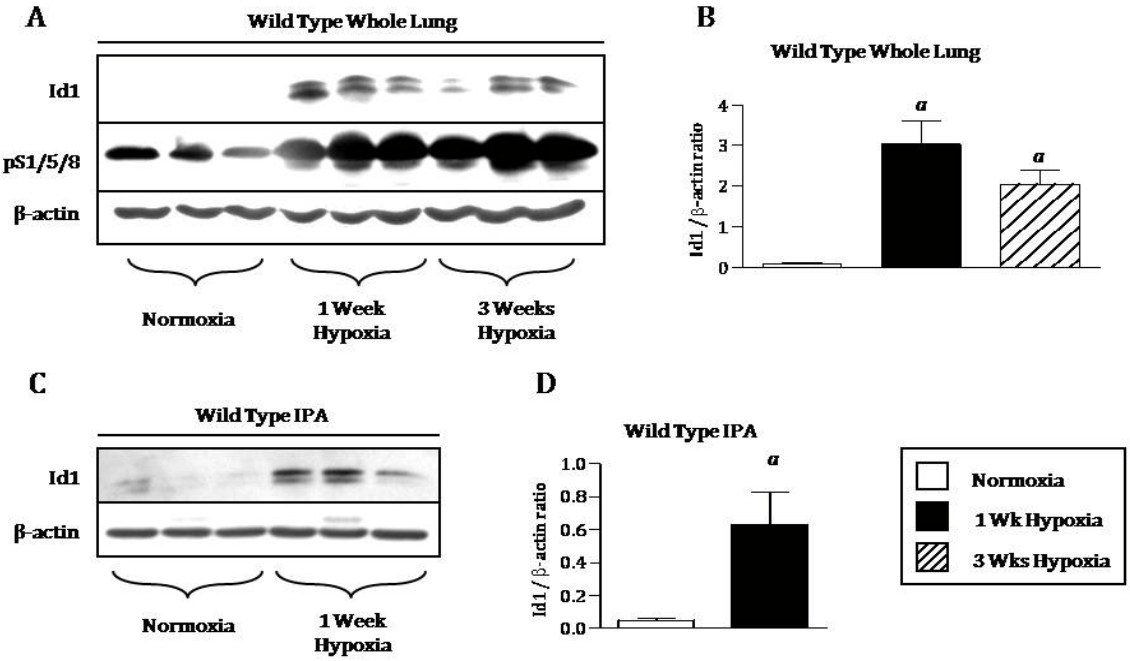

Figure 15. Regulation of Id1 expression in the hypoxic lung. A: Western blot for Id1 using rabbit monoclonal antibody Clone 195-14, phospho-Smad1/5/8 (pS1/5/8) and β-actin in normoxic, 1 week hypoxic and 3 week hypoxic wild type lung lysates. **B:** Densitometry of Id1 bands (doublet) relative to β-actin controls from A. **C:** Western blot for Id1 using anti-Id1 Clone 195-14 in normoxic and 1 week hypoxic wild type intrapulmonary artery (IPA) preparations. **D:** Densitometry of Id1 bands relative to β-actin from C. Data are expressed as mean +/- SEM. **a**: $p<0.05$ versus wild type normoxic control by One-Way ANOVA with Bonferroni correction (B) or two-tailed t-test (D).

western blot using IPAs isolated from wild type mice maintained under normoxic or hypoxic conditions. As seen in whole lungs, low levels of Id1 in IPAs isolated from normoxic mice are up-regulated after exposure to 1 week of hypoxia (Figure 15C, D).

Localization of Id1 expression in the hypoxic pulmonary vasculature

Having observed robust induction of Id1 expression in the hypoxic pulmonary vasculature, we sought to determine the precise localization of Id1 in the hypoxic lung by immunohistochemistry. For this, we first evaluated the specificity of three different commercially available Id1 antibodies by comparing staining of lung sections from wild type and *Id1 null* mice exposed to 1 week hypoxia. The first antibody we tested, a rabbit polyclonal anti-Id1 from Santa Cruz (C-20, sc-488), has been used extensively to evaluate Id1 expression domains in a variety of different tissues (1, 25, 37, 43, 54, 76, 109-110, 153, 160, 209, 216, 231, 237). This antibody gave selective staining of lung ECs in wild type but not *Id1 null* mice (Figure 16A, B, D, E). However, this antibody also gave non-specific cytoplasmic staining of bronchial and VSMCs in some of the muscularized vessels of wild type and *Id1 null* lungs (Figure 16C, F). Given this non-specific staining of VSMCs, we went on to evaluate immunohistochemical staining of the lung using two other commercially available anti-Id1 rabbit monoclonal antibodies, Clones 195-14 and 37-2 (BioCheck). Both of these antibodies have been validated in *Id1 null* mammary tissue, but there are no data on their use in mouse lungs (160). Clone 195-14 did not stain wild type or *Id1 null* lung tissue (data not shown). Clone 37-2, on the other hand, gave dominant nuclear staining in alveolar and EC compartments in wild type but not *Id1 null* lung tissue (Figure 16G-L). Therefore, studies on Id1 localization were performed using the specific rabbit monoclonal Clone 37-2.

Figure 16. Characterization of immunohistochemical staining using different Id1 antibodies. Immunoperoxidase staining for Id1 in lung sections from 1 week hypoxic wild type and *Id1 null* mice as indicated. **A-F:** Rabbit polyclonal anti-Id1 antibody (Santa Cruz, SC-488). Arrowheads denote nuclear staining in ECs which is absent in *Id1 null* lungs. Thick arrows indicate non-specific, cytoplasmic staining seen in vessel walls and bronchial smooth muscle cells in wild type and *Id1 null* mouse lungs. **G-L:** Rabbit monoclonal anti-Id1 antibody Clone 37-2 (Biocheck). Nuclear staining of ECs (arrowheads) and VSMCs within the vessel walls (thin arrows) is seen in wild type but not *Id1 null* mouse lungs. Sections were counterstained with hematoxylin. **I, L:** Inset from H and K, respectively. Bar is 50 μm. * indicates vessels.

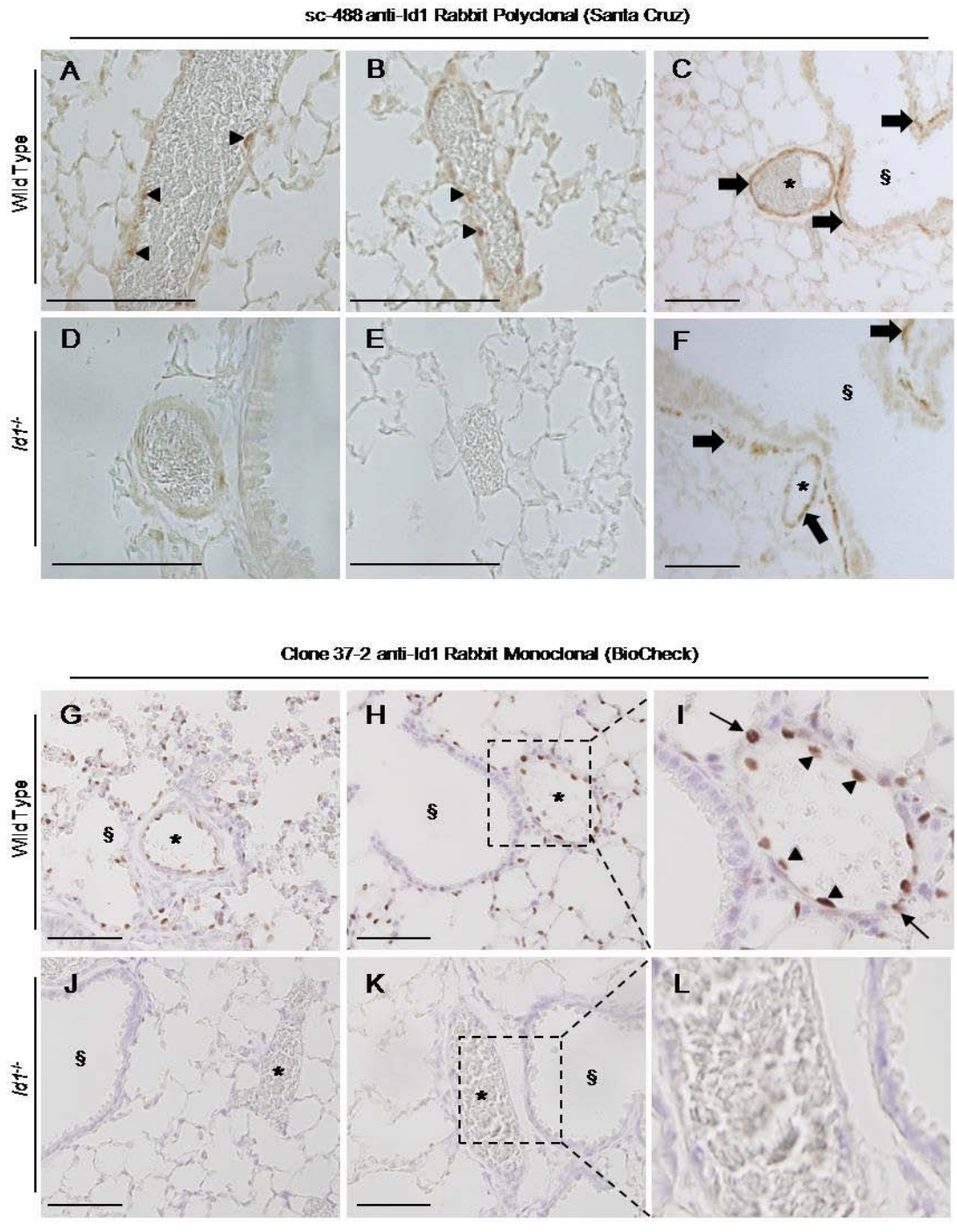
sc-488 anti-Id1 Rabbit Polyclonal (Santa Cruz)
Wild Type
Id1-/-
A
B
C
D
E
F
§
*
Clone 37-2 anti-Id1 Rabbit Monoclonal (BioCheck)
Wild Type
Id1-/-
G
H
I
J
K
L
§
*

By immunoperoxidase staining, we found that Id1 is expressed in alveolar epithelium and ECs under both normoxic and hypoxic conditions (Figure 17A-E). There is no detectable Id1 in larger airways or in bronchial smooth muscle cells using these antibodies (Figure 18). Negative staining of hypoxic *Id1 null* mouse lungs confirms antibody specificity in these studies (Figure 17F). Quantification of Id1-positive alveolar cells and vascular cells in small airway-associated vessels (20-50 μm diameter) shows that both are significantly increased in response to hypoxia (Figure 17G, H). Larger vessels (50-100 μm diameter) also tend to have increased numbers of Id1-positive cells, but this increase is not statistically significant ($p=0.077$; Figure 17I). The majority of vessel-associated Id1 expressing cells are ECs under both normoxic and hypoxic conditions (Figure 17A-E; Figure 18). However, there is a significant increase in Id1 expressing cells in the walls of these larger vessels under hypoxic conditions (mean ± SEM per vessel, normoxia: 0.158 ± 0.158 vs. hypoxia: 0.706 ± 0.122, two-tailed t-test, $p<0.03$). These cells are located within the vessel wall and have elongated nuclei typical of VSMCs and (Figure 17C, E; arrows).

To more fully characterize the cellular distribution of Id1 in the pulmonary vasculature, we performed double immunofluorescence analysis for Id1 and the smooth muscle cell marker, α-smooth muscle actin (α-SMA). For these studies, we focused on small intrapulmonary resistance vessels (20-50 μm diameter and distal to terminal bronchioles), since these vessels are the main site of pulmonary vascular remodeling in hypoxic PH (130). As in the airway-associated vessels, most Id1 expressing cells in these small peripheral vessels are inside the smooth muscle wall, consistent with their being ECs (Figure 17J-O, arrowheads). Specificity of Id1 antibody staining in these studies was again confirmed by negative staining of hypoxic *Id1 null* mouse lungs (Figure 17P). Quantification of cellular expression under hypoxic conditions revealed a selective increase in the proportion of Id1-positive VSMCs compared with peripheral vessels from normoxic lungs (Figure 17Q). There

Figure 17. Localization of Id1 expression in the hypoxic lung. A-E: Immunoperoxidase staining for Id1 in lung sections from normoxic and 1 week hypoxic wild type mice using rabbit monoclonal anti-Id1 antibody Clone 37-2 (BioCheck). **E:** inset from D. **F:** Negative staining of 1 week hypoxic lung from *Id1 null* mouse using anti-Id1 Clone 37-2. **G-I:** Quantification of Id1 positive nuclei in alveoli and both small (20-50 μm) and larger airway-associated muscularized vessels (50-100 mm) from normoxic and 1 week hypoxic wild type mouse lungs (normoxic n=4, 1 week hypoxia n=5). **J-O:** Immunofluorescence for Id1 (red) and a-SMA (green) in muscularized pulmonary vessels distal to terminal bronchioles (20-50 μm diameter) from normoxic and 1 week hypoxic wild type mice using rabbit anti-Id1 monoclonal antibody Clone 37-2. Nuclear staining with DAPI is shown in blue. **P:** Negative staining of 1 week hypoxic lung from *Id1 null* mouse using anti-Id1 Clone 37-2. **Q, R:** Quantification of cell-specific Id1 expression indices in VSMC (Q) and EC (R) compartments in 20-50 μm muscularized peripheral vessels from normoxic and 1 week hypoxic wild type mouse lungs (n=4 each group). Bar is 100 μm. * indicate vessels, arrows indicate VSMC staining, arrowheads denote EC staining. Data are expressed as mean +/- SEM. **a**: $p<0.05$ versus wild type normoxic control by two-tailed t-test.

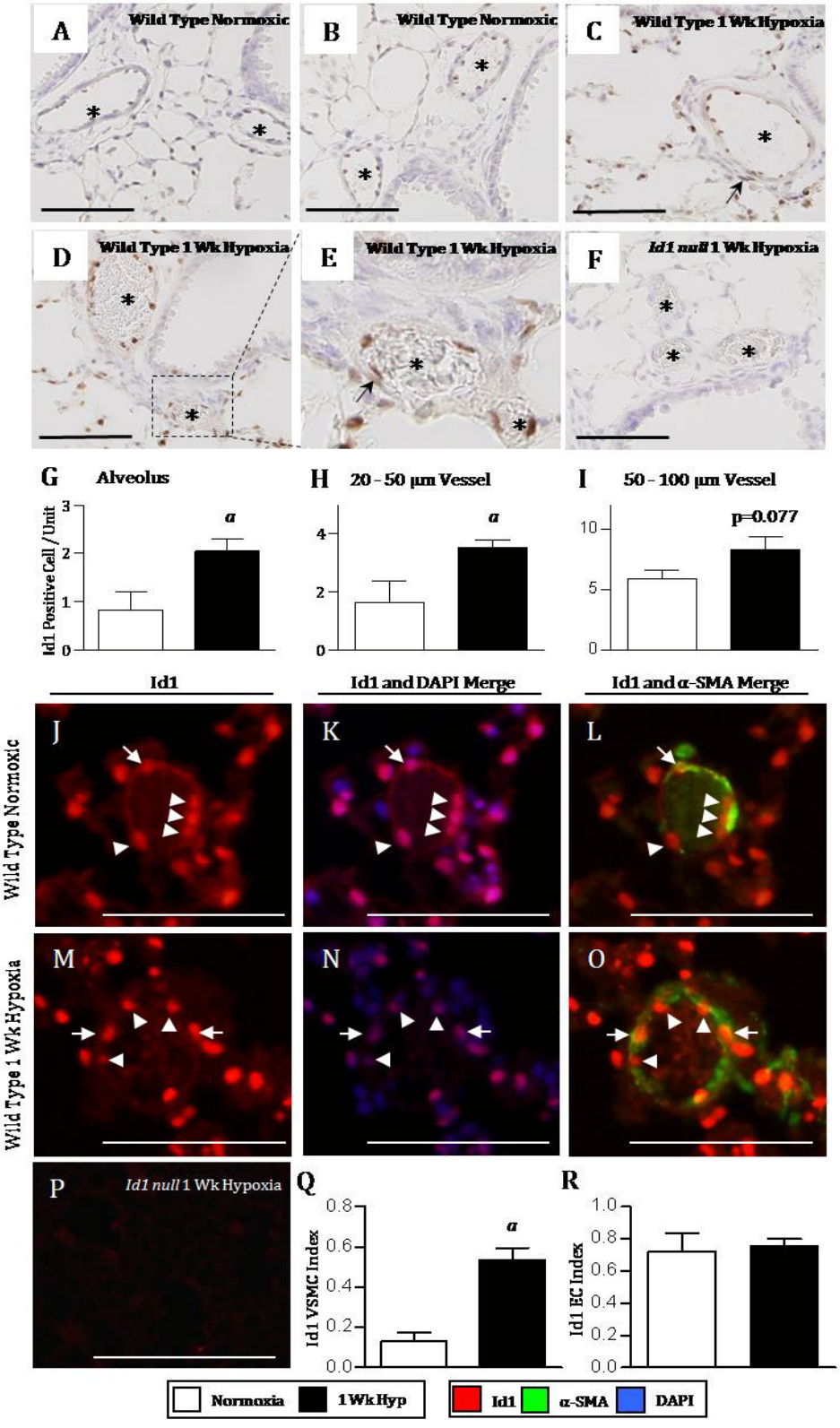
A
Wild Type Normoxic
B
Wild Type Normoxic
C
Wild Type 1 Wk Hypoxia
D
Wild Type 1 Wk Hypoxia
E
Wild Type 1 Wk Hypoxia
F
Id1 null 1 Wk Hypoxia
G
Alveolus
Id1 Positive Cell / Unit
a
H
20 - 50 µm Vessel
a
I
50 - 100 µm Vessel
p=0.077
Id1
Id1 and DAPI Merge
Id1 and α-SMA Merge
Wild Type Normoxic
Wild Type 1 Wk Hypoxia
J
K
L
M
N
O
P
Id1 null 1 Wk Hypoxia
Q
Id1 VSMC Index
a
R
Id1 EC Index
Normoxia
1 Wk Hyp
Id1
α-SMA
DAPI

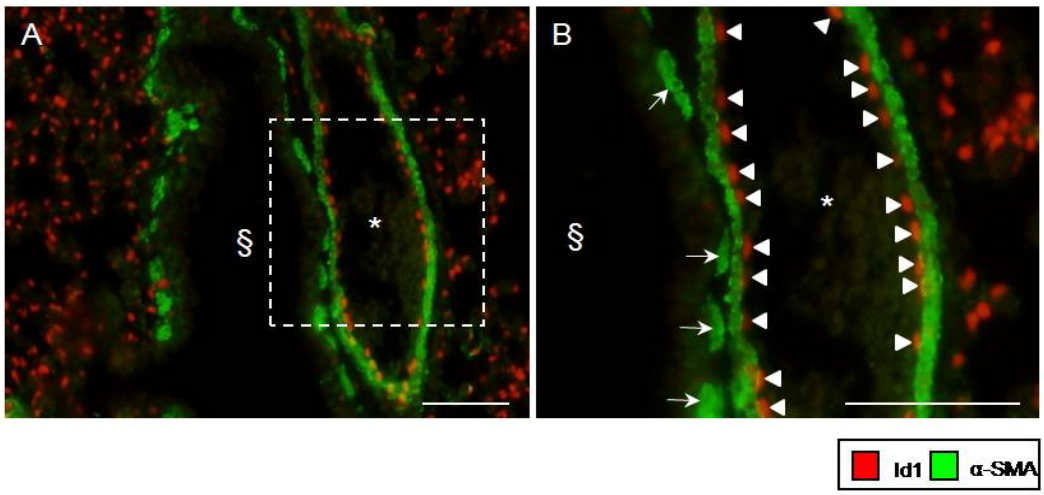

Figure 18. **Immunofluorescence for Id1 localization in hypoxic lungs. A:** Prominent endothelial staining for Id1 in a larger diameter vessel cut in longitudinal section and negative staining of bronchial smooth muscle cells using rabbit monoclonal anti-Id1 antibody Clone 37-2 (red). Tissues are counterstained with mouse anti-a-SMA antibodies (green) to identify smooth muscle cells. **B:** inset from A. Images were taken from a wild type mouse exposed to 1 week hypoxia. Bar is 100 μm. * indicates vessel, arrowheads indicate ECs, arrows indicate bronchial smooth muscle cells.

is no change in the proportion of Id1-positive ECs in vessels from normoxic or hypoxic mice (Figure 17R). Taken together, these findings indicate that there is a generalized increase in Id1-expressing cells in alveolar epithelium and small airway-associated vessels following exposure to hypoxia, and that this is associated with a specific increase in the number of Id1-positive VSMCs in both large and small intrapulmonary arteries and distal arterioles.

Role of Id1 in the development of hypoxic pulmonary hypertension

To investigate the functional role of Id1 in hypoxic PH, we obtained mutant mice with targeted disruption of the *Id1* genomic locus (230). *Id1 null* mice are viable and no apparent developmental abnormalities are observed in either gender. Western blot for Id1 expression confirmed that hypoxic induction of pulmonary Id1 expression is diminished or absent in $Id1^{+/-}$ and *Id1 null* mice, respectively (Figure 19A, the full length western blot is shown in Figure 14A). We measured RVSP in wild type, $Id1^{+/-}$ and *Id1 null* mice after exposure to 1 or 3 weeks normobaric hypoxia. There is a significant increase in RVSP in response to hypoxia in wild type and *Id1* mutant mice, but no difference in RVSP between wild type and *Id1* deficient mice under any of the treatment conditions (Figure 19B and Table 12). Male mice develop more severe PH after 3 weeks of hypoxia than female mice, but *Id1* deficiency does not modulate this effect within either gender (Table 12). No elevation of RVDP or LVDP was observed, confirming that the increase in RVSP is not due to left-sided heart failure (data not shown). These hemodynamic data are supported by measurements of RV hypertrophy, which also increase after 3 weeks of hypoxia, but reveal no differences between genotypes (Table 12). There is also no difference in sedated heart rate or hypoxia-induced increase in hematocrit between genotypes (Table 12).

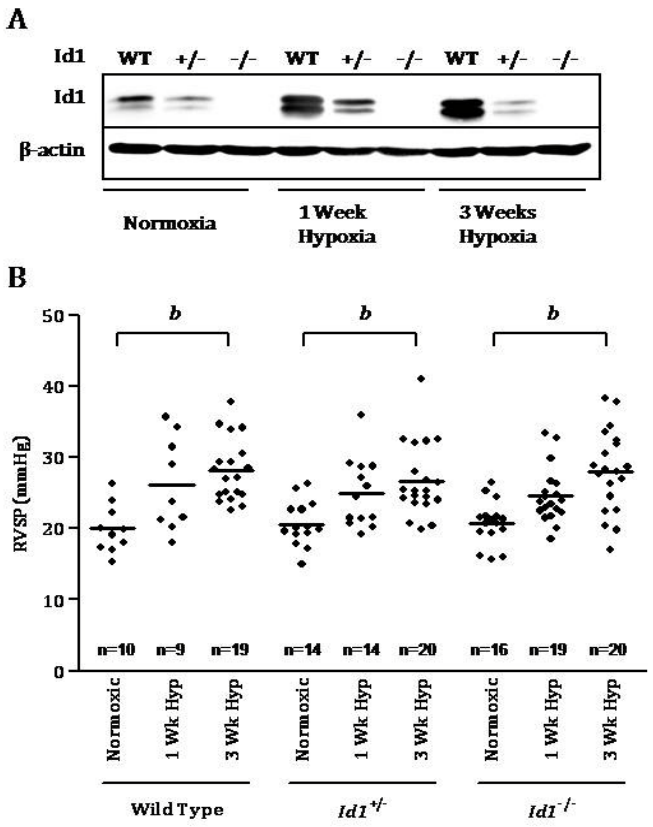

Figure 19. Hypoxic PH responses in wild type and *Id1* deficient mice. A: Representative western blot for Id1 using rabbit monoclonal antibody Clone 195-14 and β-actin in normoxic, 1 week hypoxic and 3 week hypoxic wild type, *Id1*$^{+/-}$, and *Id1 null* whole lung lysates. **B:** Right Ventricular Systolic Pressures (RVSP) in wild type, *Id1*$^{+/-}$ and *Id1 null* mice exposed to normoxia, 1 week or 3 weeks hypoxia. Mouse numbers are indicated (n). Each dot represents the mean RVSP from a single animal; bars indicate mean values for each group. **b**: $p<0.05$ versus corresponding genotype normoxic control by One-Way ANOVA with Bonferroni correction.

Table 12. Hypoxic PH in wild type and *Id1* deficient mice. Data are expressed as mean +/- SEM from wild type, *Id1*$^{+/-}$, and *Id1 null* mice exposed to normoxia, 1 week, or 3 weeks hypoxia. Mouse numbers are indicated (n). ***b***: $p<0.05$ versus corresponding genotype normoxic control, and ***c***: $p<0.05$ versus female wild type 3 week hypoxia by One-Way ANOVA with Bonferroni correction.

	Normoxia			1 Week Hypoxia			3 Weeks Hypoxia		
	Wild Type Mean±SEM (n)	*Id1*$^{+/-}$ Mean±SEM (n)	*Id1*$^{-/-}$ Mean±SEM (n)	Wild Type Mean±SEM (n)	*Id1*$^{+/-}$ Mean±SEM (n)	*Id1*$^{-/-}$ Mean±SEM (n)	Wild Type Mean±SEM (n)	*Id1*$^{+/-}$ Mean±SEM (n)	*Id1*$^{-/-}$ Mean±SEM (n)
RVSP, mmHg	19.96±1.06 (10)	20.66±0.84 (14)	20.76±0.77 (16)	26.18±2.18 (9)	24.15±1.50 (14)	24.59±0.88 (19)	28.12±1.01 *b* (19)	26.68±1.14 *b* (20)	28.04±1.29 *b* (20)
Female RVSP, mmHg	19.01±1.58 (6)	20.91±1.38 (8)	19.81±0.83 (6)	23.66±2.61 (4)	21.01±1.96 *b* (6)	23.16±0.83 *b* (10)	25.75±0.84 *b* (10)	24.91±1.01 *b* (11)	25.69±1.46 *b* (10)
Male RVSP, mmHg	21.39±1.09 (4)	20.33±0.85 (6)	21.33±1.12 (10)	28.19±3.27 (5)	26.50±1.85 *b* (8)	26.19±1.51 *b* (9)	30.75±1.52 *b c* (9)	28.85±2.08 *b* (9)	30.39±1.92 *b* (10)
RV/LV+S, mg/mg	0.257±0.008 (10)	0.245±0.005 (20)	0.258±0.009 (15)	0.291±0.016 (5)	0.302±0.011 *b* (14)	0.339±0.015 *b* (13)	0.368±0.013 *b* (17)	0.362±0.009 *b* (22)	0.360±0.007 *b* (21)
RV/Body Weight, mg/g	0.186±0.006 (10)	0.191±0.004 (20)	0.213±0.011 (15)	0.246±0.011 (4)	0.250±0.008 *b* (14)	0.263±0.01 *b* (13)	0.309±0.012 *b* (17)	0.291±0.009 *b* (22)	0.288±0.012 *b* (21)
Hematocrit,%	32.50±2.13 (7)	35.42±0.92 (21)	36.95±0.91 (11)	39.75±1.76 (8)	47.36±1.56 *b* (11)	46.76±1.21 *b* (15)	46.36±1.23 *b* (11)	50.92±1.45 *b* (13)	49.33±1.83 *b* (18)
Heart Rate, bpm	421.3±21.1 (10)	451.8±21.4 (16)	439.1±14.1 (16)	408.8±19.5 (9)	415.7±9.5 *b* (14)	415.8±10.1 *b* (20)	418.5±9.3 *b* (19)	425.8±12.9 *b* (20)	398.0±13.8 *b* (20)

To determine whether loss of Id1 expression is associated with alterations in hypoxia-induced pulmonary vascular remodeling, we evaluated the degree of hypoxia-induced peripheral vessel muscularization and proliferation in wild type, *Id1*$^{+/-}$, and *Id1 null* mouse lungs. Supporting our finding that Id1 is dispensable for the development of hypoxic PH, this characteristic increase in peripheral muscularization does not differ between genotypes (Table 13). Furthermore, while small, peripheral pulmonary vessels from hypoxic *Id1*$^{+/-}$ and *Id1* $^{-/-}$ mice tend to have an increased numbers of PCNA positive proliferating VSMCs, this increase is not statistically significant. There is no difference in EC proliferation with hypoxia between genotypes (Table 13). Collectively, these data indicate that expression of Id1 is not required for the physiologic events, vascular remodeling or vascular cell proliferation associated with the development of hypoxic PH.

Compensatory expression of other *Id* family members in *Id1* deficient mice

One explanation for our findings is that changes in expression of other Id family members compensate for loss of Id1 in *Id1 null* mice. To evaluate this, we first evaluated expression of the other Id family members, Id2-4, in normoxic and hypoxic wild type mouse lungs by western blot analyses of whole lung lysates. Pulmonary Id2 and Id3 expression levels are increased following exposure to 1 week hypoxia in wild type mice (Figure 20A-C). Id2 and Id3 are also elevated at 3 weeks of hypoxia (data not shown). In contrast, pulmonary Id4 expression is barely detectable in lung lysates from wild type mice under normoxic conditions, and there is no significant increase in Id4 expression after 1 or 3 weeks hypoxia (data not shown). To evaluate compensatory expression of *Id* family members associated with loss of Id1, we compared the expression of Id2 and Id3 in the lungs of wild type and *Id1 null* mice. There is a marked increase in expression of Id2 and

Table 13. Hypoxia-induced vascular remodeling and proliferation in wild type and *Id1* deficient mice. Data are expressed as mean +/- SEM from wild type, *Id1*$^{+/-}$, and *Id1 null* mice exposed to normoxia, 1 week, or 3 weeks hypoxia. ND: no data recorded. Mouse numbers are indicated (n). ***b***: $p<0.05$ versus corresponding genotype normoxic control by One-Way ANOVA with Bonferroni correction.

	Normoxia			1 Week Hypoxia			3 Weeks Hypoxia		
	Wild Type Mean+/-SEM (n)	Id1$^{+/-}$ Mean+/-SEM (n)	Id1$^{-/-}$ Mean+/-SEM (n)	Wild Type Mean+/-SEM (n)	Id1$^{+/-}$ Mean+/-SEM (n)	Id1$^{-/-}$ Mean+/-SEM (n)	Wild Type Mean+/-SEM (n)	Id1$^{+/-}$ Mean+/-SEM (n)	Id1$^{-/-}$ Mean+/-SEM (n)
Muscularized Vessels, %	20.37+/-2.99 (5)	18.31+/-4.24 (5)	20.35+/-3.49 (5)	53.42+/-5.18 (5)	57.68+/-7.61 *b* (5)	51.54+/-5.18 *b* (5)	45.17+/-2.29 *b* (5)	46.32+/-4.14 *b* (5)	48.37+/-6.60 *b* (5)
EC Proliferation, PCNA positive/total	0.007+/-0.004 (5)	0.022+/-0.012 (6)	0.004+/-0.004 (6)	0.071+/-0.015 (7)	0.082+/-0.014 *b* (5)	0.062+/-0.017 *b* (5)	ND	ND	ND
VSMC Proliferation, PCNA posiitve/total	0.021+/-0.009 (5)	0.018+/-0.007 (6)	0.012+/-0.004 (6)	0.076+/-0.010 (7)	0.119+/-0.016 *b* (5)	0.113+/-0.022 *b* (5)	ND	ND	ND

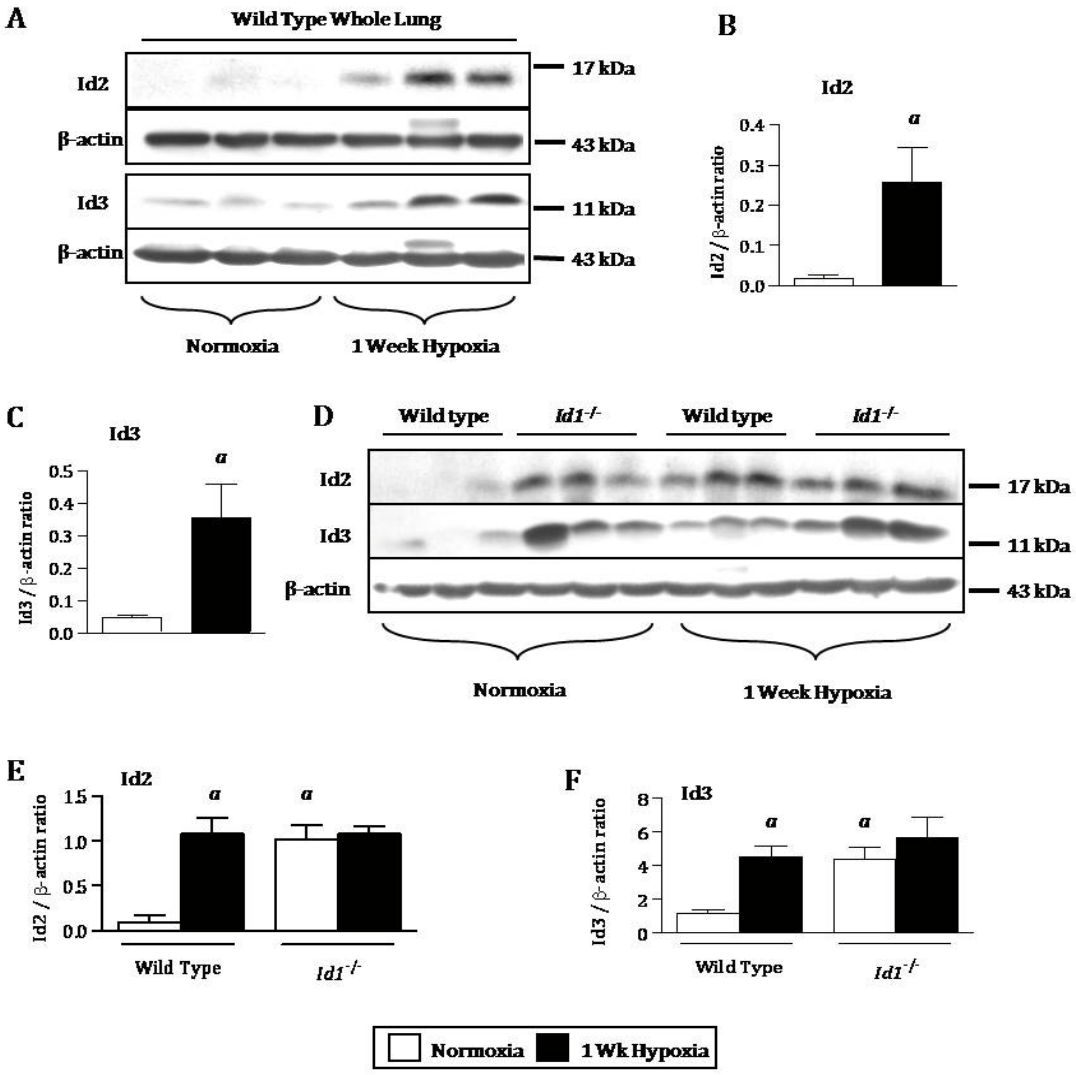

Figure 20. Regulation of pulmonary Id2 and Id3 expression in wild type and *Id1 null* mice. **A:** Western blot for Id2, Id3 and β-actin in normoxic and 1 week hypoxic wild type whole lung lysates. **B, C:** Densitometry of Id2 (B) and Id3 (C) expression relative to β-actin from A. **D:** Western blot for Id2, Id3 and β-actin in normoxic and 1 week hypoxic wild type and *Id1 null* whole lung lysates. **E, F:** Densitometry of Id2 (E) and Id3 (F) expression relative to β-actin from D. Data are expressed as mean +/- SEM. **a**: $p<0.05$ versus wild type normoxic control by two-tailed t-test (B-C) or One-Way ANOVA with Bonferroni correction (E, F).

Id3 in normoxic *Id1 null* mouse lungs, but no further increase in Id2 or Id3 expression levels are seen in *Id1 null* mice compared with wild type littermates in responses to chronic hypoxia (Figure 20D-F). These findings suggest that Id2 and/or Id3 may compensate for loss of pulmonary Id1 expression in *Id1 null* mice.

Localization of Id2 expression in the hypoxic pulmonary vasculature of wild type and *Id1 null* mice

To determine whether Id2 and/or Id3 expression could compensate for loss of Id1 in the pulmonary vasculature of *Id1 null* mice, we evaluated their cellular localization in wild type and *Id1 null* mouse lungs under normoxic and hypoxic conditions. For these studies we used commercially available rabbit monoclonal anti-Id2 and Id3 antibodies. As with Id1, we first evaluated expression in airway-associated vessels by immunoperoxidase staining of lung tissues. Since we do not have *Id2 null* mice in our facility, antibody specificity was evaluated by negative staining using rabbit IgG control for these studies (Figure 21H). Using these antibodies we show that Id2 is detectable at low levels in scattered endothelium and alveolar epithelial cells under normoxic conditions and is more easily detected and widely expressed throughout the lung after 1 week of hypoxia (Figure 21A-G). Id2-positive VSMCs are detectable in airway-associated vessels under hypoxic conditions (Figure 21C, arrow). Id2 is expressed in both endothelial and smooth muscle cell compartments of the pulmonary vasculature of *Id1 null* mice under hypoxic conditions, but is more strongly expressed throughout the lung in both normoxic and hypoxic *Id1 null* than in wild type mice (Figure 21E-G). Unlike Id1, Id2 is detectable in bronchial smooth muscle cells (Figure 21D, yellow arrows).

Figure 21. Localization of Id2 expression in wild type and *Id1 null* mouse lungs. A-G: Immunoperoxidase staining for Id2 in lung sections from normoxic and 1 week hypoxic wild type and *Id1 null* mice. **C, G:** inset from B and F, respectively. **H:** Negative staining with rabbit IgG control. **I-T:** Immunofluorescence staining for Id2 (red) and a-SMA (green) in small (20-50 μm) muscularized peripheral pulmonary vessels from normoxic and 1 week hypoxic wild type mice and *Id1 null* mice. Nuclear staining with DAPI is shown in blue. **U:** Negative staining with rabbit IgG control. **V, W:** Quantification of cell-specific Id2 indices in EC (V) and VSMC (W) compartments in peripheral vessels from normoxic and 1 week hypoxic wild type and *Id1 null* lungs (n=4 each group). Bar is 100 μm. * indicate vessels, thin arrows indicate nuclear staining in VSMCs; arrowheads indicate nuclear staining of ECs. Thick yellow arrows indicate smooth muscle cell staining in muscularized airways. Data are expressed as mean +/- SEM. **b**: $p<0.05$ versus corresponding genotype normoxic control by One-Way ANOVA with Bonferroni correction.

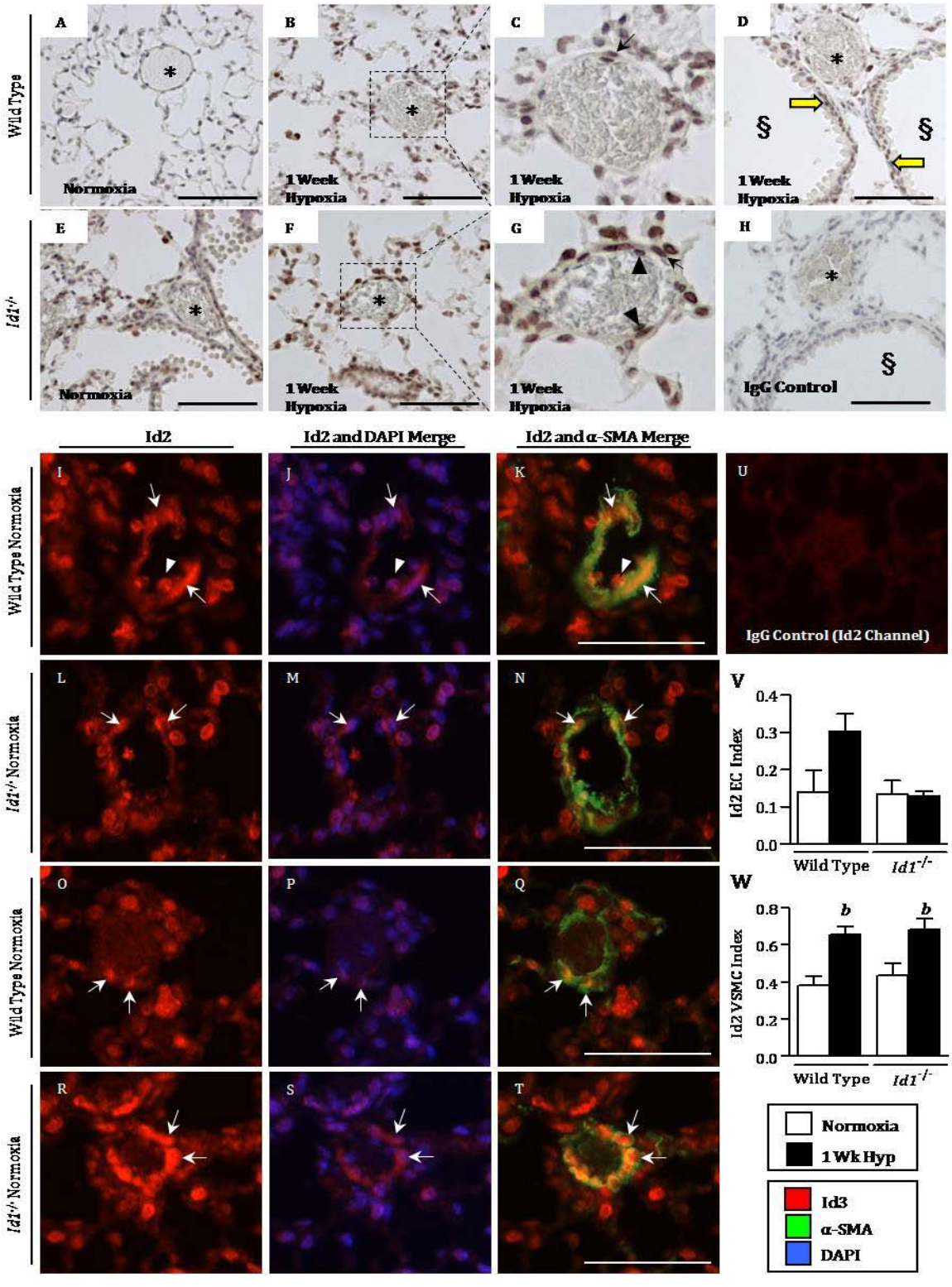
Wild Type
Id1-/-
A
B
C
D
E
F
G
H
Normoxia
1 Week Hypoxia
IgG Control
Id2
Id2 and DAPI Merge
Id2 and α-SMA Merge
Wild Type Normoxia
Id1-/- Normoxia
I
J
K
U
L
M
N
O
P
Q
R
S
T
IgG Control (Id2 Channel)
V
Id2 EC Index
0.4
0.3
0.2
0.1
0.0
Wild Type
Id1-/-
W
Id2 VSMC Index
0.8
0.6
0.4
0.2
0.0
b
Normoxia
1 Wk Hyp
Id3
α-SMA
DAPI

To evaluate the cellular expression domains of Id2 in small (20-50 μm diameter) muscularized peripheral vessels, we employed double immunofluorescence analysis using α-SMA staining to identify vascular compartments (Figure 21I-T). While Id2-positive staining of ECs tends to increase in wild type mice exposed to hypoxia, this finding was not statistically significant (p=0.42, ANOVA after Bonferroni correction; Figure 21V). *Id1 null* mice tend to have fewer Id2-positive ECs in hypoxia than wild type mice; however, this was not statistically significant (p=0.066, ANOVA after Bonferroni correction; Figure 21V). In contrast, the proportion of Id2-positive VSMCs increases with exposure to hypoxia in both wild type and *Id1 null* mice (Figure 21W). Importantly, there is no compensatory increase in Id2-expressing cells in either the endothelial or smooth muscle cell compartments of these small intrapulmonary vessels in *Id1 null* mice under normoxic or hypoxic conditions (Figure 21V, W). This indicates that increased expression of Id2 in *Id1 null* mice results from increased Id2 expression in epithelial and not vascular compartments of the lung.

Id3 expression pattern in peripheral pulmonary vessels

Immunoperoxidase staining shows that Id3 is detectable in bronchial smooth muscle, alveolar epithelium, and vascular cells under normoxic and hypoxic conditions (Figure 22A-G). As with the Id2 antibodies, since we do not have *Id3 null* mice in our facility, antibody specificity was evaluated by negative staining using rabbit IgG control for these studies (Figure 22H). Like Id1, Id3 is dominantly expressed in ECs but also in occasional VSMCs in both large and small diameter airway-associated vessels. Immunofluorescence analysis for Id3 in small muscularized peripheral vessels shows that Id3 is dominantly found in ECs (Figure 22I-T). However, the proportion of Id3-positive ECs does not increase in wild type or *Id1 null* mice exposed to hypoxia (Figure 22V). On the

Figure 22. Localization of Id3 expression in wild type and *Id1 null* mouse lungs. A-G: Immunoperoxidase staining for Id3 in lung sections of normoxic and 1 week hypoxic wild type and *Id1 null* mice. **C, G:** inset from B and F, respectively. **H:** Negative staining with rabbit IgG control. **I-T:** Immunofluorescence for Id3 (red) and a-SMA (green) in small (20-50 mm) muscularized peripheral pulmonary vessels from normoxic and 1 week hypoxic wild type mice and *Id1 null* mice. Nuclear staining with DAPI is shown in blue. **U:** Negative staining with rabbit IgG control. **V, W:** Quantification of cell-specific Id3 indices in ECs (V) and VSMCs (W) in peripheral vessels from normoxic and 1 week hypoxic wild type and *Id1 null* lungs (n=4 each group). Bar is 100 μm. * indicate vessels, thin arrows indicate nuclear staining in VSMCs; arrowheads denote nuclear staining of ECs. Thick yellow arrows indicate smooth muscle cell staining in muscularized airways. Data are expressed as mean +/- SEM. **a**: $p<0.05$ versus wild type normoxic control by One-Way ANOVA with Bonferroni correction.

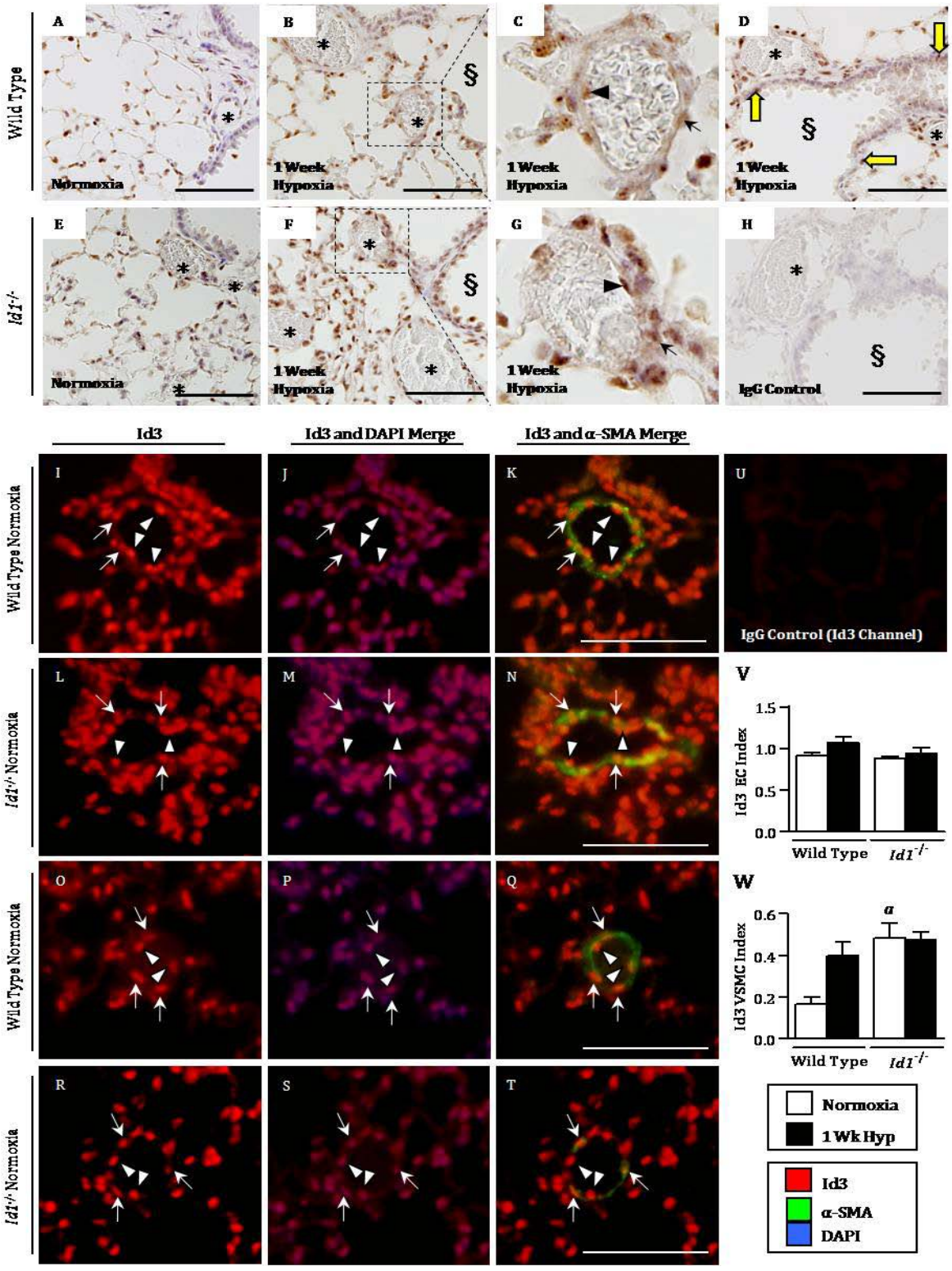
Wild Type
Id1-/-
A
B
C
D
E
F
G
H
Normoxia
1 Week Hypoxia
IgG Control
Id3
Id3 and DAPI Merge
Id3 and α-SMA Merge
Wild Type Normoxia
Id1-/- Normoxia
I
J
K
U
L
M
N
O
P
Q
R
S
T
IgG Control (Id3 Channel)
V
Id3 EC Index
1.5
1.0
0.5
0.0
Wild Type
Id1-/-
W
Id3 VSMC Index
0.6
0.4
0.2
0.0
a
Normoxia
1 Wk Hyp
Id3
α-SMA
DAPI

other hand, like Id1 there is an increase in the proportion of Id3-positive VSMCs in wild type mice under hypoxic versus normoxic conditions (Figure 22W). Importantly, the proportion of Id3-positive VSMCs is significantly increased under normoxic conditions in *Id1 null* mutant mice when compared to their wild type littermates (Figure 22W). There is no further increase in the proportion of Id3-positive VSMCs with hypoxia in *Id1 null* mouse lungs. These data indicate that Id3 is selectively up-regulated in peripheral vessel smooth muscle cells in *Id1 null* mice and suggest that Id3 may compensate for loss of Id1 expression in pulmonary VSMCs from *Id1 null* mice.

Discussion

This study provides the first complete characterization of Id1 expression and localization in the adult mouse lung and describes distinct hypoxic regulation of Id1 in small intrapulmonary resistance vessels. We show that Id1 is up-regulated in the pulmonary vasculature following prolonged exposure to hypoxia and that this is associated with an increased proportion of Id1-expressing VSMCs. Based on the previously attributed role of Id1 in promoting proliferation of various cell types (171, 186, 220), we predicted that loss of Id1 expression in *Id1 null* mice would reduce hypoxic pulmonary VSMC proliferation and remodeling. However, our genetic studies using *Id1 null* mice show that Id1 is dispensable for the development of hypoxic PH and that *Id1 null* mice show the same pulmonary vascular remodeling and smooth muscle cell proliferation responses to chronic hypoxic as their wild type littermates. We, therefore, evaluated compensatory expression of other, closely related Id family members. Id3 expression recapitulates that of Id1 in the hypoxic pulmonary vasculature, and loss of Id1 expression in *Id1 null* mice led to a selective up-

regulation of Id3 in pulmonary VSMCs. Taken together, these studies suggest that Id3 might compensate for loss of Id1 expression in *Id1 null* mice and indicate that Id1 and Id3 could play a cooperative role in regulating hypoxic PH and pulmonary vascular remodeling.

Prolonged exposure to hypoxia increases the proportion of Id1-positive VSMCs in the pulmonary vasculature. This change occurs throughout the pulmonary arterial tree, but is most pronounced in small muscularized vessels that are distal to terminal bronchioles. This is of significance since these peripheral vessels represent the dominant vessels that undergo pulmonary vascular remodeling in the hypoxic lung (130). However, these findings contrast with the observation that Bmp-dependent induction of Id1 expression is suppressed in cultured human pulmonary artery smooth muscle cells following exposure to hypoxia (222). Furthermore, our studies show that the proportion of Id1-positive ECs, unlike VSMCs, in the peripheral pulmonary vasculature is unchanged in response to hypoxia. These observations in ECs also differ from *in vitro* studies showing that Id1 expression is decreased in rat (200) and human lung ECs exposed to hypoxia (data not shown), but increased in a Bmp-dependent fashion in hypoxic mouse pulmonary microvascular ECs (54). These cell culture studies indicate that the *in vitro* hypoxic Id1 response is both context and cell type-dependent and supports our approach to evaluate the regulation of this hypoxic response in the intact pulmonary vasculature.

The mechanism by which chronic hypoxia selectively up-regulates Id1 expression in VSMCs *in vivo* is unknown. *Id1* is a transcriptional target of Bmp-activated Smads in a variety of cells types (135). In addition, our earlier studies in *Bmp4* deficient mice show that loss of hypoxic induction of Bmp4 in the lung is associated with reduced Id1 expression in VSMCs *in vivo* (54), suggesting that Id1 may be a target of Bmp4 in the intact hypoxic pulmonary vasculature. However, Id1 can also be up-regulated by hypoxia in a HIF1α-

dependent fashion (143). Furthermore, a variety of signaling pathways implicated in the development of vascular remodeling, including VEGF, IGF1, and TGF-β, can up-regulate Id1 expression in different cell types (161). This suggests that a number of Bmp-independent signaling pathways may regulate Id1 expression in the hypoxic pulmonary vasculature. These *in vitro* observations are complicated by the fact that cell-specific Id1 responses are themselves regulated by cell type and context-dependent transcriptional co-factors. For example, Bmp-dependent up-regulation of Id1 in pulmonary artery smooth muscle cells is inhibited by hypoxic-induction of the transcriptional co-repressor CtBP1 (222), while HIF-1α-dependent up-regulation of Id1 is repressed by hypoxic-induction of the transcriptional repressor ATF3 in cultured neuroblastoma cells (143). On this basis, differential hypoxic regulation of Id1 in endothelial and smooth muscle cell compartments of the pulmonary vasculature could be dependent not only on the localized expression of Bmp ligands and receptors in the hypoxic lung, but also on hypoxic induction of Bmp-independent signaling pathways and cell-specific expression of transcriptional repressors of these responses.

An earlier study from our lab has shown that reduced Id1 expression is associated with impaired hypoxia-induced pulmonary VSMC proliferation *in vivo* (54). Furthermore, previous *in vitro* studies indicate that Id1 exerts pro-proliferative effects in vascular cells (148, 172). These findings support the hypothesis that hypoxic induction of Id1 expression in VSMCs could play a role in promoting hypoxic pulmonary VSMC proliferation and remodeling. However, Yang et al. have shown that ID1 has anti-proliferative effects in cultured human pulmonary artery smooth muscle cells (233), indicating that the functional role of Id1 in regulating cell proliferation is also cell type and context dependent. Since these *in vitro* studies have failed to identify a definitive role for Id1 in regulating pulmonary VSMC function, we therefore used an *in vivo* genetic approach to evaluate smooth muscle cell responses in the intact pulmonary vasculature. For these studies, we evaluated

pulmonary vascular responses in a mouse model of hypoxic PH in which there are well-characterized changes in peripheral vessel remodeling and VSMC proliferation. However, our studies failed to detect any difference in hypoxic PH responses, VSMC proliferation, or remodeling between wild type and *Id1 null* mice. These findings indicate that expression of Id1 is dispensable in the pulmonary vascular response to chronic hypoxia. One explanation for these findings is that there is compensation for the loss of pulmonary Id1 by over-expression of other, closely related Id family members in the pulmonary vasculature. Supporting this idea, both Id2 and Id3 expression are elevated in the lungs of *Id1 null* mice. Detailed immunohistochemical analysis reveals that hypoxic regulation of Id2 is largely extra-vascular, and that *Id1 null* mice tend to have reduced hypoxic induction of Id2 in peripheral vessel ECs. These findings suggest that Id2 is unlikely to compensate for the loss of Id1 in the pulmonary vasculature. On the other hand, the expression pattern of Id3 is strikingly similar to that of Id1 in the hypoxic pulmonary vasculature. Moreover, loss of Id1 leads to a selective increase in the proportion of peripheral vessel smooth muscle cells that express Id3, suggesting that compensation for the loss of Id1 in the pulmonary vasculature occurs through increased Id3 expression. This hypothesis is consistent with the fact that Id1 and Id3 share many of the same molecular targets (161). Furthermore, *Id1/Id3* double mutant mice die with defects in angiogenesis and blood vessel stability (119), while mice with single homozygous deletion of *Id1* or *Id3* are viable (156, 230). This indicates that Id1 and Id3 play a combinatorial role in regulating vascular development and suggests that Id1 and Id3 are likely to have overlapping functions in regulating pulmonary vascular responses in the adult. However, loss of either Id1 or Id3 expression is sufficient to impair vascular cell function *in vitro* (30, 172, 215, 233, 237). Therefore, the combinatorial role of Id1 and Id3 *in vivo* cannot be addressed using isolated vascular cell culture systems. Future studies will

therefore utilize *Id1*/*Id3* double mutant mice to address their role in regulating hypoxia-induced PH and pulmonary vascular remodeling.

In summary, we have shown that Id1 is not required for vascular remodeling or hypoxic PH, but that Id3 exhibits striking compensatory expression in *Id1 null* pulmonary VSMCs *in vivo*. Since Id1 and Id3 have overlapping roles in regulating cellular proliferation and differentiation responses in a variety of cell types, we propose that the coordinated regulation of these factors in the pulmonary vasculature plays a cooperative role in regulating hypoxic pulmonary vascular remodeling. Given that *Id1* and *Id3* are established Bmp target genes, further evaluation of their combinatorial role in pulmonary vascular remodeling using compound *Id1* and *Id3* mutant mice will advance our understanding of Bmp signaling in the development of human HPAH (123).

Acknowledgments

The studies described in this chapter were a collaborative effort among several individuals. A particular debt of gratitude is owed to David Frank, Lynda Anderson, Mark Jones, Gabriella DiCarlo, Josh Smith, and the technical support at BioCheck, without whom these studies would not have been possible.

CHAPTER V

DISCUSSION AND FUTURE DIRECTIONS

The studies described in this dissertation were designed to elucidate the functional role of Bmp signaling in normal pulmonary vascular homeostasis and disease. They describe convergence of signaling pathways previously unknown to be linked, define a role for compartmentalization of signaling, and suggest functional redundancy of downstream effectors. Above all, they illustrate the intricate complexity of Bmp signaling *in vivo* and suggest that similar complexities are likely to underlie the effects of aberrant Bmp signaling in human pulmonary vascular disease. This chapter will focus on some of the major discoveries in this dissertation and align them into a cohesive model of Bmp signaling in the pulmonary vasculature.

Model of Bmp signaling in pulmonary vascular homeostasis

The studies in Chapters 2 and 3 describe a major role for Bmp2 and Bmpr2 in pulmonary vascular homeostasis through the regulation of vascular tone. According to the model in Figure 23, hypoxia-induced Bmp2 is dominantly secreted into the pulmonary circulation from the endothelium, where it then causes autocrine activation of EC-expressed Bmpr2. This signaling increases eNOS expression and, thereby, balances hypoxic vasoconstriction by increased NO production. This idea is supported by several lines of evidence: *Bmpr2* hypomorph and *Bmp2* deficient mice display attenuated hypoxic induction of eNOS expression and activity; Bmp2 regulates eNOS expression in IPAs and PECs; Bmp2

Figure 23. Model of Bmp signaling in a peripheral pulmonary vessel.

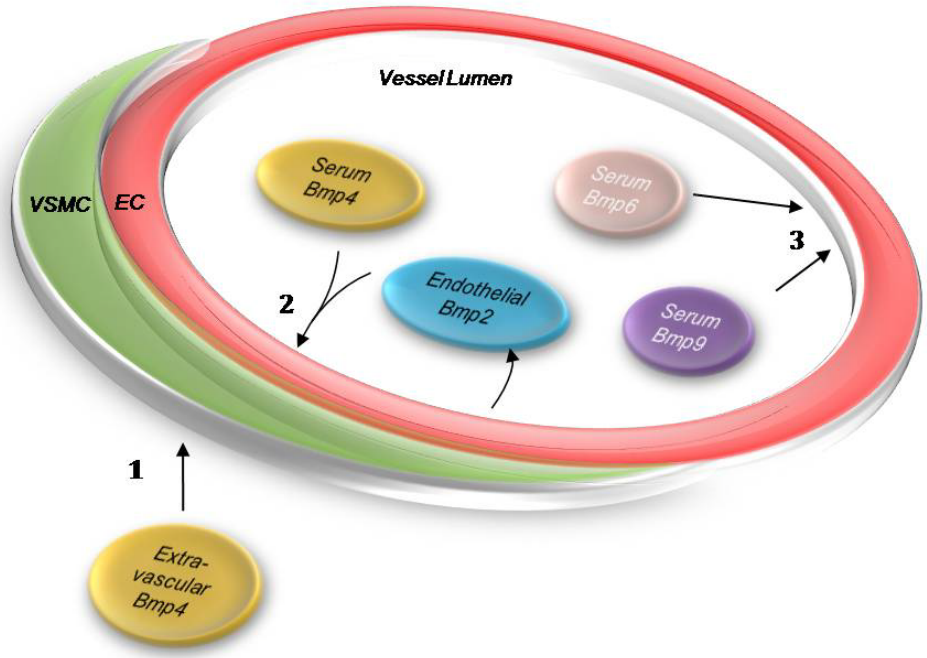

1) Extra-vascular Bmp4 dominantly promotes compensatory remodeling through Alk3 in VSMCs

2) Endothelial Bmp2 and circulating Bmp4 dominantly promote compensatory vasodilation through Bmpr2 in ECs

3) Circulating Bmp6 and Bmp9 exert unknown effects on ECs *in vivo*

increases NOS activity in wild type PECs but not in *Bmpr2* hypomorph PECs; and *Bmp2* deficient mice develop increased hypoxia-induced vascular remodeling.

Collectively, these studies indicate that Bmp2 and Bmpr2 exert protective effects in the pulmonary vasculature and that a major consequence of mutation in *Bmp2* or *Bmpr2* mutation is dysregulation of pulmonary eNOS expression and activity. It is conceivable, therefore, that overexpression of eNOS could protect against the development of hypoxic PH even in the context of impaired Bmp signaling. Proof of principle for this concept is provided in an earlier study that found mice overexpressing eNOS in ECs from the *Pre-proendothelin* promoter do not develop hypoxic PH (155). Future studies will involve crossing this *eNOS* transgene into the $Bmp2^{+/-}$ and $Bmpr2^{\Delta Ex/+}$ backgrounds. If these mice are protected from hypoxic PH, these data would argue that the major effect of reduced Bmp2- and Bmpr2-dependent signaling is impaired NO-dependent vasodilation. Another approach is to examine the functional defects associated with impaired Bmp signaling by performing arteriography upon wild type and $Bmp2^{+/-}$ IPAs. We predict that $Bmp2^{+/-}$ IPAs, similar to $Bmpr2^{\Delta Ex2/+}$ IPAs, will display impaired NO-dependent vasodilation and exogenous administration of Bmp2 will reverse this defect. Future studies will also determine the precise downstream signaling responsible for regulation of eNOS in PECs. This will be accomplished by step-wise inhibition of protein synthesis (actinomycin D and cycloheximide), evalution of protein stability (pulse-chase), and determination of effector dependency (MAPK inhibitors, dorsomorphin Smad inhibitor, and siRNA). Preliminary evidence suggests this regulation occurs Bmp2 post-transcriptionally, which is a common mechanism for regulating eNOS expression (179).

The findings in Chapters 2 and 3 have implications for the understanding of Bmp signaling in the context of human disease. For instance, proper eNOS expression level and

activity plays a critical role in maintaining low pulmonary vascular resistance (51, 197-198). Given the role of vasoconstriction in promoting vascular remodeling (138), impaired Bmp-dependent regulation of eNOS may be an early event in PAH pathogenesis. Supporting this idea, there is evidence of reduced eNOS expression in the lungs of some patients with PAH (63, 126). In regard to therapy, many of the current treatments for PAH involve vasodilator administration; however, these approaches are complex and are not always well-tolerated by the patient (158). Additionally, their long-term effectiveness is uncertain (120). By understanding the direct relationship between Bmp signaling and pulmonary vascular reactivity, it may be possible to design more targeted strategies to treat PAH.

Genetic studies performed in our lab have revealed opposing roles for Bmp2 and Bmp4 in the development of PH *in vivo*. While *Bmp2*-deficient mice display increased susceptibility to hypoxic PH and dysregulated eNOS expression and activity (3), *Bmp4* deficient mice are partially protected from hypoxic PH and show no dysregulation of eNOS (54). Thus, it was unexpected to find that Bmp2 and Bmp4 are equally capable of inducing expression of eNOS in the pulmonary vasculature *ex vivo*. One explanation for these findings is that, while Bmp2 and Bmp4 do not inherently differ in their signaling abilities, their differential effects on eNOS expression *in vivo* result from their distinct expression domains in and around the pulmonary vasculature. To test this hypothesis, future studies will generate mice in which *Bmp4* is knocked into the *Bmp2* locus (*Bmp2*$^{Bmp4/Bmp4}$ mutant mice). In this way, *Bmp4* is expressed under the regulatory control of the *Bmp2* locus. While it is possible that *Bmp2*$^{Bmp4/Bmp4}$ mutant mice might have developmental abnormalities, we do not expect this to be the case since previous studies using *Bmp4* knock-in to the *Bmp7* locus indicate that there is complete functional redundancy between different Bmp ligands in embryonic development (154). Therefore, if our hypothesis is correct, we would expect wild type and viable *Bmp2*$^{Bmp4/Bmp4}$ mice to show the same

pulmonary vascular response to chronic hypoxia. If, on the other hand, our hypothesis is incorrect, and the differential effects of Bmp2 and Bmp4 on the pulmonary vasculature result from their distinct signaling activity in vascular effector cells *in vivo*, then we would expect *Bmp2*$^{Bmp4/Bmp4}$ mice to develop more severe hypoxic PH than their wild type littermates.

Restricted patterns of Bmp2 and Bmp4 expression allow for unique separation of signaling effects by cell-type specific genetic ablation. Mice carrying alleles of *Bmp2* (*Bmp2* floxed) and *Bmp4* (*Bmp4* floxed) that can be conditionally deleted have been generated (88, 221) and are currently breeding in our facility. By crossing floxed mice with mice expressing Cre recombinase in certain cell types (e.g., endothelial Scl-Cre (65); smooth muscle αSMA-Cre (223)), the specific cell type contributing the protective expression of *Bmp2* and exacerbating expression of *Bmp4* in hypoxia can be dissected. For those cell types where no specific *Cre* transgene has been reported, such as type I pneumocytes, intrapulmonary adenoviral delivery of *Cre* serves as an alternative approach. Given the limited resolution ability of the reporter mice used in our studies, we are unable to rule out combinatorial expression of *Bmp2* or *Bmp4* by multiple cell types. Thus, a detailed study utilizing several *Cre* transgenic mice provides the resolution necessary. Our results argue that deletion of *Bmp2* in the endothelial compartment would result in dysregulation of eNOS and exacerbated hypoxic PH, while deletion of *Bmp4* in lung epithelia would protect from hypoxic PH by reducing VSMC proliferation and remodeling.

Additionally, once the cell-type specific expression patterns of Bmp2/4 are determined, overexpression of each ligand in specific compartments could provide functional evidence of their role in the development of hypoxic PH. Presently, mice overexpressing *Bmp2* in smooth muscle cells are in progress (142), but other vascular-

expressed transgenic lines have not been reported. Validation of *Bmp4* transgenic mice are in progress in our lab. Our results suggest that overexpression of Bmp2 or Bmp4 in the endothelium would protect against hypoxic PH, while overexpression in VSMCs or epithelia would exacerbate hypoxic PH. Additionally, these mice will provide a means to perform future epistasis experiments to evaluate the relationship between ligands and downstream targets (described below).

In addition to local tissue production of BMP2 and BMP4 in the lung, BMP4, BMP6, and BMP9 have been found to circulate at biologically active concentrations in human serum (38, 77). These ligands would have direct access to pulmonary vascular beds, suggesting that they could play a role in vascular homeostasis. Unlike Bmp4 and Bmp6, which are pro-angiogenic *in vitro* (75, 167), Bmp9 signals through Alk1 to inhibit Vegf-induced angiogenesis (177). Of note, Bmp9 is not inhibited by Noggin (180), suggesting that selective antagonism by Noggin could determine the net pro- vs. anti-angiogenic effects of Bmp ligands *in vivo*. However, the functional role of Bmp6 and Bmp9 *in vivo* is unknown. Future studies will generate *Bmp9* deficient mice and utilize available *Bmp6* deficient mice (190) to answer these questions.

Earlier findings from our lab suggest that Bmp4 promotes hypoxic vascular remodeling through VSMC proliferation (54). This likely occurs through Alk3 since another group has shown that, like *Bmp4* deficiency (54), patchy deletion of *Alk3* in VSMCs impairs hypoxia-induced pulmonary vascular remodeling (49). However, the effectors that lie downstream of these signaling events are unknown. One possibility is the well-characterized Bmp target gene *Id1*, whose expression is reduced in pulmonary VSMCs of *Bmp4* deficient mice (54). In Chapter 4, we show that hypoxia selectively up-regulates Id1 expression in peripheral pulmonary VSMCs. Surprisingly, though, Id1 expression is not

necessary for the development of hypoxic vascular remodeling or PH *in vivo*. One explanation for this result is that a closely related protein functionally compensates for the loss of Id1 expression. Supporting this idea, expression of both Id2 and Id3 is elevated in the lungs of *Id1 null* mice. While the hypoxic regulation of Id2 is largely extra-vascular, the expression pattern of Id3 is strikingly similar to that of Id1 in the pulmonary vasculature. Moreover, loss of Id1 leads to a selective increase in the proportion of peripheral vessel smooth muscle cells that express Id3, suggesting that compensation for the loss of Id1 in the pulmonary vasculature occurs through increased Id3 expression. This hypothesis is consistent with the fact that Id1 and Id3 share many of the same molecular targets (161). Furthermore, *Id1/Id3* double mutant mice die with defects in angiogenesis and blood vessel stability (119), while mice with single homozygous deletion of *Id1* or *Id3* are viable (156, 230). This indicates that Id1 and Id3 play a combinatorial role in regulating vascular development and suggests that Id1 and Id3 are likely to have overlapping functions in regulating pulmonary vascular responses in the adult. One method to test this possibility is through combinatorial knockdown of Id1 and Id3 expression *in vitro* by siRNA. Earlier studies have shown that loss of either Id1 or Id3 expression is sufficient to impair vascular cell function *in vitro* (30, 172, 215, 233, 237). Therefore, double knockdown of *Id1/Id3* would be predicted to exacerbate these defects. An obvious limitation of this approach is the artificial context in which functionality is assessed. Therefore, we are currently generating *Id1*/*Id3* double mutant mice to address their role in regulating hypoxia-induced PH and pulmonary vascular remodeling *in vivo*.

Our studies were unable to conclusively show that Id1 mediates the effects of Bmp4 upon hypoxic vascular remodeling. Future studies will utilize *Bmp4* transgenic mice (described above) to evaluate this possibility. Provided that, as predicted, Bmp4 overexpression in alveolar epithelium leads to increased pulmonary vascular remodeling,

these mice would be crossed to *Id1/Id3* double mutants. If deficiency of *Id1/Id3* abrogates vascular remodeling in *Bmp4* transgenic mice, this would provide the necessary epistatic data to establish these effectors as being downstream of Bmp4 *in vivo.*

Chronic hypoxia as a model of PAH

For our functional evaluation of Bmp signaling the development of PH, we chose to utilize the well-established mouse model of chronic hypoxia. In response to hypoxia, mice develop many of the signs of human PAH, but rarely develop the severe obliterative lesions seen in humans (reviewed in (196)). Therefore, chronic hypoxia in mice has been criticized as a poor model for this human disease (218). While we agree this is an obvious limitation, findings using the chronic hypoxia model provide insight into how the Bmp signaling pathway can modify pulmonary vascular function. Therefore, even though these mice do not develop severe vascular remodeling, they show defects in pulmonary vascular function that might also occur in the early course of human disease. In addition to modeling early pulmonary vascular disease in PAH, studies using the chronic hypoxia model are also relevant to the analysis of alveolar hypoxia, which plays a critical role in promoting PH associated with chronic lung disease (reviewed in (163)). Since chronic lung disease is the most common cause of PH worldwide, findings using the chronic hypoxia model have clinical implications for our understanding of an important human disease.

The true strength of the chronic hypoxia model comes when combined with genetic manipulation in mice (as we have done), thus allowing for evaluation of specific gene function *in vivo*. However, future studies will attempt to establish better models of human PAH in the mouse, thereby more closely mimicking human disease while retaining the ability to perform genetic manipulation in the intact animal. Potential models include

enhancing vascular contractility by chronic infusion of serotonin and inducing inflammatory stress by intrapulmonary adenovirus delivery of 5-lipoxygenase. Both of these models have been used in the field previously (116, 192) and, when crossed into susceptible genetic backgrounds, might lead to new insights into the development of PAH.

NMD-positive versus NMD–negative *BMPR2* mutations in the pathogenesis of HPAH

The *Bmpr2* hypomorph (*Bmpr2*$^{\Delta Ex2/+}$) mice used in our study (Chapter 2) differ from the *Bmpr2*$^{+/-}$ mutant mouse used in earlier studies. Unlike the null allele of *Bmpr2*$^{+/-}$ mutants, *Bmpr2* hypomorphs express a truncated isoform of Bmpr2 (Bmpr2-ΔEx2) that is readily detectable by western blot. This mutant protein, which exactly replicates an inherited mutation in one HPAH family, is retained intracellularly due to defective trafficking. Interestingly, *Bmpr2*$^{\Delta Ex2/+}$ mutant mice are susceptible to hypoxic PH (55), while *Bmpr2*$^{+/-}$ mutant mice are not (17, 116). This raises the possibility that the phenotype of *Bmpr2*$^{\Delta Ex2/+}$ mutant mice might be attributable to effects caused by the expression and/or retention of Bmpr2-ΔEx2 instead of haploinsufficiency as in *Bmpr2*$^{+/-}$ mutant mice. Support for this idea comes from the finding that patients who are predicted to express partially-inactivated BMPR2 isoforms have earlier onset and more severe disease than patients carrying mutations that are predicted to be unexpressed (9).

To explore this possibility further, future studies will compare the consequences of *Bmpr2*$^{+/-}$ and *Bmpr2*$^{\Delta Ex2/+}$ mutations. Since previous studies were performed on *Bmpr2*$^{+/-}$ and *Bmpr2*$^{\Delta Ex2/+}$ mutant mice under different experimental conditions and genetic backgrounds, future studies will address this question by direct comparison of the hypoxic PH phenotype in wild type, *Bmpr2*$^{+/-}$, and *Bmpr2*$^{\Delta Ex2/+}$ mutant mice that we have now backcrossed onto a pure C57Bl/6 background for 9 generations. We expect these studies to

show that *Bmpr2*$^{\Delta Ex2/+}$ mutant mice do indeed develop more severe hypoxic PH *in vivo.* Once this finding is established, the regulation of eNOS in *Bmpr2*$^{+/-}$ mutant mice will be evaluated. If our finding of impaired Bmp-mediated regulation of eNOS is due to *Bmpr2* haploinsufficiency, we predict that, like *Bmpr2*$^{\Delta Ex2/+}$ mutant mice, *Bmpr2*$^{+/-}$ mutant mice will display eNOS dysregulation. However, if dominant negative interference by Bmpr2-ΔEx2 is to blame, *Bmpr2*$^{+/-}$ mutant mice would not be expected to share this phenotype.

Besides dominant negative effects, ER stress is another possible mechanism by which retention of Bmpr2-ΔEx2 might lead to hypoxic PH. Activation of ER stress can induce the unfolded protein response, which causes a variety of cellular effects and when uncorrected leads to apoptosis (reviewed in (81, 91)). Therefore, future studies will evaluate activation of these pathways in *Bmpr2*$^{\Delta Ex2/+}$ mutant mice and isolated PECs. Because Bmpr2 is principally expressed in ECs, we predict that VSMCs, in which Bmpr2 is less strongly expressed, are less affected by Bmpr2-ΔEx2 retention. In order to test this possibility, these studies will be repeated in pulmonary VSMCs isolated from wild type and *Bmpr2*$^{\Delta Ex2/+}$ mutant mice.

It is of great interest to evaluate if forced shuttling of Bmpr2-ΔEx2 to the cell surface partially restores signaling and whether this is sufficient to abrogate the hypoxic PH seen in *Bmpr2*$^{\Delta Ex2/+}$ mutant mice. To answer this question, chemical chaperones (such as glycerol, 4-PBA, and thapsigargin) will be used *in vitro* and the trafficking of Bmpr2-ΔEx2 evaluated in *Bmpr2*$^{\Delta Ex2/+}$ PECs by biotinylation and immunofluorescent localization. If cell surface localization is achieved, the rescue of downstream signaling, and ultimately the hypoxic PH phenotype, in this scenario will be determined. *In vitro* proof of principle has been provided by rescue of an artificially overexpressed Bmpr2 isoform that is retained in the ER (189).

However, our studies have the distinct advantage of mutant expression from the endogenous locus *in vivo*.

Induced pluripotent stem cells in the study of HPAH

The findings described in this dissertation provide insight into the role of Bmp signaling in pulmonary vascular homeostasis and could be of significant clinical relevance to human HPAH. However, definitive evidence from functional studies in human tissue is lacking. It is quite likely that the effects of Bmp pathway mutations are cell-type specific, but access to appropriate human tissue is limited and typically end-stage disease. One approach to circumvent this limitation comes from recent advances in the ability to generate induced pluripotent stem (iPS) cells from human skin fibroblasts, which can then be differentiated into a variety of cell types (201, 228). New studies are defining protocols to derive vascular cells, including ECs and VSMCs, from human iPS cells (191, 204). Future efforts will utilize this technology to generate vascular cells from a library of normal and HPAH patient skin fibroblasts that exists at Vanderbilt University. These will provide the first means to study functional defects that lead to the development of HPAH in the appropriate human cell types. Of particular clinical interest will be the evaluation of NMD+ and NMD- *BMPR2* mutations, and whether agents that promote translational read-through (reviewed in (112)) can partially restore signaling of NMD+ *BMPR2* mutations.

Concluding remarks

Genetic studies in mice have firmly established that Bmp signaling is essential for vascular development and homeostasis. The studies in this dissertation add to this

foundation by demonstrating that the Bmp pathway directly regulates pulmonary vascular tone, by defining a role for compartmentalization of Bmp signaling in the lung, and by suggesting compensation among closely-related downstream effectors. Our findings have implications for understanding the molecular pathogenesis of HPAH and other, more common forms of PH not associated with *BMPR2* mutations. Additionally, we have identified potential interventions, such as protein refolding agents and cell-specific modulation of Bmp signaling components in the pulmonary vasculature, which may assist in future therapies for this important group of human diseases.

BIBLIOGRAPHY

1. **Abdollahi A, Hahnfeldt P, Maercker C, Gröne H-J, Debus J, Ansorge W, Folkman J, Hlatky L, and Huber PE**. Endostatin's Antiangiogenic Signaling Network. *Molecular Cell* 13: 649-663, 2004.

2. **Allendorph GP, Vale WW, and Choe S**. Structure of the ternary signaling complex of a TGF-beta superfamily member. *Proc Natl Acad Sci U S A* 103: 7643-7648, 2006.

3. **Anderson L, Lowery JW, Frank DB, Novitskaya T, Jones M, Mortlock DP, Chandler RL, and de Caestecker MP**. Bmp2 and Bmp4 exert opposing effects in hypoxic pulmonary hypertension. *Am J Physiol Regul Integr Comp Physiol* 298: R833-842, 2010.

4. **Andersson O, Bertolino P, and Ibanez CF**. Distinct and cooperative roles of mammalian Vg1 homologs GDF1 and GDF3 during early embryonic development. *Dev Biol* 311: 500-511, 2007.

5. **Andersson O, Reissmann E, and Ibanez CF**. Growth differentiation factor 11 signals through the transforming growth factor-beta receptor ALK5 to regionalize the anterior-posterior axis. *EMBO Rep* 7: 831-837, 2006.

6. **Andriopoulos B, Jr., Corradini E, Xia Y, Faasse SA, Chen S, Grgurevic L, Knutson MD, Pietrangelo A, Vukicevic S, Lin HY, and Babitt JL**. BMP6 is a key endogenous regulator of hepcidin expression and iron metabolism. *Nat Genet* 41: 482-487, 2009.

7. **Arthur HM, Ure J, Smith AJH, Renforth G, Wilson DI, Torsney E, Charlton R, Parums DV, Jowett T, Marchuk DA, Burn J, and Diamond AG**. Endoglin, an Ancillary TGF[beta] Receptor, Is Required for Extraembryonic Angiogenesis and Plays a Key Role in Heart Development. *Developmental Biology* 217: 42-53, 2000.

8. **Atkinson C, Stewart S, Upton PD, Machado R, Thomson JR, Trembath RC, and Morrell NW**. Primary pulmonary hypertension is associated with reduced pulmonary vascular expression of type II bone morphogenetic protein receptor. *Circulation* 105: 1672-1678, 2002.

9. **Austin ED, Phillips JA, Cogan JD, Hamid R, Yu C, Stanton KC, Phillips CA, Wheeler LA, Robbins IM, Newman JH, and Loyd JE**. Truncating and missense BMPR2

mutations differentially affect the severity of heritable pulmonary arterial hypertension. *Respir Res* 10: 87, 2009.

10. **Babitt JL, Huang FW, Wrighting DM, Xia Y, Sidis Y, Samad TA, Campagna JA, Chung RT, Schneyer AL, Woolf CJ, Andrews NC, and Lin HY**. Bone morphogenetic protein signaling by hemojuvelin regulates hepcidin expression. *Nat Genet* 38: 531-539, 2006.

11. **Babitt JL, Zhang Y, Samad TA, Xia Y, Tang J, Campagna JA, Schneyer AL, Woolf CJ, and Lin HY**. Repulsive guidance molecule (RGMa), a DRAGON homologue, is a bone morphogenetic protein co-receptor. *J Biol Chem* 280: 29820-29827, 2005.

12. **Baek D, Villen J, Shin C, Camargo FD, Gygi SP, and Bartel DP**. The impact of microRNAs on protein output. *Nature* 455: 64-71, 2008.

13. **Barbara NP, Wrana JL, and Letarte M**. Endoglin is an accessory protein that interacts with the signaling receptor complex of multiple members of the transforming growth factor-beta superfamily. *J Biol Chem* 274: 584-594, 1999.

14. **Barbara NP, Wrana JL, and Letarte M**. Endoglin Is an Accessory Protein That Interacts with the Signaling Receptor Complex of Multiple Members of the Transforming Growth Factor-β Superfamily. *Journal of Biological Chemistry* 274: 584-594, 1999.

15. **Beck H, Drahushuk K, Jacoby D, Higgins D, and Lein P**. Bone morphogenetic protein-5 (BMP-5) promotes dendritic growth in cultured sympathetic neurons. *BMC Neuroscience* 2: 12, 2001.

16. **Belik J, Jerkic M, McIntyre BAS, Pan J, Leen J, Yu LX, Henkelman RM, Toporsian M, and Letarte M**. Age-dependent endothelial nitric oxide synthase uncoupling in pulmonary arteries of endoglin heterozygous mice. *Am J Physiol Lung Cell Mol Physiol* 297: L1170-1178, 2009.

17. **Beppu H, Ichinose F, Kawai N, Jones RC, Yu PB, Zapol WM, Miyazono K, Li E, and Bloch KD**. BMPR-II heterozygous mice have mild pulmonary hypertension and an impaired pulmonary vascular remodeling response to prolonged hypoxia. *Am J Physiol Lung Cell Mol Physiol* 287: L1241-1247, 2004.

18. **Beppu H, Kawabata M, Hamamoto T, Chytil A, Minowa O, Noda T, and Miyazono K**. BMP Type II Receptor Is Required for Gastrulation and Early Development of Mouse Embryos. *Developmental Biology* 221: 249-258, 2000.

19. **Blanco FJ, Santibanez JF, Guerrero-Esteo M, Langa C, Vary CP, and Bernabeu C**. Interaction and functional interplay between endoglin and ALK-1, two components of the endothelial transforming growth factor-beta receptor complex. *J Cell Physiol* 204: 574-584, 2005.

20. **Bostrom K, Watson KE, Horn S, Wortham C, Herman IM, and Demer LL**. Bone morphogenetic protein expression in human atherosclerotic lesions. *J Clin Invest* 91: 1800-1809, 1993.

21. **Bourdeau A, Cymerman U, Paquet ME, Meschino W, McKinnon WC, Guttmacher AE, Becker L, and Letarte M**. Endoglin expression is reduced in normal vessels but still detectable in arteriovenous malformations of patients with hereditary hemorrhagic telangiectasia type 1. *Am J Pathol* 156: 911-923, 2000.

22. **Boyle S, Misfeldt A, Chandler KJ, Deal KK, Southard-Smith EM, Mortlock DP, Baldwin HS, and de Caestecker M**. Fate mapping using Cited1-CreERT2 mice demonstrates that the cap mesenchyme contains self-renewing progenitor cells and gives rise exclusively to nephronic epithelia. *Dev Biol* 313: 234-245, 2008.

23. **Brown MA, Zhao Q, Baker KA, Naik C, Chen C, Pukac L, Singh M, Tsareva T, Parice Y, Mahoney A, Roschke V, Sanyal I, and Choe S**. Crystal Structure of BMP-9 and Functional Interactions with Pro-region and Receptors. *Journal of Biological Chemistry* 280: 25111-25118, 2005.

24. **Butt E, Abel K, Krieger M, Palm D, Hoppe V, Hoppe J, and Walter U**. cAMP- and cGMP-dependent protein kinase phosphorylation sites of the focal adhesion vasodilator-stimulated phosphoprotein (VASP) in vitro and in intact human platelets. *J Biol Chem* 269: 14509-14517, 1994.

25. **Chambers RC, Leoni P, Kaminski N, Laurent GJ, and Heller RA**. Global expression profiling of fibroblast responses to transforming growth factor-beta1 reveals the induction of inhibitor of differentiation-1 and provides evidence of smooth muscle cell phenotypic switching. *Am J Pathol* 162: 533-546, 2003.

26. **Chan MC, Hilyard AC, Wu C, Davis BN, Hill NS, Lal A, Lieberman J, Lagna G, and Hata A**. Molecular basis for antagonism between PDGF and the TGFbeta family of signalling pathways by control of miR-24 expression. *EMBO J* 29: 559-573, 2010.

27. **Chandler RL, Chandler KJ, McFarland KA, and Mortlock DP**. Bmp2 transcription in osteoblast progenitors is regulated by a distant 3' enhancer located 156.3 kilobases from the promoter. *Mol Cell Biol* 27: 2934-2951, 2007.

28. **Chang H, Brown CW, and Matzuk MM**. Genetic analysis of the mammalian transforming growth factor-beta superfamily. *Endocr Rev* 23: 787-823, 2002.

29. **Chang H, Huylebroeck D, Verschueren K, Guo Q, Matzuk MM, and Zwijsen A**. Smad5 knockout mice die at mid-gestation due to multiple embryonic and extraembryonic defects. *Development* 126: 1631-1642, 1999.

30. **Chen X, Zankl A, Niroomand F, Liu Z, Katus HA, Jahn L, and Tiefenbacher C**. Upregulation of ID protein by growth and differentiation factor 5 (GDF5) through a smad-dependent and MAPK-independent pathway in HUVSMC. *J Mol Cell Cardiol* 41: 26-33, 2006.

31. **Coggins MP, and Bloch KD**. Nitric oxide in the pulmonary vasculature. *Arterioscler Thromb Vasc Biol* 27: 1877-1885, 2007.

32. **Corriere MA, Rogers CM, Eliason JL, Faulk J, Kume T, Hogan BL, and Guzman RJ**. Endothelial Bmp4 is induced during arterial remodeling: effects on smooth muscle cell migration and proliferation. *J Surg Res* 145: 142-149, 2008.

33. **Csiszar A, Ahmad M, Smith KE, Labinskyy N, Gao Q, Kaley G, Edwards JG, Wolin MS, and Ungvari Z**. Bone morphogenetic protein-2 induces proinflammatory endothelial phenotype. *Am J Pathol* 168: 629-638, 2006.

34. **Csiszar A, Labinskyy N, Jo H, Ballabh P, and Ungvari Z**. Differential proinflammatory and prooxidant effects of bone morphogenetic protein-4 in coronary and pulmonary arterial endothelial cells. *Am J Physiol Heart Circ Physiol* 295: H569-577, 2008.

35. **Csiszar A, Smith KE, Koller A, Kaley G, Edwards JG, and Ungvari Z**. Regulation of bone morphogenetic protein-2 expression in endothelial cells: role of nuclear factor-kappaB activation by tumor necrosis factor-alpha, H2O2, and high intravascular pressure. *Circulation* 111: 2364-2372, 2005.

36. **Daly AC, Randall RA, and Hill CS**. Transforming growth factor beta-induced Smad1/5 phosphorylation in epithelial cells is mediated by novel receptor complexes and is essential for anchorage-independent growth. *Mol Cell Biol* 28: 6889-6902, 2008.

37. **Darby S, Cross S, Brown N, Hamdy F, and Robson C**. BMP-6 over-expression in prostate cancer is associated with increased Id-1 protein and a more invasive phenotype. *The Journal of Pathology* 214: 394-404, 2008.

38. **David L, Mallet C, Keramidas M, Lamande N, Gasc JM, Dupuis-Girod S, Plauchu H, Feige JJ, and Bailly S**. Bone morphogenetic protein-9 is a circulating vascular quiescence factor. *Circ Res* 102: 914-922, 2008.

39. **David L, Mallet C, Mazerbourg S, Feige J-J, and Bailly S**. Identification of BMP9 and BMP10 as functional activators of the orphan activin receptor-like kinase 1 (ALK1) in endothelial cells. *Blood* 109: 1953-1961, 2007.

40. **David L, Mallet C, Mazerbourg S, Feige JJ, and Bailly S**. Identification of BMP9 and BMP10 as functional activators of the orphan activin receptor-like kinase 1 (ALK1) in endothelial cells. *Blood* 109: 1953-1961, 2007.

41. **Davis BN, Hilyard AC, Lagna G, and Hata A**. SMAD proteins control DROSHA-mediated microRNA maturation. *Nature* 454: 56-61, 2008.

42. **de Caestecker M**. The transforming growth factor-[beta] superfamily of receptors. *Cytokine & Growth Factor Reviews* 15: 1-11, 2004.

43. **de Candia P, Solit DB, Giri D, Brogi E, Siegel PM, Olshen AB, Muller WJ, Rosen N, and Benezra R**. Angiogenesis impairment in Id-deficient mice cooperates with an Hsp90 inhibitor to completely suppress HER2/neu-dependent breast tumors. *Proceedings of the National Academy of Sciences of the United States of America* 100: 12337-12342, 2003.

44. **de Jesus Perez VA, Alastalo TP, Wu JC, Axelrod JD, Cooke JP, Amieva M, and Rabinovitch M**. Bone morphogenetic protein 2 induces pulmonary angiogenesis via Wnt-beta-catenin and Wnt-RhoA-Rac1 pathways. *J Cell Biol* 184: 83-99, 2009.

45. **Delot EC, Bahamonde ME, Zhao M, and Lyons KM**. BMP signaling is required for septation of the outflow tract of the mammalian heart. *Development* 130: 209-220, 2003.

46. **Di Pasquale E, and Brivanlou AH**. Bone morphogenetic protein 15 (BMP15) acts as a BMP and Wnt inhibitor during early embryogenesis. *J Biol Chem* 284: 26127-26136, 2009.

47. **Ebisawa T, Tada K, Kitajima I, Tojo K, Sampath T, Kawabata M, Miyazono K, and Imamura T**. Characterization of bone morphogenetic protein-6 signaling pathways in osteoblast differentiation. *J Cell Sci* 112: 3519-3527, 1999.

48. **El-Bizri N, Guignabert C, Wang L, Cheng A, Stankunas K, Chang CP, Mishina Y, and Rabinovitch M**. SM22alpha-targeted deletion of bone morphogenetic

protein receptor 1A in mice impairs cardiac and vascular development, and influences organogenesis. *Development* 135: 2981-2991, 2008.

49. **El-Bizri N, Wang L, Merklinger SL, Guignabert C, Desai T, Urashima T, Sheikh AY, Knutsen RH, Mecham RP, Mishina Y, and Rabinovitch M**. Smooth muscle protein 22alpha-mediated patchy deletion of Bmpr1a impairs cardiac contractility but protects against pulmonary vascular remodeling. *Circ Res* 102: 380-388, 2008.

50. **Erlacher L, McCartney J, Piek E, ten Dijke P, Yanagishita M, Oppermann H, and Luyten FP**. Cartilage-derived morphogenetic proteins and osteogenic protein-1 differentially regulate osteogenesis. *J Bone Miner Res* 13: 383-392, 1998.

51. **Fagan KA, Fouty BW, Tyler RC, Morris KG, Jr., Hepler LK, Sato K, LeCras TD, Abman SH, Weinberger HD, Huang PL, McMurtry IF, and Rodman DM**. The pulmonary circulation of homozygous or heterozygous eNOS-null mice is hyperresponsive to mild hypoxia. *J Clin Invest* 103: 291-299, 1999.

52. **Fleming I, and Busse R**. Molecular mechanisms involved in the regulation of the endothelial nitric oxide synthase. *Am J Physiol Regul Integr Comp Physiol* 284: R1-12, 2003.

53. **Fraidenraich D, Stillwell E, Romero E, Wilkes D, Manova K, Basson CT, and Benezra R**. Rescue of cardiac defects in id knockout embryos by injection of embryonic stem cells. *Science* 306: 247-252, 2004.

54. **Frank DB, Abtahi A, Yamaguchi DJ, Manning S, Shyr Y, Pozzi A, Baldwin HS, Johnson JE, and de Caestecker MP**. Bone Morphogenetic Protein 4 Promotes Pulmonary Vascular Remodeling in Hypoxic Pulmonary Hypertension. *Circ Res* 97: 496-504, 2005.

55. **Frank DB, Lowery J, Anderson L, Brink M, Reese J, and de Caestecker M**. Increased susceptibility to hypoxic pulmonary hypertension in Bmpr2 mutant mice is associated with endothelial dysfunction in the pulmonary vasculature. *Am J Physiol Lung Cell Mol Physiol* 294: L98-109, 2008.

56. **Freeze HH**. Use of glycosidases to study protein trafficking. *Curr Protoc Cell Biol* Chapter 15: Unit 15 12, 2001.

57. **Fritz DT, Liu D, Xu J, Jiang S, and Rogers MB**. Conservation of Bmp2 post-transcriptional regulatory mechanisms. *J Biol Chem* 279: 48950-48958, 2004.

58. **Fujiwara M, Yagi H, Matsuoka R, Akimoto K, Furutani M, Imamura S, Uehara R, Nakayama T, Takao A, Nakazawa M, and Saji T**. Implications of mutations of activin receptor-like kinase 1 gene (ALK1) in addition to bone morphogenetic protein receptor II gene (BMPR2) in children with pulmonary arterial hypertension. *Circ J* 72: 127-133, 2008.

59. **Gallione C, Aylsworth AS, Beis J, Berk T, Bernhardt B, Clark RD, Clericuzio C, Danesino C, Drautz J, Fahl J, Fan Z, Faughnan ME, Ganguly A, Garvie J, Henderson K, Kini U, Leedom T, Ludman M, Lux A, Maisenbacher M, Mazzucco S, Olivieri C, Ploos van Amstel JK, Prigoda-Lee N, Pyeritz RE, Reardon W, Vandezande K, Waldman JD, White RI, Jr., Williams CA, and Marchuk DA**. Overlapping spectra of SMAD4 mutations in juvenile polyposis (JP) and JP-HHT syndrome. *Am J Med Genet A* 152A: 333-339, 2010.

60. **Gallione CJ, Richards JA, Letteboer TG, Rushlow D, Prigoda NL, Leedom TP, Ganguly A, Castells A, Ploos van Amstel JK, Westermann CJ, Pyeritz RE, and Marchuk DA**. SMAD4 mutations found in unselected HHT patients. *J Med Genet* 43: 793-797, 2006.

61. **Galvin KM, Donovan MJ, Lynch CA, Meyer RI, Paul RJ, Lorenz JN, Fairchild-Huntress V, Dixon KL, Dunmore JH, Gimbrone MA, Jr., Falb D, and Huszar D**. A role for smad6 in development and homeostasis of the cardiovascular system. *Nat Genet* 24: 171-174, 2000.

62. **Gamer LW, Nove J, Levin M, and Rosen V**. BMP-3 is a novel inhibitor of both activin and BMP-4 signaling in Xenopus embryos. *Dev Biol* 285: 156-168, 2005.

63. **Giaid A, and Saleh D**. Reduced expression of endothelial nitric oxide synthase in the lungs of patients with pulmonary hypertension. *N Engl J Med* 333: 214-221, 1995.

64. **Goldman DC, Hackenmiller R, Nakayama T, Sopory S, Wong C, Kulessa H, and Christian JL**. Mutation of an upstream cleavage site in the BMP4 prodomain leads to tissue-specific loss of activity. *Development* 133: 1933-1942, 2006.

65. **Gothert JR, Gustin SE, van Eekelen JA, Schmidt U, Hall MA, Jane SM, Green AR, Gottgens B, Izon DJ, and Begley CG**. Genetically tagging endothelial cells in vivo: bone marrow-derived cells do not contribute to tumor endothelium. *Blood* 104: 1769-1777, 2004.

66. **Goumans MJ, Valdimarsdottir G, Itoh S, Lebrin F, Larsson J, Mummery C, Karlsson S, and ten Dijke P**. Activin receptor-like kinase (ALK)1 is an antagonistic mediator of lateral TGFbeta/ALK5 signaling. *Mol Cell* 12: 817-828, 2003.

67. **Greenwald J, Groppe J, Gray P, Wiater E, Kwiatkowski W, Vale W, and Choe S**. The BMP7/ActRII Extracellular Domain Complex Provides New Insights into the Cooperative Nature of Receptor Assembly. *Molecular Cell* 11: 605-617, 2003.

68. **Hagen M, Fagan K, Steudel W, Carr M, Lane K, Rodman DM, and West J**. Interaction of interleukin-6 and the BMP pathway in pulmonary smooth muscle. *Am J Physiol Lung Cell Mol Physiol* 292: L1473-1479, 2007.

69. **Halbrooks PJ, Ding R, Wozney JM, and Bain G**. Role of RGM coreceptors in bone morphogenetic protein signaling. *J Mol Signal* 2: 4, 2007.

70. **Han RNN, Babaei S, Robb M, Lee T, Ridsdale R, Ackerley C, Post M, and Stewart DJ**. Defective Lung Vascular Development and Fatal Respiratory Distress in Endothelial NO Synthase-Deficient Mice: A Model of Alveolar Capillary Dysplasia? *Circ Res* 94: 1115-1123, 2004.

71. **Harrison RE, Flanagan JA, Sankelo M, Abdalla SA, Rowell J, Machado RD, Elliott CG, Robbins IM, Olschewski H, McLaughlin V, Gruenig E, Kermeen F, Halme M, Raisanen-Sokolowski A, Laitinen T, Morrell NW, and Trembath RC**. Molecular and functional analysis identifies ALK-1 as the predominant cause of pulmonary hypertension related to hereditary haemorrhagic telangiectasia. *J Med Genet* 40: 865-871, 2003.

72. **Hassoun PM, Mouthon L, Barbera JA, Eddahibi S, Flores SC, Grimminger F, Jones PL, Maitland ML, Michelakis ED, Morrell NW, Newman JH, Rabinovitch M, Schermuly R, Stenmark KR, Voelkel NF, Yuan JX, and Humbert M**. Inflammation, growth factors, and pulmonary vascular remodeling. *J Am Coll Cardiol* 54: S10-19, 2009.

73. **Hatta T, Konishi H, Katoh E, Natsume T, Ueno N, Kobayashi Y, and Yamazaki T**. Identification of the ligand-binding site of the BMP type IA receptor for BMP-4. *Peptide Science* 55: 399-406, 2000.

74. **Hebert DN, Garman SC, and Molinari M**. The glycan code of the endoplasmic reticulum: asparagine-linked carbohydrates as protein maturation and quality-control tags. *Trends Cell Biol* 15: 364-370, 2005.

75. **Heinke J, Wehofsits L, Zhou Q, Zoeller C, Baar KM, Helbing T, Laib A, Augustin H, Bode C, Patterson C, and Moser M**. BMPER is an endothelial cell regulator and controls bone morphogenetic protein-4-dependent angiogenesis. *Circ Res* 103: 804-812, 2008.

76. **Henke E, Perk J, Vider J, de Candia P, Chin Y, Solit DB, Ponomarev V, Cartegni L, Manova K, Rosen N, and Benezra R**. Peptide-conjugated antisense

oligonucleotides for targeted inhibition of a transcriptional regulator in vivo. *Nat Biotech* 26: 91-100, 2008.

77. **Herrera B, and Inman GJ**. A rapid and sensitive bioassay for the simultaneous measurement of multiple bone morphogenetic proteins. Identification and quantification of BMP4, BMP6 and BMP9 in bovine and human serum. *BMC Cell Biol* 10: 20, 2009.

78. **Higashi Y, Noma K, Yoshizumi M, and Kihara Y**. Endothelial function and oxidative stress in cardiovascular diseases. *Circ J* 73: 411-418, 2009.

79. **Hong K-H, Lee YJ, Lee E, Park SO, Han C, Beppu H, Li E, Raizada MK, Bloch KD, and Oh SP**. Genetic Ablation of the Bmpr2 Gene in Pulmonary Endothelium Is Sufficient to Predispose to Pulmonary Arterial Hypertension. *Circulation* 118: 722-730, 2008.

80. **Hong KH, Lee YJ, Lee E, Park SO, Han C, Beppu H, Li E, Raizada MK, Bloch KD, and Oh SP**. Genetic ablation of the BMPR2 gene in pulmonary endothelium is sufficient to predispose to pulmonary arterial hypertension. *Circulation* 118: 722-730, 2008.

81. **Hosoi T, and Ozawa K**. Endoplasmic reticulum stress in disease: mechanisms and therapeutic opportunities. *Clin Sci (Lond)* 118: 19-29, 2010.

82. **Huang Z, Wang D, Ihida-Stansbury K, Jones PL, and Martin JF**. Defective pulmonary vascular remodeling in Smad8 mutant mice. *Hum Mol Genet* 18: 2791-2801, 2009.

83. **Iavarone A, and Lasorella A**. ID proteins as targets in cancer and tools in neurobiology. *Trends in Molecular Medicine* 12: 588-594, 2006.

84. **Itoh F, Itoh S, Goumans MJ, Valdimarsdottir G, Iso T, Dotto GP, Hamamori Y, Kedes L, Kato M, and ten Dijke Pt P**. Synergy and antagonism between Notch and BMP receptor signaling pathways in endothelial cells. *EMBO J* 23: 541-551, 2004.

85. **Jadrich JL, O'Connor MB, and Coucouvanis E**. The TGF beta activated kinase TAK1 regulates vascular development in vivo. *Development* 133: 1529-1541, 2006.

86. **Jat PS, Noble MD, Ataliotis P, Tanaka Y, Yannoutsos N, Larsen L, and Kioussis D**. Direct derivation of conditionally immortal cell lines from an H-2Kb-tsA58 transgenic mouse. *Proc Natl Acad Sci U S A* 88: 5096-5100, 1991.

87. **Jerkic M, Rivas-Elena JV, Prieto M, Carron R, Sanz-Rodriguez F, Perez-Barriocanal F, Rodriguez-Barbero A, Bernabeu C, and Lopez-Novoa JM**. Endoglin regulates nitric oxide-dependent vasodilatation. *FASEB J* 18: 609-611, 2004.

88. **Jiao K, Kulessa H, Tompkins K, Zhou Y, Batts L, Baldwin HS, and Hogan BL**. An essential role of Bmp4 in the atrioventricular septation of the mouse heart. *Genes Dev* 17: 2362-2367, 2003.

89. **Jin W, Yun C, Kim HS, and Kim SJ**. TrkC binds to the bone morphogenetic protein type II receptor to suppress bone morphogenetic protein signaling. *Cancer Res* 67: 9869-9877, 2007.

90. **Johnson DW, Berg JN, Baldwin MA, Gallione CJ, Marondel I, Yoon SJ, Stenzel TT, Speer M, Pericak-Vance MA, Diamond A, Guttmacher AE, Jackson CE, Attisano L, Kucherlapati R, Porteous ME, and Marchuk DA**. Mutations in the activin receptor-like kinase 1 gene in hereditary haemorrhagic telangiectasia type 2. *Nat Genet* 13: 189-195, 1996.

91. **Kapoor A, and Sanyal AJ**. Endoplasmic reticulum stress and the unfolded protein response. *Clin Liver Dis* 13: 581-590, 2009.

92. **Keller S, Nickel J, Zhang JL, Sebald W, and Mueller TD**. Molecular recognition of BMP-2 and BMP receptor IA. *Nat Struct Mol Biol* 11: 481-488, 2004.

93. **Kirkbride KC, Townsend TA, Bruinsma MW, Barnett JV, and Blobe GC**. Bone Morphogenetic Proteins Signal through the Transforming Growth Factor-β Type III Receptor. *Journal of Biological Chemistry* 283: 7628-7637, 2008.

94. **Kirsch T, Nickel J, and Sebald W**. BMP-2 antagonists emerge from alterations in the low-affinity binding epitope for receptor BMPR-II. *EMBO J* 19: 3314-3324, 2000.

95. **Kirsch T, Nickel J, and Sebald W**. Isolation of recombinant BMP receptor IA ectodomain and its 2:1 complex with BMP-2. *FEBS Letters* 468: 215-219, 2000.

96. **Kirsch T, Sebald W, and Dreyer MK**. Crystal structure of the BMP-2-BRIA ectodomain complex. *Nat Struct Biol* 7: 492-496, 2000.

97. **Kishigami S, and Mishina Y**. BMP signaling and early embryonic patterning. *Cytokine Growth Factor Rev* 16: 265-278, 2005.

98. **Koenig BB, Cook JS, Wolsing DH, Ting J, Tiesman JP, Correa PE, Olson CA, Pecquet AL, Ventura F, and Grant RA**. Characterization and cloning of a receptor for BMP-2 and BMP-4 from NIH 3T3 cells. *Mol Cell Biol* 14: 5961-5974, 1994.

99. **Kuns-Hashimoto R, Kuninger D, Nili M, and Rotwein P**. Selective binding of RGMc/hemojuvelin, a key protein in systemic iron metabolism, to BMP-2 and neogenin. *Am J Physiol Cell Physiol* 294: C994-C1003, 2008.

100. **Lagna G, Nguyen PH, Ni W, and Hata A**. BMP-dependent activation of caspase-9 and caspase-8 mediates apoptosis in pulmonary artery smooth muscle cells. *Am J Physiol Lung Cell Mol Physiol* 291: L1059-1067, 2006.

101. **Lamping K, and Faraci F**. Enhanced vasoconstrictor responses in eNOS deficient mice. *Nitric Oxide* 8: 207-213, 2003.

102. **Lan Y, Liu B, Yao H, Li F, Weng T, Yang G, Li W, Cheng X, Mao N, and Yang X**. Essential role of endothelial Smad4 in vascular remodeling and integrity. *Mol Cell Biol* 27: 7683-7692, 2007.

103. **Lawson KA, Dunn NR, Roelen BA, Zeinstra LM, Davis AM, Wright CV, Korving JP, and Hogan BL**. Bmp4 is required for the generation of primordial germ cells in the mouse embryo. *Genes Dev* 13: 424-436, 1999.

104. **Lebrin F, Goumans MJ, Jonker L, Carvalho RL, Valdimarsdottir G, Thorikay M, Mummery C, Arthur HM, and ten Dijke P**. Endoglin promotes endothelial cell proliferation and TGF-beta/ALK1 signal transduction. *Embo J* 23: 4018-4028, 2004.

105. **Lechleider RJ, Ryan JL, Garrett L, Eng C, Deng C, Wynshaw-Boris A, and Roberts AB**. Targeted mutagenesis of Smad1 reveals an essential role in chorioallantoic fusion. *Dev Biol* 240: 157-167, 2001.

106. **Lee TC, Zhao YD, Courtman DW, and Stewart DJ**. Abnormal Aortic Valve Development in Mice Lacking Endothelial Nitric Oxide Synthase. *Circulation* 101: 2345-2348, 2000.

107. **Lee TK, Poon RT, Yuen AP, Ling MT, Wang XH, Wong YC, Guan XY, Man K, Tang ZY, and Fan ST**. Regulation of angiogenesis by Id-1 through hypoxia-inducible factor-1alpha-mediated vascular endothelial growth factor up-regulation in hepatocellular carcinoma. *Clin Cancer Res* 12: 6910-6919, 2006.

108. **Lesca G, Burnichon N, Raux G, Tosi M, Pinson S, Marion MJ, Babin E, Gilbert-Dussardier B, Riviere S, Goizet C, Faivre L, Plauchu H, Frebourg T, Calender A, and Giraud S**. Distribution of ENG and ACVRL1 (ALK1) mutations in French HHT patients. *Hum Mutat* 27: 598, 2006.

109. **Li AG, Wang D, Feng X-H, and Wang X-J**. Latent TGF[beta]1 overexpression in keratinocytes results in a severe psoriasis-like skin disorder. *EMBO J* 23: 1770-1781, 2004.

110. **Li H, Gerald WL, and Benezra R**. Utilization of Bone Marrow-Derived Endothelial Cell Precursors in Spontaneous Prostate Tumors Varies with Tumor Grade. *Cancer Res* 64: 6137-6143, 2004.

111. **Li W, Mital S, Ojaimi C, Csiszar A, Kaley G, and Hintze TH**. Premature death and age-related cardiac dysfunction in male eNOS-knockout mice. *Journal of Molecular and Cellular Cardiology* 37: 671-680, 2004.

112. **Linde L, and Kerem B**. Introducing sense into nonsense in treatments of human genetic diseases. *Trends Genet* 24: 552-563, 2008.

113. **Liu D, Wang J, Kinzel B, Mueller M, Mao X, Valdez R, Liu Y, and Li E**. Dosage-dependent requirement of BMP type II receptor for maintenance of vascular integrity. *Blood* 110: 1502-1510, 2007.

114. **Liu F, Ventura F, Doody J, and Massague J**. Human type II receptor for bone morphogenic proteins (BMPs): extension of the two-kinase receptor model to the BMPs. *Mol Cell Biol* 15: 3479-3486, 1995.

115. **Long L, Crosby A, Yang X, Southwood M, Upton PD, Kim D-K, and Morrell NW**. Altered Bone Morphogenetic Protein and Transforming Growth Factor-{beta} Signaling in Rat Models of Pulmonary Hypertension: Potential for Activin Receptor-Like Kinase-5 Inhibition in Prevention and Progression of Disease. *Circulation* 119: 566-576, 2009.

116. **Long L, MacLean MR, Jeffery TK, Morecroft I, Yang X, Rudarakanchana N, Southwood M, James V, Trembath RC, and Morrell NW**. Serotonin increases susceptibility to pulmonary hypertension in BMPR2-deficient mice. *Circ Res* 98: 818-827, 2006.

117. **Lonn P, Moren A, Raja E, Dahl M, and Moustakas A**. Regulating the stability of TGFbeta receptors and Smads. *Cell Res* 19: 21-35, 2009.

118. **Lowery JW, Anderson L, DiCarlo GE, Jones MT, and deCaestecker MP**. Functional redundancy between Id1 and Id3 in hypoxic pulmonary hypertension. *submitted* 2009.

119. **Lyden D, Young AZ, Zagzag D, Yan W, Gerald W, O'Reilly R, Bader BL, Hynes RO, Zhuang Y, Manova K, and Benezra R**. Id1 and Id3 are required for neurogenesis, angiogenesis and vascularization of tumour xenografts. *Nature* 401: 670-677, 1999.

120. **Macchia A, Marchioli R, Tognoni G, Scarano M, Marfisi R, Tavazzi L, and Rich S**. Systematic review of trials using vasodilators in pulmonary arterial hypertension: why a new approach is needed. *Am Heart J* 159: 245-257, 2010.

121. **Machado RD, Aldred MA, James V, Harrison RE, Patel B, Schwalbe EC, Gruenig E, Janssen B, Koehler R, Seeger W, Eickelberg O, Olschewski H, Elliott CG, Glissmeyer E, Carlquist J, Kim M, Torbicki A, Fijalkowska A, Szewczyk G, Parma J, Abramowicz MJ, Galie N, Morisaki H, Kyotani S, Nakanishi N, Morisaki T, Humbert M, Simonneau G, Sitbon O, Soubrier F, Coulet F, Morrell NW, and Trembath RC**. Mutations of the TGF-beta type II receptor BMPR2 in pulmonary arterial hypertension. *Hum Mutat* 27: 121-132, 2006.

122. **Machado RD, Eickelberg O, Elliott CG, Geraci MW, Hanaoka M, Loyd JE, Newman JH, Phillips JA, 3rd, Soubrier F, Trembath RC, and Chung WK**. Genetics and genomics of pulmonary arterial hypertension. *J Am Coll Cardiol* 54: S32-42, 2009.

123. **Machado RD, Pauciulo MW, Thomson JR, Lane KB, Morgan NV, Wheeler L, Phillips Iii JA, Newman J, Williams D, Galiè N, Manes A, McNeil K, Yacoub M, Mikhail G, Rogers P, Corris P, Humbert M, Donnai D, Martensson G, Tranebjaerg L, Loyd JE, Trembath RC, and Nichols WC**. BMPR2 Haploinsufficiency as the Inherited Molecular Mechanism for Primary Pulmonary Hypertension. *The American Journal of Human Genetics* 68: 92-102, 2001.

124. **Machado RD, Pauciulo MW, Thomson JR, Lane KB, Morgan NV, Wheeler L, Phillips JA, 3rd, Newman J, Williams D, Galie N, Manes A, McNeil K, Yacoub M, Mikhail G, Rogers P, Corris P, Humbert M, Donnai D, Martensson G, Tranebjaerg L, Loyd JE, Trembath RC, and Nichols WC**. BMPR2 haploinsufficiency as the inherited molecular mechanism for primary pulmonary hypertension. *Am J Hum Genet* 68: 92-102, 2001.

125. **Macías-Silva M, Hoodless PA, Tang SJ, Buchwald M, and Wrana JL**. Specific Activation of Smad1 Signaling Pathways by the BMP7 Type I Receptor, ALK2. *Journal of Biological Chemistry* 273: 25628-25636, 1998.

126. **Mason NA, Springall DR, Burke M, Pollock J, Mikhail G, Yacoub MH, and Polak JM**. High expression of endothelial nitric oxide synthase in plexiform lesions of pulmonary hypertension. *J Pathol* 185: 313-318, 1998.

127. **Mazerbourg S, and Hsueh AJ**. Genomic analyses facilitate identification of receptors and signalling pathways for growth differentiation factor 9 and related orphan bone morphogenetic protein/growth differentiation factor ligands. *Hum Reprod Update* 12: 373-383, 2006.

128. **Mazerbourg S, Klein C, Roh J, Kaivo-Oja N, Mottershead DG, Korchynskyi O, Ritvos O, and Hsueh AJ**. Growth differentiation factor-9 signaling is mediated by the type I receptor, activin receptor-like kinase 5. *Mol Endocrinol* 18: 653-665, 2004.

129. **McAllister KA, Grogg KM, Johnson DW, Gallione CJ, Baldwin MA, Jackson CE, Helmbold EA, Markel DS, McKinnon WC, Murrell J, and et al.** Endoglin, a TGF-beta binding protein of endothelial cells, is the gene for hereditary haemorrhagic telangiectasia type 1. *Nat Genet* 8: 345-351, 1994.

130. **Meyrick BO, and Perkett EA**. The sequence of cellular and hemodynamic changes of chronic pulmonary hypertension induced by hypoxia and other stimuli. *Am Rev Respir Dis* 140: 1486-1489, 1989.

131. **Miller AA, Hislop AA, Vallance PJ, and Haworth SG**. Deletion of the eNOS gene has a greater impact on the pulmonary circulation of male than female mice. *Am J Physiol Lung Cell Mol Physiol* 289: L299-366, 2005.

132. **Miriyala S, Gongora Nieto MC, Mingone C, Smith D, Dikalov S, Harrison DG, and Jo H**. Bone morphogenic protein-4 induces hypertension in mice: role of noggin, vascular NADPH oxidases, and impaired vasorelaxation. *Circulation* 113: 2818-2825, 2006.

133. **Mitchell D, Pobre EG, Mulivor AW, Grinberg AV, Castonguay R, Monnell TE, Solban N, Ucran JA, Pearsall RS, Underwood KW, Seehra J, and Kumar R**. ALK1-Fc inhibits multiple mediators of angiogenesis and suppresses tumor growth. *Mol Cancer Ther* 9: 379-388, 2010.

134. **Miyazono K, Kamiya Y, and Morikawa M**. Bone morphogenetic protein receptors and signal transduction. *J Biochem* 147: 35-51, 2010.

135. **Miyazono K, and Miyazawa K**. Id: A Target of BMP Signaling. *Sci STKE* 2002: pe40-, 2002.

136. **Moore RK, Otsuka F, and Shimasaki S**. Molecular basis of bone morphogenetic protein-15 signaling in granulosa cells. *J Biol Chem* 278: 304-310, 2003.

137. **Moore RK, and Shimasaki S**. Molecular biology and physiological role of the oocyte factor, BMP-15. *Mol Cell Endocrinol* 234: 67-73, 2005.

138. **Morrell NW, Adnot S, Archer SL, Dupuis J, Jones PL, MacLean MR, McMurtry IF, Stenmark KR, Thistlethwaite PA, Weissmann N, Yuan JX, and Weir EK**. Cellular and molecular basis of pulmonary arterial hypertension. *J Am Coll Cardiol* 54: S20-31, 2009.

139. **Morrell NW, Yang X, Upton PD, Jourdan KB, Morgan N, Sheares KK, and Trembath RC**. Altered growth responses of pulmonary artery smooth muscle cells from patients with primary pulmonary hypertension to transforming growth factor-beta(1) and bone morphogenetic proteins. *Circulation* 104: 790-795, 2001.

140. **Morty RE, Nejman B, Kwapiszewska G, Hecker M, Zakrzewicz A, Kouri FM, Peters DM, Dumitrascu R, Seeger W, Knaus P, Schermuly RT, and Eickelberg O**. Dysregulated Bone Morphogenetic Protein Signaling in Monocrotaline-Induced Pulmonary Arterial Hypertension. *Arterioscler Thromb Vasc Biol* 27: 1072-1078, 2007.

141. **Moustakas A, and Heldin CH**. The regulation of TGFbeta signal transduction. *Development* 136: 3699-3714, 2009.

142. **Nakagawa Y, Ikeda K, Nakano R, Uraoka M, Koide M, Akakabe Y, and Matsubara H**. Abstract 5811: Dual Function of Bone Morphogenetic Protein-2 in the Progression of Atherosclerotic Lesion and Atherosclerotic Intimal Calcification in vivo. *Circulation* 120: S1153-d-, 2009.

143. **Nemetski SM, and Gardner LB**. Hypoxic regulation of Id-1 and activation of the unfolded protein response are aberrant in neuroblastoma. *J Biol Chem* 282: 240-248, 2007.

144. **Newfeld SJ, Wisotzkey RG, and Kumar S**. Molecular evolution of a developmental pathway: phylogenetic analyses of transforming growth factor-beta family ligands, receptors and Smad signal transducers. *Genetics* 152: 783-795, 1999.

145. **Nickel J, Dreyer MK, Kirsch T, and Sebald W**. The Crystal Structure of the BMP-2:BMPR-IA Complex and the Generation of BMP-2 Antagonists. *J Bone Joint Surg Am* 83: S7-14, 2001.

146. **Nickel J, Sebald W, Groppe JC, and Mueller TD**. Intricacies of BMP receptor assembly. *Cytokine Growth Factor Rev* 20: 367-377, 2009.

147. **Nishitoh H, Ichijo H, Kimura M, Matsumoto T, Makishima F, Yamaguchi A, Yamashita H, Enomoto S, and Miyazono K**. Identification of Type I and Type II Serine/Threonine Kinase Receptors for Growth/Differentiation Factor-5. *Journal of Biological Chemistry* 271: 21345-21352, 1996.

148. **Nishiyama K, Takaji K, Kataoka K, Kurihara Y, Yoshimura M, Kato A, Ogawa H, and Kurihara H**. Id1 gene transfer confers angiogenic property on fully differentiated endothelial cells and contributes to therapeutic angiogenesis. *Circulation* 112: 2840-2850, 2005.

149. **Norton JD, Deed RW, Craggs G, and Sablitzky F**. Id helix-loop-helix proteins in cell growth and differentiation. *Trends Cell Biol* 8: 58-65, 1998.

150. **Oelze M, Mollnau H, Hoffmann N, Warnholtz A, Bodenschatz M, Smolenski A, Walter U, Skatchkov M, Meinertz T, and Munzel T**. Vasodilator-stimulated phosphoprotein serine 239 phosphorylation as a sensitive monitor of defective nitric oxide/cGMP signaling and endothelial dysfunction. *Circ Res* 87: 999-1005, 2000.

151. **Oh SP, Seki T, Goss KA, Imamura T, Yi Y, Donahoe PK, Li L, Miyazono K, ten Dijke P, Kim S, and Li E**. Activin receptor-like kinase 1 modulates transforming growth factor-beta 1 signaling in the regulation of angiogenesis. *Proc Natl Acad Sci U S A* 97: 2626-2631, 2000.

152. **Onichtchouk D, Chen YG, Dosch R, Gawantka V, Delius H, Massague J, and Niehrs C**. Silencing of TGF-beta signalling by the pseudoreceptor BAMBI. *Nature* 401: 480-485, 1999.

153. **Ouyang XS, Wang X, Lee DTW, Tsao SW, and Wong YC**. Up-regulation of TRPM-2, MMP-7 and ID-1 during sex hormone-induced prostate carcinogenesis in the Noble rat. *Carcinogenesis* 22: 965-973, 2001.

154. **Oxburgh L, Dudley AT, Godin RE, Koonce CH, Islam A, Anderson DC, Bikoff EK, and Robertson EJ**. BMP4 substitutes for loss of BMP7 during kidney development. *Developmental Biology* 286: 637-646, 2005.

155. **Ozaki M, Kawashima S, Yamashita T, Ohashi Y, Rikitake Y, Inoue N, Hirata KI, Hayashi Y, Itoh H, and Yokoyama M**. Reduced hypoxic pulmonary vascular remodeling by nitric oxide from the endothelium. *Hypertension* 37: 322-327, 2001.

156. **Pan L, Sato S, Frederick JP, Sun XH, and Zhuang Y**. Impaired immune responses and B-cell proliferation in mice lacking the Id3 gene. *Mol Cell Biol* 19: 5969-5980, 1999.

157. **Park C, Lavine K, Mishina Y, Deng CX, Ornitz DM, and Choi K**. Bone morphogenetic protein receptor 1A signaling is dispensable for hematopoietic development but essential for vessel and atrioventricular endocardial cushion formation. *Development* 133: 3473-3484, 2006.

158. **Park MH**. Advances in diagnosis and treatment in patients with pulmonary arterial hypertension. *Catheterization and Cardiovascular Interventions* 71: 205-213, 2008.

159. **Park SO, Lee YJ, Seki T, Hong K-H, Fliess N, Jiang Z, Park A, Wu X, Kaartinen V, Roman BL, and Oh SP**. ALK5- and TGFBR2-independent role of ALK1 in the pathogenesis of hereditary hemorrhagic telangiectasia type 2. *Blood* 111: 633-642, 2008.

160. **Perk J, Gil-Bazo I, Chin Y, de Candia P, Chen JJS, Zhao Y, Chao S, Cheong W, Ke Y, Al-Ahmadie H, Gerald WL, Brogi E, and Benezra R**. Reassessment of Id1 Protein Expression in Human Mammary, Prostate, and Bladder Cancers Using a Monospecific Rabbit Monoclonal Anti-Id1 Antibody. *Cancer Res* 66: 10870-10877, 2006.

161. **Perk J, Iavarone A, and Benezra R**. Id family of helix-loop-helix proteins in cancer. *Nat Rev Cancer* 5: 603-614, 2005.

162. **Pregizer S, and Mortlock DP**. Control of BMP gene expression by long-range regulatory elements. *Cytokine Growth Factor Rev* 20: 509-515, 2009.

163. **Preston IR**. Clinical perspective of hypoxia-mediated pulmonary hypertension. *Antioxid Redox Signal* 9: 711-721, 2007.

164. **Quinlan TR, Li D, Laubach VE, Shesely EG, Zhou N, and Johns RA**. eNOS-deficient mice show reduced pulmonary vascular proliferation and remodeling to chronic hypoxia. *Am J Physiol Lung Cell Mol Physiol* 279: L641-650, 2000.

165. **Rabinovitch M**. Molecular pathogenesis of pulmonary arterial hypertension. *J Clin Invest* 118: 2372-2379, 2008.

166. **Ramos M, Lame MW, Segall HJ, and Wilson DW**. The BMP type II receptor is located in lipid rafts, including caveolae, of pulmonary endothelium in vivo and in vitro. *Vascul Pharmacol* 44: 50-59, 2006.

167. **Ren R, Charles PC, Zhang C, Wu Y, Wang H, and Patterson C**. Gene expression profiles identify a role for cyclooxygenase 2-dependent prostanoid generation in BMP6-induced angiogenic responses. *Blood* 109: 2847-2853, 2007.

168. **Rigelsky CM, Jennings C, Lehtonen R, Minai OA, Eng C, and Aldred MA**. BMPR2 mutation in a patient with pulmonary arterial hypertension and suspected hereditary hemorrhagic telangiectasia. *Am J Med Genet A* 146A: 2551-2556, 2008.

169. **Rosenzweig BL, Imamura T, Okadome T, Cox GN, Yamashita H, ten Dijke P, Heldin CH, and Miyazono K**. Cloning and characterization of a human type II receptor for bone morphogenetic proteins. *Proc Natl Acad Sci U S A* 92: 7632-7636, 1995.

170. **Ross S, and Hill CS**. How the Smads regulate transcription. *Int J Biochem Cell Biol* 40: 383-408, 2008.

171. **Ruzinova MB, and Benezra R**. Id proteins in development, cell cycle and cancer. *Trends in Cell Biology* 13: 410-418, 2003.

172. **Sakurai D, Tsuchiya N, Yamaguchi A, Okaji Y, Tsuno NH, Kobata T, Takahashi K, and Tokunaga K**. Crucial Role of Inhibitor of DNA Binding/Differentiation in the Vascular Endothelial Growth Factor-Induced Activation and Angiogenic Processes of Human Endothelial Cells. *J Immunol* 173: 5801-5809, 2004.

173. **Samad TA, Rebbapragada A, Bell E, Zhang Y, Sidis Y, Jeong SJ, Campagna JA, Perusini S, Fabrizio DA, Schneyer AL, Lin HY, Brivanlou AH, Attisano L, and Woolf CJ**. DRAGON, a bone morphogenetic protein co-receptor. *J Biol Chem* 280: 14122-14129, 2005.

174. **Sammar M, Sieber C, and Knaus P**. Biochemical and functional characterization of the Ror2/BRIb receptor complex. *Biochem Biophys Res Commun* 381: 1-6, 2009.

175. **Sammar M, Stricker S, Schwabe GC, Sieber C, Hartung A, Hanke M, Oishi I, Pohl J, Minami Y, Sebald W, Mundlos S, and Knaus P**. Modulation of GDF5/BRI-b signalling through interaction with the tyrosine kinase receptor Ror2. *Genes Cells* 9: 1227-1238, 2004.

176. **Santibanez JF, Letamendia A, Perez-Barriocanal F, Silvestri C, Saura M, Vary CP, Lopez-Novoa JM, Attisano L, and Bernabeu C**. Endoglin increases eNOS expression by modulating Smad2 protein levels and Smad2-dependent TGF-beta signaling. *J Cell Physiol* 210: 456-468, 2007.

177. **Scharpfenecker M, van Dinther M, Liu Z, van Bezooijen RL, Zhao Q, Pukac L, Lowik CW, and ten Dijke P**. BMP-9 signals via ALK1 and inhibits bFGF-induced endothelial cell proliferation and VEGF-stimulated angiogenesis. *J Cell Sci* 120: 964-972, 2007.

178. **Scherner O, Meurer SK, Tihaa L, Gressner AM, and Weiskirchen R**. Endoglin differentially modulates antagonistic transforming growth factor-beta1 and BMP-7 signaling. *J Biol Chem* 282: 13934-13943, 2007.

179. **Searles CD**. Transcriptional and posttranscriptional regulation of endothelial nitric oxide synthase expression. *Am J Physiol Cell Physiol* 291: C803-816, 2006.

180. **Seemann P, Brehm A, Konig J, Reissner C, Stricker S, Kuss P, Haupt J, Renninger S, Nickel J, Sebald W, Groppe JC, Ploger F, Pohl J, Schmidt-von Kegler M, Walther M, Gassner I, Rusu C, Janecke AR, Dathe K, and Mundlos S**. Mutations in GDF5 reveal a key residue mediating BMP inhibition by NOGGIN. *PLoS Genet* 5: e1000747, 2009.

181. **Seki T, Yun J, and Oh SP**. Arterial endothelium-specific activin receptor-like kinase 1 expression suggests its role in arterialization and vascular remodeling. *Circ Res* 93: 682-689, 2003.

182. **Selbach M, Schwanhausser B, Thierfelder N, Fang Z, Khanin R, and Rajewsky N**. Widespread changes in protein synthesis induced by microRNAs. *Nature* 455: 58-63, 2008.

183. **Shao ES, Lin L, Yao Y, and Bostrom KI**. Expression of vascular endothelial growth factor is coordinately regulated by the activin-like kinase receptors 1 and 5 in endothelial cells. *Blood* 114: 2197-2206, 2009.

184. **Shi Y, and Massague J**. Mechanisms of TGF-beta signaling from cell membrane to the nucleus. *Cell* 113: 685-700, 2003.

185. **Shintani M, Yagi H, Nakayama T, Saji T, and Matsuoka R**. A new nonsense mutation of SMAD8 associated with pulmonary arterial hypertension. *J Med Genet* 46: 331-337, 2009.

186. **Sikder HA, Devlin MK, Dunlap S, Ryu B, and Alani RM**. Id proteins in cell growth and tumorigenesis. *Cancer Cell* 3: 525-530, 2003.

187. **Simonneau G, Galie N, Rubin LJ, Langleben D, Seeger W, Domenighetti G, Gibbs S, Lebrec D, Speich R, Beghetti M, Rich S, and Fishman A**. Clinical classification of pulmonary hypertension. *J Am Coll Cardiol* 43: 5S-12S, 2004.

188. **Simonneau G, Robbins IM, Beghetti M, Channick RN, Delcroix M, Denton CP, Elliott CG, Gaine SP, Gladwin MT, Jing ZC, Krowka MJ, Langleben D, Nakanishi N, and Souza R**. Updated clinical classification of pulmonary hypertension. *J Am Coll Cardiol* 54: S43-54, 2009.

189. **Sobolewski A, Rudarakanchana N, Upton PD, Yang J, Crilley TK, Trembath RC, and Morrell NW**. Failure of bone morphogenetic protein receptor trafficking in pulmonary arterial hypertension: potential for rescue. *Hum Mol Genet* 17: 3180-3190, 2008.

190. **Solloway MJ, Dudley AT, Bikoff EK, Lyons KM, Hogan BL, and Robertson EJ**. Mice lacking Bmp6 function. *Dev Genet* 22: 321-339, 1998.

191. **Sone M, Itoh H, Yamahara K, Yamashita JK, Yurugi-Kobayashi T, Nonoguchi A, Suzuki Y, Chao TH, Sawada N, Fukunaga Y, Miyashita K, Park K, Oyamada N, Taura D, Tamura N, Kondo Y, Nito S, Suemori H, Nakatsuji N, Nishikawa S, and Nakao K**. Pathway for differentiation of human embryonic stem cells to vascular cell components and their potential for vascular regeneration. *Arterioscler Thromb Vasc Biol* 27: 2127-2134, 2007.

192. **Song Y, Coleman L, Shi J, Beppu H, Sato K, Walsh K, Loscalzo J, and Zhang YY**. Inflammation, endothelial injury, and persistent pulmonary hypertension in heterozygous BMPR2-mutant mice. *Am J Physiol Heart Circ Physiol* 295: H677-690, 2008.

193. **Song Y, Jones JE, Beppu H, Keaney JF, Jr., Loscalzo J, and Zhang YY**. Increased susceptibility to pulmonary hypertension in heterozygous BMPR2-mutant mice. *Circulation* 112: 553-562, 2005.

194. **Sorescu GP, Sykes M, Weiss D, Platt MO, Saha A, Hwang J, Boyd N, Boo YC, Vega JD, Taylor WR, and Jo H**. Bone morphogenic protein 4 produced in endothelial cells by oscillatory shear stress stimulates an inflammatory response. *J Biol Chem* 278: 31128-31135, 2003.

195. **Srinivasan S, Hanes MA, Dickens T, Porteous ME, Oh SP, Hale LP, and Marchuk DA**. A mouse model for hereditary hemorrhagic telangiectasia (HHT) type 2. *Hum Mol Genet* 12: 473-482, 2003.

196. **Stenmark KR, Meyrick B, Galie N, Mooi WJ, and McMurtry IF**. Animal models of pulmonary arterial hypertension: the hope for etiological discovery and pharmacological cure. *Am J Physiol Lung Cell Mol Physiol* 297: L1013-1032, 2009.

197. **Steudel W, Ichinose F, Huang PL, Hurford WE, Jones RC, Bevan JA, Fishman MC, and Zapol WM**. Pulmonary vasoconstriction and hypertension in mice with targeted disruption of the endothelial nitric oxide synthase (NOS 3) gene. *Circ Res* 81: 34-41, 1997.

198. **Steudel W, Scherrer-Crosbie M, Bloch KD, Weimann J, Huang PL, Jones RC, Picard MH, and Zapol WM**. Sustained pulmonary hypertension and right ventricular hypertrophy after chronic hypoxia in mice with congenital deficiency of nitric oxide synthase 3. *J Clin Invest* 101: 2468-2477, 1998.

199. **Takahashi H, Goto N, Kojima Y, Tsuda Y, Morio Y, Muramatsu M, and Fukuchi Y**. Downregulation of type II bone morphogenetic protein receptor in hypoxic pulmonary hypertension. *Am J Physiol Lung Cell Mol Physiol* 290: L450-458, 2006.

200. **Takahashi K, Kogaki S, Matsushita T, Nasuno S, Kurotobi S, and Ozono K**. Hypoxia Induces Alteration of Bone Morphogenetic Protein Receptor Signaling in Pulmonary Artery Endothelial Cell. *Pediatric Research* 61: 392-397 310.1203/pdr.1200b1013e3180332cba, 2007.

201. **Takahashi K, Tanabe K, Ohnuki M, Narita M, Ichisaka T, Tomoda K, and Yamanaka S**. Induction of pluripotent stem cells from adult human fibroblasts by defined factors. *Cell* 131: 861-872, 2007.

202. **Takeda M, Otsuka F, Nakamura K, Inagaki K, Suzuki J, Miura D, Fujio H, Matsubara H, Date H, Ohe T, and Makino H**. Characterization of the bone morphogenetic protein (BMP) system in human pulmonary arterial smooth muscle cells isolated from a sporadic case of primary pulmonary hypertension: roles of BMP type IB receptor (activin receptor-like kinase-6) in the mitotic action. *Endocrinology* 145: 4344-4354, 2004.

203. **Takeda M, Otsuka F, Nakamura K, Inagaki K, Suzuki J, Miura D, Fujio H, Matsubara H, Date H, Ohe T, and Makino H**. Characterization of the Bone Morphogenetic Protein (BMP) System in Human Pulmonary Arterial Smooth Muscle Cells Isolated from a Sporadic Case of Primary Pulmonary Hypertension: Roles of BMP Type IB Receptor (Activin Receptor-Like Kinase-6) in the Mitotic Action. *Endocrinology* 145: 4344-4354, 2004.

204. **Taura D, Sone M, Homma K, Oyamada N, Takahashi K, Tamura N, Yamanaka S, and Nakao K**. Induction and isolation of vascular cells from human induced pluripotent stem cells--brief report. *Arterioscler Thromb Vasc Biol* 29: 1100-1103, 2009.

205. **ten Dijke P, Korchynskyi O, Valdimarsdottir G, and Goumans M-J**. Controlling cell fate by bone morphogenetic protein receptors. *Molecular and Cellular Endocrinology* 211: 105-113, 2003.

206. **ten Dijke P, Yamashita H, Sampath TK, Reddi AH, Estevez M, Riddle DL, Ichijo H, Heldin CH, and Miyazono K**. Identification of type I receptors for osteogenic protein-1 and bone morphogenetic protein-4. *Journal of Biological Chemistry* 269: 16985-16988, 1994.

207. **Toporsian M, Gros R, Kabir MG, Vera S, Govindaraju K, Eidelman DH, Husain M, and Letarte M**. A Role for Endoglin in Coupling eNOS Activity and Regulating Vascular Tone Revealed in Hereditary Hemorrhagic Telangiectasia. *Circ Res* 96: 684-692, 2005.

208. **Toporsian M, Jerkic M, Zhou YQ, Kabir MG, Yu LX, McIntyre BA, Davis A, Wang YJ, Stewart DJ, Belik J, Husain M, Henkelman M, and Letarte M**. Spontaneous adult-onset pulmonary arterial hypertension attributable to increased endothelial oxidative stress in a murine model of hereditary hemorrhagic telangiectasia. *Arterioscler Thromb Vasc Biol* 30: 509-517, 2010.

209. **Uehara N, Chou Y-C, Galvez J, de-Candia P, Cardiff R, Benezra R, and Shyamala G**. Id-1 is not expressed in the luminal epithelial cells of mammary glands. *Breast Cancer Res* 5: R25 - R29, 2003.

210. **Umulis D, O'Connor MB, and Blair SS**. The extracellular regulation of bone morphogenetic protein signaling. *Development* 136: 3715-3728, 2009.

211. **Upton PD, and Morrell NW**. TGF-beta and BMPR-II pharmacology--implications for pulmonary vascular diseases. *Curr Opin Pharmacol* 9: 274-280, 2009.

212. **Urist MR**. Bone: formation by autoinduction. *Science* 150: 893-899, 1965.

213. **Urist MR, and Strates BS**. Bone morphogenetic protein. *J Dent Res* 50: 1392-1406, 1971.

214. **Urness LD, Sorensen LK, and Li DY**. Arteriovenous malformations in mice lacking activin receptor-like kinase-1. *Nat Genet* 26: 328-331, 2000.

215. **Valdimarsdottir G, Goumans MJ, Rosendahl A, Brugman M, Itoh S, Lebrin F, Sideras P, and ten Dijke P**. Stimulation of Id1 expression by bone morphogenetic

protein is sufficient and necessary for bone morphogenetic protein-induced activation of endothelial cells. *Circulation* 106: 2263-2270, 2002.

216. **Vandeputte DAA, Troost D, Leenstra S, Ijlst-Keizers H, Ramkema M, Bosch DA, Baas F, Das NK, and Aronica E**. Expression and distribution of id helix-loop-helix proteins in human astrocytic tumors. *Glia* 38: 329-338, 2002.

217. **Vitt UA, Mazerbourg S, Klein C, and Hsueh AJ**. Bone morphogenetic protein receptor type II is a receptor for growth differentiation factor-9. *Biol Reprod* 67: 473-480, 2002.

218. **Voelkel NF, and Tuder RM**. Hypoxia-induced pulmonary vascular remodeling: a model for what human disease? *J Clin Invest* 106: 733-738, 2000.

219. **West J, Harral J, Lane K, Deng Y, Ickes B, Crona D, Albu S, Stewart D, and Fagan K**. Mice expressing BMPR2R899X transgene in smooth muscle develop pulmonary vascular lesions. *Am J Physiol Lung Cell Mol Physiol* 295: L744-755, 2008.

220. **Wong YC, Wang X, and Ling MT**. Id-1 expression and cell survival. *Apoptosis* 9: 279-289, 2004.

221. **Wu LA, Yuan G, Yang G, Ortiz-Gonzalez I, Yang W, Cui Y, MacDougall M, Donly KJ, Harris S, and Chen S**. Immortalization and characterization of mouse floxed Bmp2/4 osteoblasts. *Biochem Biophys Res Commun* 386: 89-95, 2009.

222. **Wu X, Chang MS, Mitsialis SA, and Kourembanas S**. Hypoxia regulates bone morphogenetic protein signaling through C-terminal-binding protein 1. *Circ Res* 99: 240-247, 2006.

223. **Wu Z, Yang L, Cai L, Zhang M, Cheng X, Yang X, and Xu J**. Detection of epithelial to mesenchymal transition in airways of a bleomycin induced pulmonary fibrosis model derived from an alpha-smooth muscle actin-Cre transgenic mouse. *Respir Res* 8: 1, 2007.

224. **Xia Y, Babitt JL, Sidis Y, Chung RT, and Lin HY**. Hemojuvelin regulates hepcidin expression via a selective subset of BMP ligands and receptors independently of neogenin. *Blood* 111: 5195-5204, 2008.

225. **Xia Y, Yu PB, Sidis Y, Beppu H, Bloch KD, Schneyer AL, and Lin HY**. Repulsive guidance molecule RGMa alters utilization of bone morphogenetic protein (BMP) type II receptors by BMP2 and BMP4. *J Biol Chem* 282: 18129-18140, 2007.

226. **Yamaji N, Celeste AJ, Thies RS, Song JJ, Bernier SM, Goltzman D, Lyons KM, Nove J, Rosen V, and Wozney JM**. A Mammalian Serine/Threonine Kinase Receptor Specifically Binds BMP-2 and BMP-4. *Biochemical and Biophysical Research Communications* 205: 1944-1951, 1994.

227. **Yamaji N, Celeste AJ, Thies RS, Song JJ, Bernier SM, Goltzman D, Lyons KM, Nove J, Rosen V, and Wozney JM**. A mammalian serine/threonine kinase receptor specifically binds BMP-2 and BMP-4. *Biochem Biophys Res Commun* 205: 1944-1951, 1994.

228. **Yamanaka S**. A fresh look at iPS cells. *Cell* 137: 13-17, 2009.

229. **Yamashita H, ten Dijke P, Huylebroeck D, Sampath TK, Andries M, Smith JC, Heldin CH, and Miyazono K**. Osteogenic protein-1 binds to activin type II receptors and induces certain activin-like effects. *J Cell Biol* 130: 217-226, 1995.

230. **Yan W, Young AZ, Soares VC, Kelley R, Benezra R, and Zhuang Y**. High incidence of T-cell tumors in E2A-null mice and E2A/Id1 double-knockout mice. *Mol Cell Biol* 17: 7317-7327, 1997.

231. **Yang C-L, Kurczab T, Down G, Kealey T, and Langlands K**. Gene expression profiling of the ageing rat vibrissa follicle. *British Journal of Dermatology* 153: 22-28, 2005.

232. **Yang F, West AP, Jr., Allendorph GP, Choe S, and Bjorkman PJ**. Neogenin interacts with hemojuvelin through its two membrane-proximal fibronectin type III domains. *Biochemistry* 47: 4237-4245, 2008.

233. **Yang J, Davies RJ, Southwood M, Long L, Yang X, Sobolewski A, Upton PD, Trembath RC, and Morrell NW**. Mutations in bone morphogenetic protein type II receptor cause dysregulation of Id gene expression in pulmonary artery smooth muscle cells: implications for familial pulmonary arterial hypertension. *Circ Res* 102: 1212-1221, 2008.

234. **Yang X, Castilla LH, Xu X, Li C, Gotay J, Weinstein M, Liu PP, and Deng CX**. Angiogenesis defects and mesenchymal apoptosis in mice lacking SMAD5. *Development* 126: 1571-1580, 1999.

235. **Yang X, Long L, Southwood M, Rudarakanchana N, Upton PD, Jeffery TK, Atkinson C, Chen H, Trembath RC, and Morrell NW**. Dysfunctional Smad signaling contributes to abnormal smooth muscle cell proliferation in familial pulmonary arterial hypertension. *Circ Res* 96: 1053-1063, 2005.

236. **Zhang H, and Bradley A**. Mice deficient for BMP2 are nonviable and have defects in amnion/chorion and cardiac development. *Development* 122: 2977-2986, 1996.

237. **Zhang H, Lawson WE, Polosukhin VV, Pozzi A, Blackwell TS, Litingtung Y, and Chiang C**. Inhibitor of differentiation 1 promotes endothelial survival in a bleomycin model of lung injury in mice. *Am J Pathol* 171: 1113-1126, 2007.

238. **Zhang S, Fantozzi I, Tigno DD, Yi ES, Platoshyn O, Thistlethwaite PA, Kriett JM, Yung G, Rubin LJ, and Yuan JX**. Bone morphogenetic proteins induce apoptosis in human pulmonary vascular smooth muscle cells. *Am J Physiol Lung Cell Mol Physiol* 285: L740-754, 2003.

239. **Zhang YE**. Non-Smad pathways in TGF-beta signaling. *Cell Res* 19: 128-139, 2009.

240. **Zhao GQ**. Consequences of knocking out BMP signaling in the mouse. *Genesis* 35: 43-56, 2003.